Production and Decay Characteristics of Paramagnetic Defects in Quartz: Applications to ESR Dating

by

Shin Toyoda

Abstract

Electron spin resonance (ESR) detects paramagnetic defects and radicals created by natural radiation and accumulated in minerals in geologic time scale. Quartz is a mineral abundant in volcanic and sedimentary rocks. ESR dating using the mineral has been used to elucidate history of tectonic activities in the Quarternary.

Although ESR dating has been popular, basic studies on thermal stabilities of paramagnetic centers are lacking. This thesis deals with formation and decay characteristics of paramagnetic defects in natural quartz. The findings in the characteristics were utilized to solve some problems in ESR dating using quartz.

Many of paramagnetic defects in quartz have been well characterized in the field of solid state physics as reviewed in the first half of Chapter 1 in this thesis. However, little have been known about their formation and decay kinetics although formation and decay kinetics are of interest to investigate history of thermal events and formation ages of minerals. Only a few studies in ESR dating is made on thermal stabilities and decay kinetics as reviewed in the latter half of Chapter 1.

As the results of annealing experiments, paramagnetic defects (E_1', Al, and Ti centers) in quartz extracted from a granite were found to reduce their numbers on heating following a second order decay kinetics. A procedure is proposed to estimate the number of oxygen vacancies in quartz. The possible decay process of the paramagnetic centers are discussed in Chapter 2 as well as formation and decay mechanisms of E' centers and oxygen vacancies.

Some new applications of ESR dating are described in Chapter 3 using the findings in formation and decay characteristics of paramagnetic defects. Closure temperatures, at which the clock of dating starts, for ESR dating in the cases of using oxygen vacancies and Al, and Ti centers were obtained for the first time. Thermal history around an old intrusive rock is investigated using concentrations of oxygen vacancies in metamorphic rocks.

A new technique is proposed to estimate the temperature of prehistoric heat treatment for stone implements by using the ratio between E' center and oxygen vacancies. An Archaeological problems of firing stone implements of American Indians' is solved with ESR. Concentration of oxygen vacancies is correlated with total accumulated doses given by β and γ rays for volcanic rocks whose ages are between 10 and 1800 Ma. A possibility was investigated for ESR dating for the early Earth.

Lastly, the effect of atmospheric ^{222}Rn activities on the annual dose rate in ESR and TL dating was estimated and given in Appendix.

Table of Contents

1. INTRODUCTION

1–1 General Introduction

Lattice defects with an unpaired electron created by natural radiation in minerals are observed with electron spin resonance (ESR). Microwave absorption is caused by transfer of electron spins between the energy levels splitted by Zeeman effect in static magnetic field. The accumulated dose from natural radiation given to a specific sample is estimated by relative ESR intensity and by enhancement of the signal by artificial γ ray irradiation. The idea of ESR dating was first proposed by Duchesne *et al.* (1961), but ESR dating of coal did not succeed because radicals in coal were not formed by natural radiation but by chemical reactions. Zeller (1968) tried ESR dating of some minerals but again he did not succeed because the samples were too old for ESR dating.

This method was first practically applied to calcite of stalactite in Akiyoshi cave (Ikeya, 1975). A systematic studies are going on in earth science beyond the limitation of ^{14}C dating up to a few million years (Ikeya, 1988, Ikeya and Miki, 1985). ESR dating has been practically applied to Quaternary samples utilizing speleothems made of calcite (e.g. Ikeya, 1975), mollusks made of calcite and aragonite (e.g. Ikeya and Ohmura, 1981), corals made of aragonite (e.g. Ikeya and Ohmura, 1983; Ikeda *et al.*, 1991), tooth enamel made of hydroxyapatite (e.g. Grün and Invarnati, 1985), bones made of hydroxyapatite (Ikeya and Miki, 1980), gypsum (e.g. Ikeya, 1985), and quartz (e.g. Ikeya *et al.*, 1982). Possibilities of dating have been pointed out for other apatites (Ishii and Ikeya, in press), zircon (Taguchi *et al.*, 1985), halite and $NaHCO_3$ (Ikeya, 1988), and for ice and dry ice at a low temperature, on the surfaces of the outer planets (Tsukamoto *et al.*, submitted).

α–quartz is an abundant mineral in geological field occurring in volcanic, metamorphic, and sedimentary rocks. It is the only mineral practically applied to ESR dating of volcanic materials. ESR dating using quartz has contributed to various fields in earth sciences, such as structural geology and tephrochronology, and in Archaeology.

The tectonic movement has been active accompanied with faulting and volcanic

activities especially in Quaternary time, representing the last 1.7 Ma. Quartz is the only promising mineral to elucidate the history of tectonic activities by ESR dating method, especially for the gap between ^{14}C and K–Ar methods. Several kind of centers of different thermal stabilities may solve the history of the activities.

In this chapter, the principle of ESR dating method, crystal structure and point defects in quartz and reports on ESR dating are reviewed. Problems in ESR dating using quartz are also summarized.

1–2 Principle of ESR dating

Paramagnetic defects created by natural ionizing radiation are accumulated in minerals. The accumulation starts at the time of zeroing process, for which four mechanisms have been proposed, mineralization, heat, sunlight, and shear stress. Most ESR ages obtained for carbonates are mineralization age. In the case for quartz, ESR ages have been obtained of the rest three kind of events. The heating age is obtained for volcanic rocks and tuffs. Sedimentation ages have been obtained assuming bleaching of centers by sun light (e.g. Tanaka *et al.*, 1985). ESR dating of active fault movement assumes that the paramagnetic centers in intra fault materials are reset by shear stress at the time of faulting (Ikeya *et al.*, 1982).

Total accumulated dose for a sample is obtained by additive dose method, i.e., extrapolation of signal enhancement curve to the zero ordinate. An ESR age, T, is derived from the equation

$$TD = \int_0^T D(t)\ dt$$

where TD is a total accumulated dose and D(t) is an annual dose rate, time dependent in general. D(t) is measured by thermoluminescence dosimeter or calculated from concentrations of radioactive nuclides of the layer as a summation of dose rates given by α β, and γ rays (Nambi and Aitken, 1986). Cosmic rays are also considered in many cases. The effectiveness of defect production of α rays relative to that of β and γ rays has been

investigated (e.g. Yokoyama, 1982) and is now still in discussion. ^{238}U, ^{235}U, ^{232}Th, ^{40}K, and their daughter nuclides have been considered as the sources of ionizing radiation. The initial acquisition of nuclides in radioactive disequilibrium is responsible for time dependence of annual dose rate, D(t) (e.g., Ikeya and Ohmura, 1983). The time dependence of D(t) has been investigated for corals, speleothems and bones, but no radioactive disequilibrium has been considered in the cases of volcanic materials.

1-3 Crystal structure of quartz

α-quartz has a trigonal lattice which contains three silicon atoms and six oxygen atoms in the coordination unit (LePage and Donnay, 1976). A schematic structure of α quartz is shown in Fig.1-1 and Fig.1-2a. The unit cell parameters are a=0.49134 nm and c=0.54152 nm at room temperature (LePage and Donnay, 1976). Each silicon atom has four oxygen neighbors, approximately tetrahedrally positioned. Each tetrahedron bonded together sharing all four oxygen atoms with next ones. One oxygen has two bonds whose lengths are 0.1611 nm (long bond) and 0.1607 nm (short bond) at room temperature (LePage and Donnay, 1976). One silicon has two long bonds and two short bonds.

1-4 Paramagnetic defects in quartz

(1) E' centers

E' centers are defects associated with oxygen vacancies. The investigations of paramagnetic species of E' centers began in 1956 (Weeks, 1956). Six types of E' centers have been identified: E'_1, E'_2, E'_4, E''_1, E''_2, and E''_3. Little is known about the corresponding precursors of these defects (Weil, 1984).

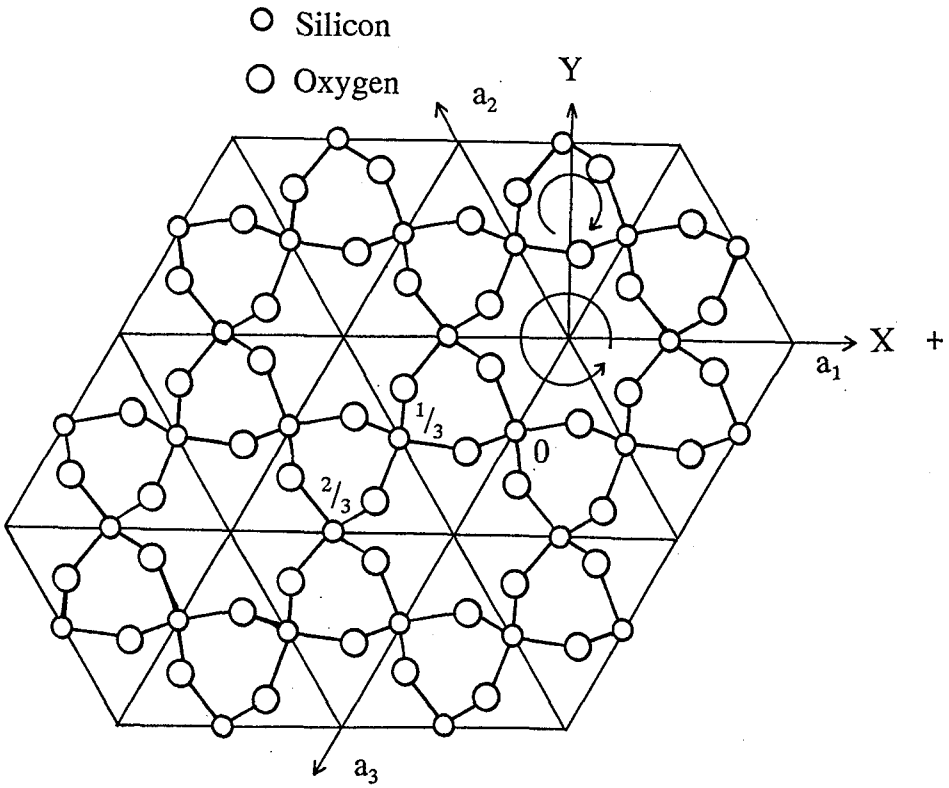

Fig.1-1 Projection of right α quartz atomic positions onto the plane perpendicular to c axis, showing two-fold axes a_j (i=1,2,3). (partially modified after Weil, 1984) The unit cell parameters are a=0.49134 nm and c=0.54152 nm at room temperature.

The best known type is E_1' center, where an electron is trapped at an oxygen vacancy. The form is $[O_3Si{\cdot}SiO_3]^+$. Weeks (1956) first reported electron and hole centers created by neutron-irradiation in quartz. E_1' center was characterized in detail by Silsbee (1961) using ESR. The spectrum shows a strong central line with anisotropic g factors of 2.00179, 2.00053, and 2.00030 (Jani *et al.*, 1983, see Table 1-1), and three hyperfine structures with splittings at 400, 9, and 8 G when the magnetic field is parallel to the crystal c-axis. The disposition of atoms around the defect has been investigated by these hyperfine structures. Silsbee (1961) proposed that the 400G splitting is due to hyperfine interaction with ^{29}Si. The idea was supported by the study by Griscom (1979) investigating E' center in ^{29}Si enriched quartz glasses. It is also consistent with the model proposed by Feigl *et al.* (1974). According to the model, an unpaired electron is in a single silicon sp^3 orbital oriented along a bond direction into the vacancy. The silicon having the electron relaxes toward the vacancy while the other silicon, in the opposite side, having positive charge mainly relaxes away into the basal plane of its three oxygen neighbors (see Fig.1-2b). Their model agrees rather well with the spin Hamiltonian parameters obtained by Silsbee (1961), but does not explain the weak hyperfine structures.

Griscom (1980) studied E' center in fused silica and concluded that the two weak hyperfine structures might be due to protons but not silicons. On the other hand, Jani *et al.* (1983) showed that these hyperfine structures are associated with ^{29}Si by an ENDOR study and proposed a divacancy model where another oxygen atom between Si(0) and Si(4) (see Fig.1-2a) is also missing.

Rudra and Fowler (1987) theoretically simulated the structure of their model and concluded that unpaired electron cannot be localized at the vacancy between Si(0) and Si(1) in the electronic structure of minimum energy. The authors also calculated the energy level for formation of an E'_1 center from a neutral oxygen vacancy (0/+) to be −5.5 eV under the lowest energy level of conduction band according to the model by Feigl *et al.* (1974). The energy level of bonding state of neutral oxygen vacancy, and that for changing from negatively charged state to neutral (0/−) and from single to double positively charged state (+/2+) were also calculated to be −6.7, −0.7, and −7.7 eV, respectively (see Fig.1-3).

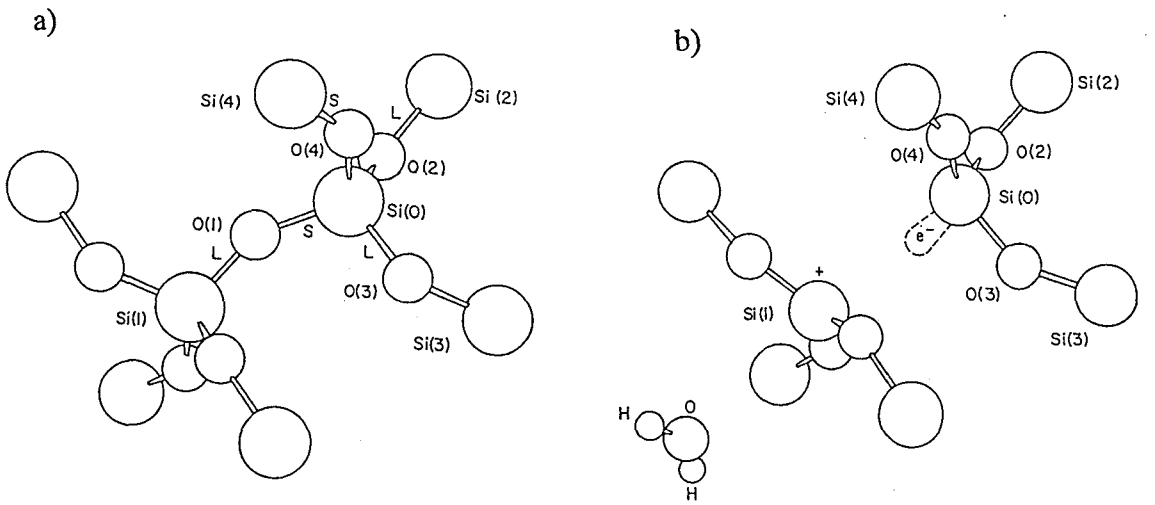

Fig.1–2 a) A part of atomic dispositions of quartz. (after Rudra and Fowler, 1987). b) Minimum energy planar configuration of E_1' center calculated by Rudra and Fowler (1987).

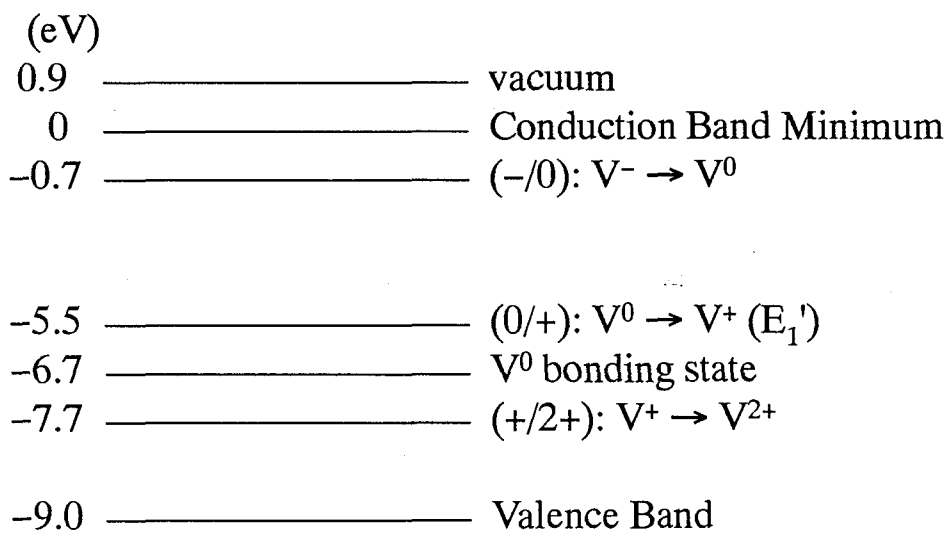

Fig. 1–3 Energy levels, relative to conduction band minimum, of defects associated with an oxygen vacancy in quartz theoretically calculated by Rudra and Fowler (1987). V^0, V^+, and V^{2+} denote oxygen vacancies with two, one, and no electrons, respectively.

The formation process of E'_1 center is a significant issue remained. It is created by fast neutron irradiation (Weeks 1956, Garrison *et al.* 1981) as well as by electron (Jani *et al.* 1983) and by γ ray irradiation at a heavy dose (Wieser and Regulla, 1989) with attendant heating at 300°C. Jani *et al.* (1983) studied the relation between E'_1 formation and the temperature of electron irradiation. They reported that the temperature above 200K at electron irradiation is required for the formation of E'_1 centers. The authors pointed out that its formation is related with mobility of interstitial alkali ions because the ions become mobile above 200K. Semi-quantitative analysis for correlation between decay of $[AlO_4]^0$ and formation of E'_1 centers suggested that holes released from $[AlO_4]^0$ are trapped at neutral oxygen vacancies with two electron to form E'_1 centers when sample is heated at 200 to 300°C.

Other states of oxygen vacancy trapping an electron (E_2' and E_4') were investigated (e.g. Rudra *et al.*, 1985; Halliburton *et al.*, 1979). A hyperfine structure was found caused by a hydrogen atom. E" type centers with two electrons (S=1) (e.g. Bossoli *et al.*, 1982) have been also observed.

(2) Aluminum Hole Center

The ESR signal of a paramagnetic defect concerning to aluminum was first observed by Griffith *et al.* (1954). Its electronic structure was attributed to $[AlO_4]^0$ where a hole is trapped in a nonbonding p-orbital of an oxygen anion linking a substitutional aluminum (O'Brien, 1955). Results of an ELDOR experiment (Taylor and Farnell, 1964) showed that the hole associated with a given aluminum impurity moves back and forth between the two oxygens linking the aluminum with long bonds. Line width was observed to be broadened with increasing temperature. Schnadt and Räuber (1971) obtained the activation energy for hopping process to be 70±10 meV by observing change of linewidths. The authors also pointed out that this hopping process is responsible for dielectric loss.

Precise angular dependence of ESR spectrum was studied by Nuttal and Weil (1981a) to determine accurate spin Hamiltonian parameters including ^{17}O and ^{29}Si hyperfine matrices. ENDOR studies have been made (Barker, 1975; Bossoli and Halliburton, 1983).

An ESR spectrum of $[AlO_4]^0$, when the magnetic field is parallel to c-axis (B//c) is shown in Fig. 1-4a. The observed spectrum is more complex than the one only with

hyperfine structure by ^{27}Al (I=5/2, 100% abundance) because of nuclear Zeeman and quadruple terms as indicated by numerical simulation (Fig. 1-4b, Nuttall and Weil, 1981a). It was also showed that small aluminum nuclear Zeeman and quadrupole interaction gives a large contribution to the spectrum features. Calculated energy levels and possible transitions are shown in Fig.1-4c. g factors are listed in Table 1-1.

An excited state, $[AlO_4]_{es}$, was observed above 100 K where a hole is trapped at the other pair of oxygens (Schnadt and Schneider, 1970). The energetical separation of the excited state from the ground state was determined to be 30±6 meV.

The normal state with Al replacing Si is $[AlO_4/M^+]^0$, which is diamagnetic, where M^+ is and ion for charge compensation. A hole is created on an oxygen ion nearest neighbor to Al at the time of irradiation. The cation M^+ diffuses away at the time of irradiation at room temperature or when the sample was warmed after irradiation at a low temperature (77K) (Hitt and Martin, 1983). Consequently, Aluminum hole center, $[AlO_4]^0$, is formed by ionizing irradiation (see Fig.1-6, Weil, 1984).

Other unstable aluminum associated centers, precursors of $[AlO_4]^0$, have been reported, such as $[AlO_4/M^+]^+$ (Nuttall and Weil, 1981b), and $[AlO_4]^+$ (Nuttall and Weil, 1981c). We only observe the spectrum of $[AlO_4]^0$ in natural quartz samples. A powder spectrum of $[AlO_4]^0$ is shown in Fig.1-5 (Schnadt and Räuber, 1971) and in Fig.1-9 (McMorris, 1971).

(3) Germanium centers

There have been many kind of germanium centers reported (Weil, 1984). Anderson and Weil (1959) first reported germanium centers in quartz. Two distinct types of anisotropic g-tensors were characterized to be designated A and C. The optical absorption bands around 280 nm was attributed to this center because of the correlation between them. The spectrum consisted of four independent anisotropic lines, each characterized by negative g-shifts and hyperfine quartet structure due to alkali ions with their nuclear spin of 3/2 (^7Li or ^{23}Na) (Weil and Anderson, 1961). The last authors presumed that unpaired electron was localized predominantly on a germanium ion replacing a silicon site and that it interacted with a charge compensating interstitial alkali ion. It seems reasonable to postulate that the Li^+ ions in the two centers occur at opposite sides of the tetrahedron, at or near channel sites $a_>$ and $a_<$ (Weil, 1984) shown in Fig.1-7.

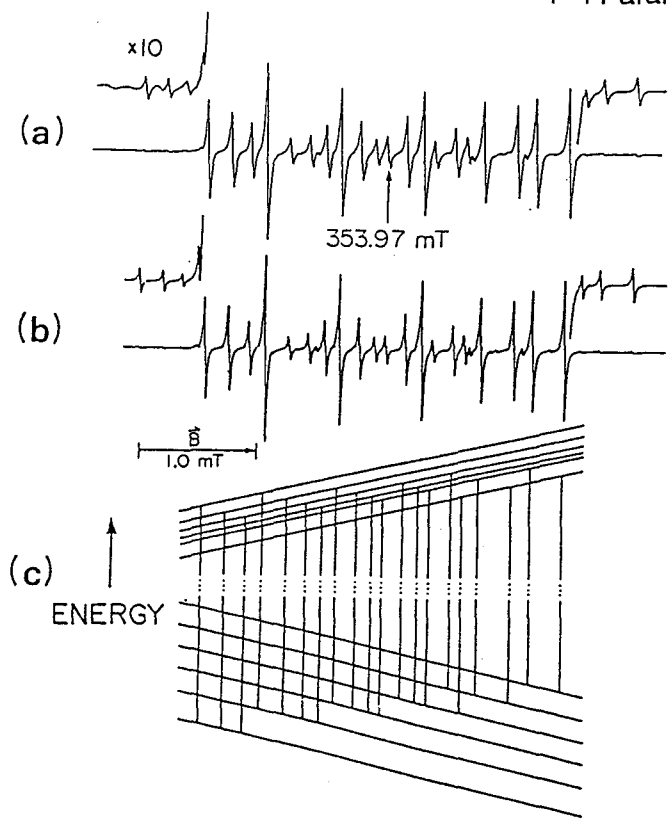

Fig.1-4 ESR spectrum of $[AlO_4]^0$ (after Nuttal and Weil, 1981a) (a) Experimental spectrum (T=35K, B//c), arrow indicates g_c=2.01810 (b) Spectrum calculated using the spin-Hamiltonian parameter matrices obtained. (c) Energy level diagram showing observed transitions between ^{27}Al hyperfine levels.

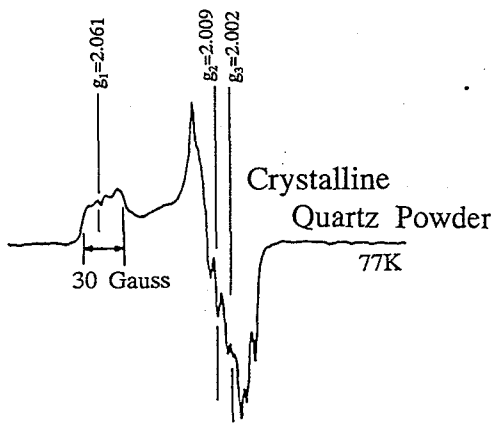

Fig.1-5 The powder ESR spectrum of $[AlO_4]^0$ (after Schnadt and Räuber, 1971).

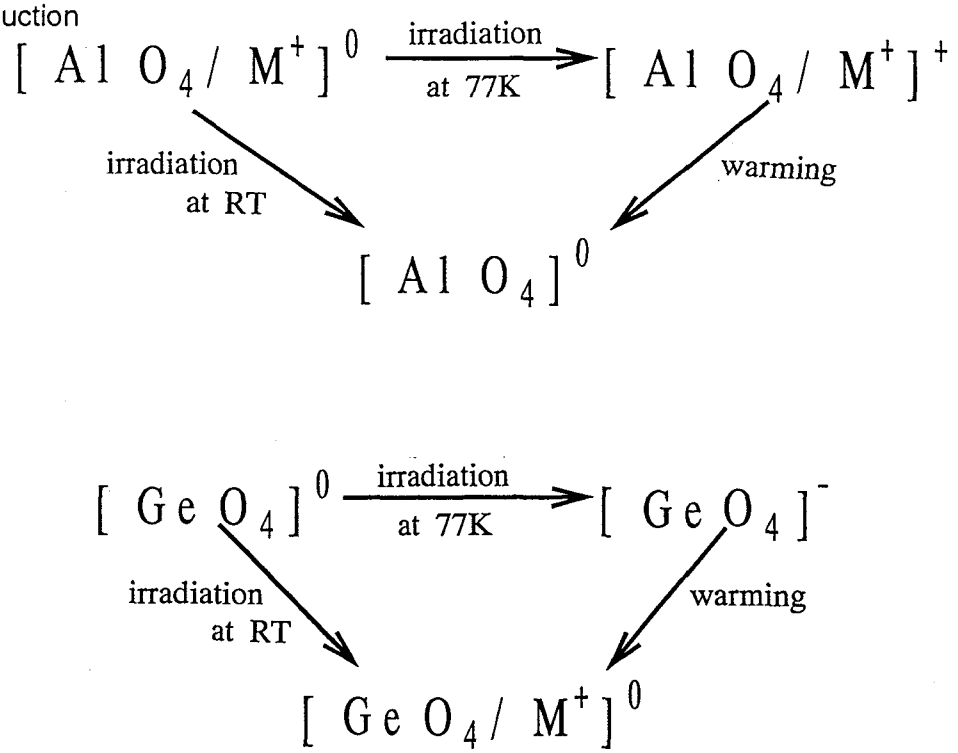

Fig.1-6 Schemes for redox reactions of Al and Ge ions substitutional for silicon in quartz (after Weil, 1984). Before irradiation, AlO_4 is a potential electron donor whereas GeO_4 is a potential electron acceptor.

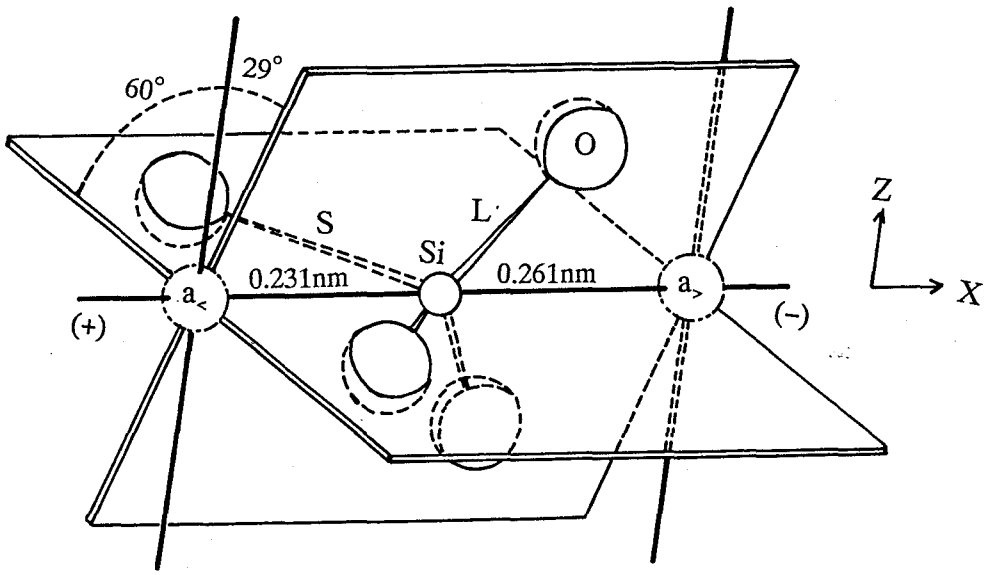

Fig.1-7 SiO_4 tetrahedron in quartz (after Weil, 1984). Symbols $a_>$ and $a_<$ locate possible sites for an interstitial atom/ion in the middle of a large c-axis channel at its intersection with two-fold axis a_1.

Anisotropic g factors for $[GeO_4(A)/Li^+]$, $[GeO_4(C)/Li^+]$, $[GeO_4(A)/Na^+]$, and $[GeO_4(C)/Na^+]$ were obtained by Mackey (1963). The author also observed $[GeO_4]^-$, alias Ge(I), and $[GeO_4]^-_{es}$, alias Ge(II). The formation mechanism for the Ge centers was discussed as the following. The precursor, $[GeO_4]^0$, traps an electron to form $[GeO_4]^-$ at 77K irradiation. An alkali metallic ion, Li^+ or Na^+, comes to this site as a charge compensator on warming to room temperature to form charge compensated germanium centers (see Fig.1-6). When quartz is irradiated at room temperature, the both processes occur to form latter centers. As for $[GeO_4(C)/Na^+]^0$, this center decays gradually at room temperature.

Accurate spin Hamiltonian parameters were obtained by Weil (1971a) at room temperature as shown in Table 1-1. He also reported that the principal axes of g and A(^{73}Ge) matrices coincide. Anderson *et al.* (1974) confirmed the correlation between optical absorption and ESR signal intensity and showed that thermoluminescence of 485 nm is correlated with decay of A and C germanium centers. This luminescence had been observed by McMorris (1971) to be correlated with aluminum hole centers. The decay of germanium centers was reported by UV (Anderson *et al.*, 1959) and sun light irradiation (Tanaka *et al.*, 1985). In natural quartz, a powdered spectrum was obtained by McMorris (1971) as shown in Fig.1-8.

Other Ge related centers unstable at room temperature have been reported, for example, $[GeO_4/H^-Li^+_2]^0$ (Weil, 1971b).

(4) Titanium centers

Substitutional titanium atoms trap unpaired electron and also trap alkali cation as a charge compensator to form titanium centers as in the case of germanium centers. There are two types of centers (1 and 2, or B and A), as for Ge centers. Wright *et al.* (1963) first reported, in a rose quartz, titanium centers with Li^+ and/or Na^+ and H^+, i. e., $[TiO_4/M^+]^0_2$ and $[TiO_4/H^+]^0_2$ (A-Ti-H), which are stable at room temperature.

Spin Hamiltonian parameters of $[TiO_4/Li^+]^0_1$ (B-Ti-Li) and $[TiO_4/Li^+]^0_2$ (A-Ti-M) and of $[TiO_4/H^+]^0_1$ (B-Ti-H) and $[TiO_4/H^+]^0_2$ (A-Ti-H) were investigated by Rinneberg and Weil (1972). Titanium center with Na^+, $[TiO_4/Na^+]^0_2$ (A-Ti-Na), was found by Okada *et al.* (1971) in α quartz replacing Li^+ with Na^+ by using a diffusion technique.

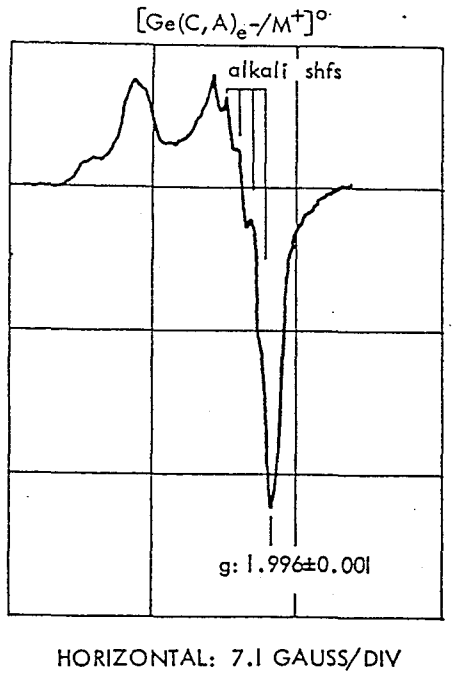

Fig.1–8 A powder ESR spectrum of Ge center (composite of $[GeO_4(A)/M^+]^0$ and $[GeO_4(C)/M^+]^0$) observed in γ ray irradiated natural rose quartz (McMorris, 1971).

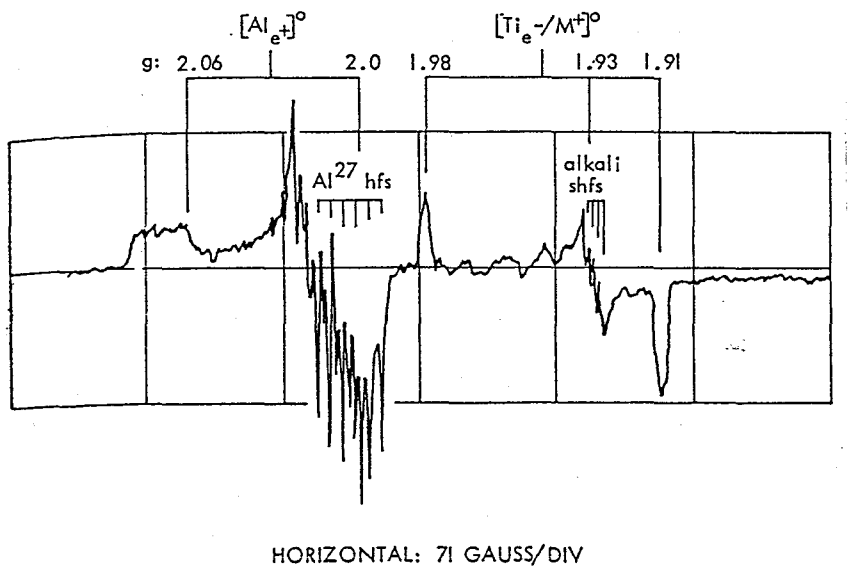

Fig.1–9 A powder ESR spectrum of Al center ($[AlO_4]^0$) and Ti center ($[TiO_4/M^+]^0$) observed in γ ray irradiated natural rose quartz (McMorris, 1971).

Okada *et al.* (1971) also reported that $[TiO_4/Li^+]^0_1$ (B-Ti-Li) and $[TiO_4/H^+]^0_1$ (B-Ti-H) decayed rapidly at room temperature. Principal g values and directions of Ti associated centers are summarized in Table 1-1.

The formation mechanism is the same as for Ge centers as described by Weil (1984). The precursor state $[TiO_4]^0$ traps an electron to form $[TiO_4^-]$ below 20 K (Isoya and Weil, 1979). Diffusion of ions, M^+ convert the center to a charge compensated state $[TiO_4/M^+]^0$ on warming.

ENDOR, pulse ESR, and ESEEM techniques have recently been applied for further characterization of these centers (e. g. Isoya *et al.* 1983a) to determine quadrupole matrix Q_{7Li} and hyperfine matrix A_{6Li} and also more accurate spin Hamiltonian parameters. A powder spectrum of titanium centers is shown in Fig.1-9 (McMorris, 1971).

(5) Oxygen hole related and Peroxy centers

Stapelbroek *et al.* (1979) identified two distinct oxygen-associated trapped-hole centers in samples of room-temperature γ irradiated, high-purity fused silica. One is denoted by 'wet' OHC, a hole trapped in a single non-bonding 2p orbital of oxygen. It is effectively formed in silica with high OH content. Its anisotropic g factors are 2.0010, 2.0095, and 2.078 (weighed average). They presumed that one hydrogen of paired OH in silica is removed by irradiation and that a hole is trapped at the remaining oxygen (see Fig.1-10).

The other is denoted by 'dry' OHC. Its intensity is much lager than that of 'wet' OHC in silica with low OH content. Its anisotropic g factors are 2.0014, 2.0074, and 2.067 (weighed average). The authors' tentative model for this center, which is O^{2-} radical replacing a bridging oxygen was confirmed by their subsequent study (Friebele *et al.* 1979). In ancient flint, Garrison *et al.* (1981) observed an ESR signal, with roughly the same g factors with this center. The signal is similar to the one observed in crystalline quartz irradiated by fast neutrons. They assigned this signal to peroxy center and tried ESR dating.

On the other hand, a set of ESR lines occurring in six symmetry related sites were observed in natural quartz in the temperature range of 10-30K (Baker and Robinson, 1983). They stated the spectrum is probably due to O_2^-, an electron at a peroxy linkage.

Table 1–1 Selected data for principal g factors and directions reported for paramagnetic defects in quartz.

Center	g values	θ (°)	ϕ (°)	Reference
E_1'	2.00179	114.5	227.7	
	2.00053	134.5	344.4	Jani *et al.* (1983)
	2.00030	125.4	118.7	
$[AlO_4]^0$	2.060208	119.25	57.62	Nuttal and Weil
	2.008535	124.43	305.05	(1981a)
	2.001948	131.65	177.49	
$[GeO_4(A)/Li^+]^0$	1.9913	23.7	90	
	1.99965	90	0	Weil (1971a)
	2.0014	66.3	270	
$[GeO_4(C)/Li^+]^0$	2.0000	26.1	90	
	1.9973	90	0	Weil (1971a)
	1.9962	63.9	270	
$[TiO_4(A)/Li^+]^0$	1.97887	159.4	90	
	1.93094	90	0	Isoya *et al.* (1983)
	1.91193	69.4	90	
$[TiO_4(A)/H^+]^0$	1.9856	28.9	255.2	Rinneberg and Weil
	1.9151	62.1	92.3	(1972)
	1.9310	82.8	358.5	
$[TiO_4(A)/Na^+]^0$	1.9675	15.9	270	
	1.9536	90	0	Okada *et al.* (1971)
	1.8994	74.1	90	

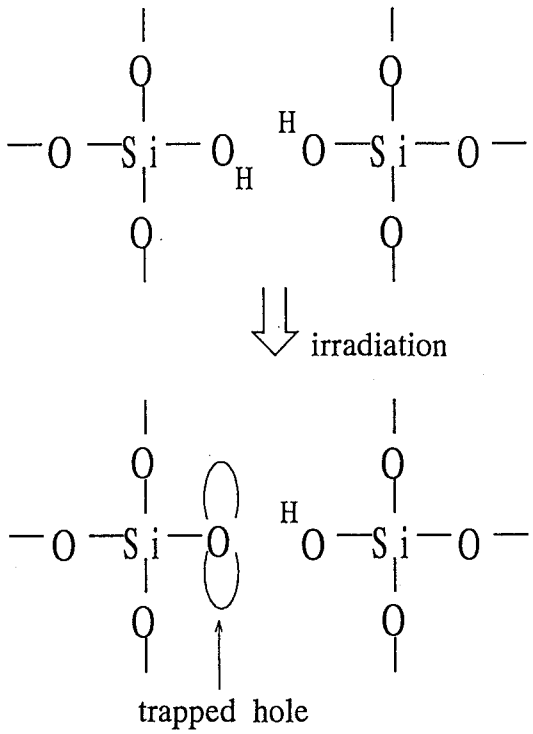

Fig.1-10 Suggested model for the formation of the "wet" OHC (oxygen hole center) (Stapelbroek *et al.* 1979).

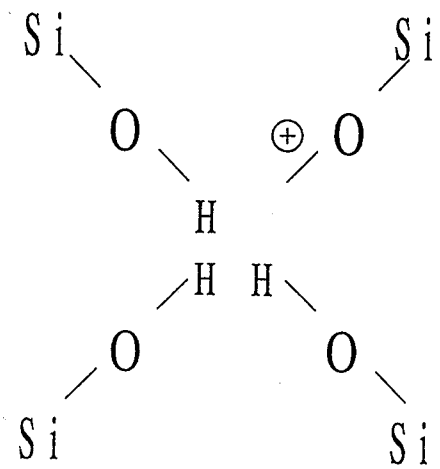

Fig.1-11 A model for hydrogenic hole center with the form of $[O(HO)_3]^0$ (Nuttal and Weil, 1980). The center is formed by trapping a hole in a p-orbital of an oxygen atom associated with one of the four hydrogen atoms replacing a silicon site as $[H_4O_4]$.

(6) Other centers

Many other paramagnetic centers in quartz have been reported but have never been used for ESR dating. It might be worth checking the following centers for their use in ESR dating. Two types of hydrogenic hole centers having the form $[(HO)_4]^+$ and $[O(HO)_3]^0$ were identified by their complex hyperfine structures due to hydrogens (Nuttal and Weil, 1980). The former is formed by trapping a hole in a p–orbital of an oxygen atom associated with one of the four hydrogen atoms replacing a silicon site as $[H_4O_4]$. The precursor state traps a hole at one of oxygen atoms and releases the proton associated with the oxygen atom to form the latter center while the sample is subsequently sitting at room temperature for an order of one year after irradiation.

Atomic hydrogen (Isoya *et al.* 1983b) and atomic copper and silver (Davis and Weil 1978) are paramagnetic states, which are reported to be unstable above 120K and at room temperature, respectively. Phosphorus centers were investigated by Uchida *et al.* (1979). The one kind of them linked with Al ion was discovered in natural quartz (Maschmeyer and Lehmann, 1982). They attributed the rose color to this kind of centers.

Fe centers are not so well characterized. The electronic form of some of them are established, for example, S_1 as $[FeO_4/Li^+]^0$, S_2 as $[FeO_4/H^+]^0$ (Becker and Lehmann, 1980), and I as $[FeO_4]^-$ (Momborquette *et al.*, 1984). The color of amethyst is found to be due to substitutional Fe^{4+} ($3d^4$) replacing Si^{4+} (Cox, 1976).

In summary, some of paramagnetic defects in quartz have been well characterized, but others have not yet. The spin Hamiltonian parameters of the former have been de–fined exactly. However, there would be further investigation needed to realize the forma–tion and decay kinetics of the centers because little are known about them. For example, the fate of electrons released on irradiation from the eventual donors in the absence of substitutional acceptor ions continues to constitute an important mystery (Weil, 1984).

1-5 Application to ESR dating

(1) Fault movement

Ikeya *et al.* (1982) first used quartz for ESR dating of a fault, where quartz grains were extracted from fault gouge, based on the assumption that fault movements bleaches ESR signal of E' centers by grinding. The concentrations of E' centers* (Miki and Ikeya, 1982) and of E' and Ge** centers (Ariyama, 1985) were shown to be reduced by frictional grinding. The defect formation yield was enhanced in quartz grains close to the fault plane at Rokko fault near Osaka (Ikeya *et al.*, 1983).

The aim of subsequent papers on ESR dating of fault movements has been to determine the geological condition that completely resets E' centers and other impurity centers (Fukuchi, 1988, 1989; Tanaka, 1989). Buhay *et al.* (1988) proposed a criteria that if total accumulated dose for some grain size fractions are same, it would indicate complete reset of centers for the specific sample.

Fukuchi (1989) attributed the source of mechanical bleaching or mechanical annealing to local frictional heat rather than to the grinding or dislocation movement. He studied thermal stabilities of Ge, Al***, and oxygen hole centers, and reported that the signal intensities do not decrease following a simple exponential decay, but did not discuss their kinetics.

*The paramagnetic center related to an oxygen vacancy has been described as "E' center" in the reports in the field of ESR dating. The "E' center" observed in natural quartz denote the E_1' center, confirmed by its anisotropic g factors described in Section 2-1.

**It is not clear which germanium associated center the author used.

***Al center denotes the center with a form $[AlO_4]^0$.

(2) Volcanic ashes and rocks

ESR dating of volcanic rocks was first tried using ESR signals of Ge center at

g=1.997 and unidentified signal at g=2.011 in quartz from a welded tuff sampled at north-east Japan for additive dose method (Shimokawa *et al.*, 1984). Fukuchi (1986) assigned the latter signal at g=2.011 as that of oxygen hole center (OHC), but Ikeya *et al.* (1990) pointed out that the signals at g=1.997 and at g=2.011 are the two of four hyper-fine lines of methyl radicals.

Al center was used in the subsequent study, for ESR dating of a tuff (Imai *et al.*, 1985) from the same sequence as Shimokawa *et al.* (1984). The obtained age was consistent with that by fission-track dating method. Quaternary tephras at Mt. Osorezan, western Japan, (Shimokawa and Imai, 1985; Imai and Shimokawa, 1988) and Quaternary volcanic rocks at central Japan (Shimokawa *et al.*, 1988) were also dated by ESR using Al and Ti* centers quartz.

Thermal reset of paramagnetic defects in quartz from sediment baked by lava flow was assumed to date volcanic eruption ages (Yokoyama *et al.*, 1985) where the ages obtained for Al and Ti centers were consistent with each other.

The ages obtained by using these centers with different thermal stability should be the same if the sample had cooled rapidly, while different ages may be obtained when the sample had cooled slowly. It was presumed that both eruption and alteration ages could be obtained by ESR dating of one sample utilizing different centers in quartz of different thermal stabilities (Shimokawa and Imai, 1987). Ages obtained for "Ge center" and "OHC" signals were consistent with fission-track age while the age for Al center with TL (thermoluminescence) age. The result of annealing experiment supported the idea: i.e., Al centers decayed at lower temperature than "Ge center" and "OHC" did.

Recently, Odom and Rink (1989) reported that the intensity of E' centers and of peroxy centers in granitic quartz are correlated with the age in the time range of 0.1-1400 Ma. They suggested that these centers in granitic quartz may be used as geochronometer of the above age range, far beyond the limitation so far considered. Recoiled nuclides by α decays were proposed to be the possible cause of defect formation. Their subsequent paper (Rink and Odom, 1991) investigated the α emitters in quartz and tried to evaluate the α-recoil effect.

*Ti center denotes the center with a form $[TiO_4/Li^+]^0$ as confirmed in Chapter 2.

(3) Flint

A few efforts have been devoted to ESR dating of flint to obtain the age of specific human activities because flint was used after heating to make tools by ancient people in such cases. ESR signals of impurity centers have never been used for dating of flint of archaeological sites. Garrison *et al.* (1981) first tried ESR dating of flint. The authors observed the signals of E' centers and 'dry' OHC in flint and reported that the signals were not increased by artificial γ ray irradiation but by fast neutron irradiation. Griffith *et al.* (1983) discussed what signal is appropriate for ESR dating of heated chert. The authors reported two components of E' centers. Recently, Porat and Schwartz (1991) reported that the characteristics of "E' center" in flint satisfy the criteria for the use of the signal for ESR dating. However, they did not show any ground for the signal assignment of E' center. Garrison (1989) discussed the characterization of E' centers and of 'OHC' in flints, but he did not propose the method for practical dating.

Some workers tried to use ESR signals for the identification of heat treatment of flint. It is possible to discuss the firing technology of ancient human beings from the temperature of heat treatment for flint. Organic radicals have been discussed for the candidate for identification of heat treatment, such as carbon radical (Robins *et al.*, 1978) and methyl radicals (Griffith *et al.*, 1982). The ESR intensities of these radicals were reported to be enhanced on heating. Wieser *et al.* (1986) showed that temperature estimation may be possible using organic radicals. Recently, perinaphthenyl radicals were observed in flints (Chandra *et al.*, 1988).

1-6 Problems in ESR dating using quartz: Scope of the present thesis

Studies on ESR dating using quartz are not so popular as that using carbonate. Scientists working on ESR dating should obtain accurate ages so that ESR dating using quartz is widely accepted. In addition, the ESR signals whose sources and formation mechanisms are well characterized should be used. The thermal stability should be checked to show that the signals are stable in the age range of samples and to show what event (thermal and/or mechanical) defines the ESR age.

Quartz is the only promising mineral to elucidate thermal history of tectonic activities, especially in a low temperature range. ESR can detect the activity sensitively. Paramagnetic defects are annealed at lower temperatures than the one, at which the clocks of other dating methods are reset. If the thermal stabilities of the centers are defined quantitatively, the thermal history of tectonic activity would be discussed quantitatively by using ESR dating technique.

The sources of ESR signals of E', Al and Ti centers are well characterized but formation mechanism of E' centers has not been well established. Sources of some other signals have not been established. Quantitative studies on thermal stabilities are scarce. Lifetimes for Al center obtained to be 1.8–3.8 Ma (Imai *et al.*, 1985) and to be 2.4 Ma (Shimokawa *et al.*, 1987) assuming first order decay kinetics are the only quantitative value for the ESR signals in quartz. There are several studies achieving stepwise heating experiment (e.g. Yokoyama *et al.*, 1985), but parameters for thermal stability were not obtained. Shimokawa and Imai (1987) presumed that eruption and alteration ages were obtained by using ESR signals of different thermal stability. However, they did not describe degree of thermal event at the time of "alteration".

In this thesis, thermal stabilities of Al and Ti center are studied in detail. The formation and decay kinetics of E' centers are investigated in relation with its precursor state, oxygen vacancies with two electrons in Chapter 2. The knowledge about formation and decay kinetics leads some new applications to geochronology and Archaeology in Chapter 3. The degree of thermal events that reset Al , Ti, and E' centers will be discussed. A new technique to know ancient heating is developed using the relation between E' center and oxygen vacancy. The possibility for ESR dating of Ma–Ga range using oxygen vacancy is also studied.

2. Decay and production characteristics of paramagnetic defects in crystalline quartz

2–1 Thermal decay of E'_1, Al, and Ti centers

Although many of paramagnetic defects have been studied to define their models and electronic structures, little of their formation and decay kinetics have been studied as described in Chapter 1. It is, however, important to define decay kinetics and to study thermal stabilities of the defects especially for investigating thermal history and assessment of geothermal area with ESR dating technique. Ikeya (1983) first discussed thermal stability of paramagnetic defects in relation with ESR dating technique, but only first order decay kinetics was considered. Shimokawa and Imai (1987) gave a half life of about 2.4 Ma at room temperature for Al centers in quartz taken from a volcanic ash. Fukuchi (1989) studied thermal stabilities of Ge, Al, and oxygen hole centers, and reported that the signal intensities do not decrease following a simple exponential decay, but he did not discuss their kinetics.

In this chapter, thermal stabilities of E'_1 centers, Al hole centers, and Ti centers were studied for quartz in granite by isochronal and isothermal annealing experiments. The activation energies of the defects were obtained. The decay kinetics of these defects in the granite is discussed.

(1) Experiment

Quartz grains were separated from the Mannari Granite in Okayama Prefecture, Japan. About 200g of the granite was gently crushed and sieved. The grains were washed in 6N HCl for 1 day then rinsed by water. After dried, magnetic minerals were removed using a portable magnetic separator. Other minerals whose densities are smaller than quartz grains were removed by using sodium polytungstate solution. Finally, separated quartz grains were etched by a 20% HF solution for 2 hours to remove remaining plagio–

clase. The obtained quartz was 100% purity as confirmed by an X-ray diffraction study. However, reliable concentration of trace elements in quartz were not obtained because of small amount of amorphous matter, which is probably plagioclase degenerated by the HF solution.

ESR spectra were obtained with a commercial ESR spectrometer (JEOL RE-1X), where the field modulation width was 0.1 mT with frequency of 100 kHz. The signals of E', Al, and Ti centers were observed as shown in Fig.2-1a-d. The intensity of E' centers was measured with microwave power of 10^{-2} mW at room temperature and the peak to peak height at g=2.001 was taken as its intensity.

The signals of Al centers were observed with microwave power of 5mW at liquid nitrogen temperature. The average peak to peak height at g=2.018 of six measurements by rotating the sample in the cavity was taken as its intensity. Imai and Shimokawa (1988) measured the intensity of Al centers with modulation width of 0.5mT to avoid variation of intensities. However, in the present experiments, other ESR signals such as peroxy centers overlapped to Al centers. Their intensities were comparable to that of Al centers when the sample was heated and the intensity of Al centers became weak. Therefore, the peak to peak height at g=2.018 was taken as the intensity although the height varied (up to 13%) with rotating the sample in the cavity. The average value was reproducible within 4% variation.

The intensity of Ti centers was measured in the same condition as that for Al centers. The average of the base to peak height at g=1.91 was taken. The variation of the heights was within 8%, and that of average value was within 3%.

One of the aliquots was isochronally heated to determine the temperatures of isothermal annealing experiment and to study the correlation between the defects. A series of aliquots was isothermally heated at temperatures of 150-420°C for 0 to 480 minutes. The signal intensities of E', Al, and Ti centers were measured at each time step at several temperatures.

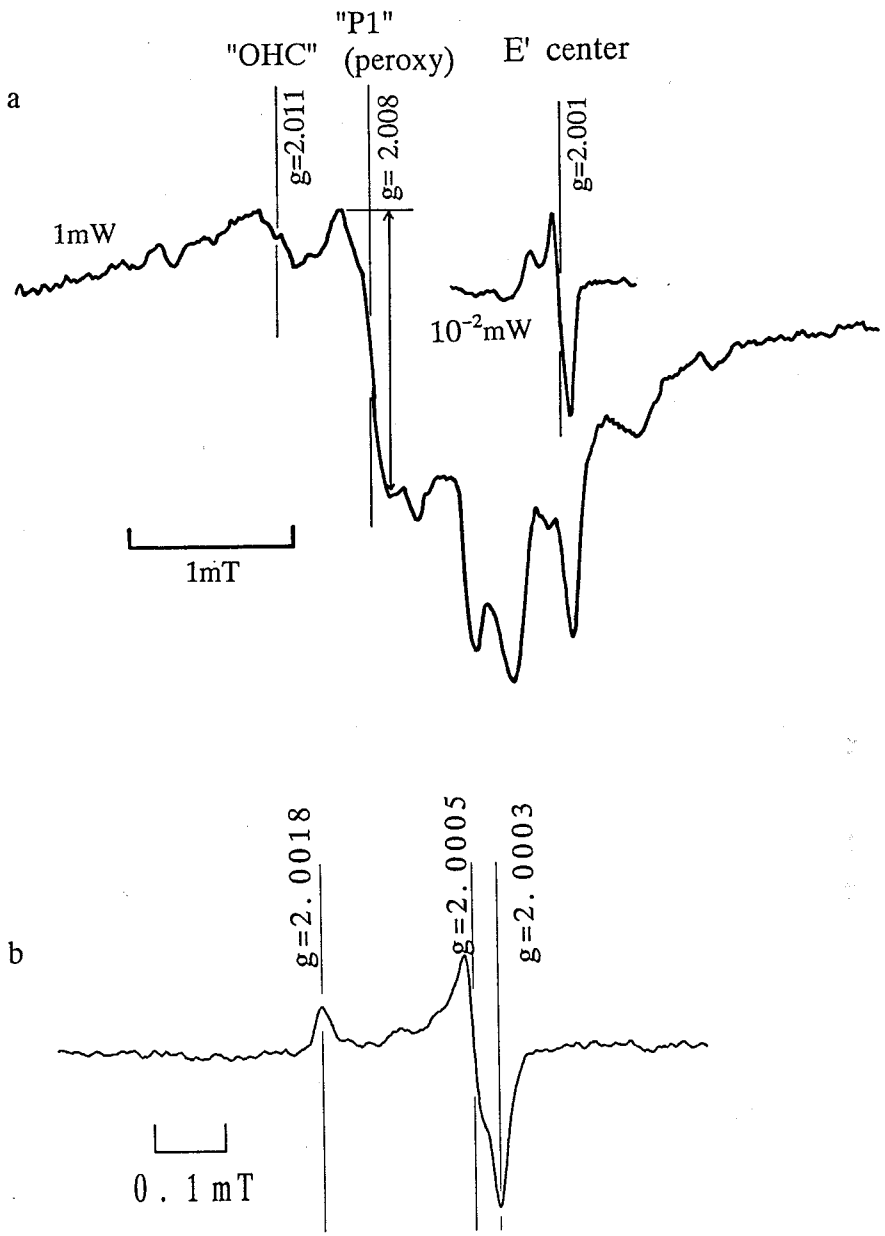

Fig.2-1 a) ESR signals observed at room temperature in quartz from Mannari granite. The signal of E' center is observed at g=2.001 with the microwave power of 0.01 mW. b) Expanded spectrum around g=2.001. The g factors obtained are consistent with those by Jani *et al.* (1983).

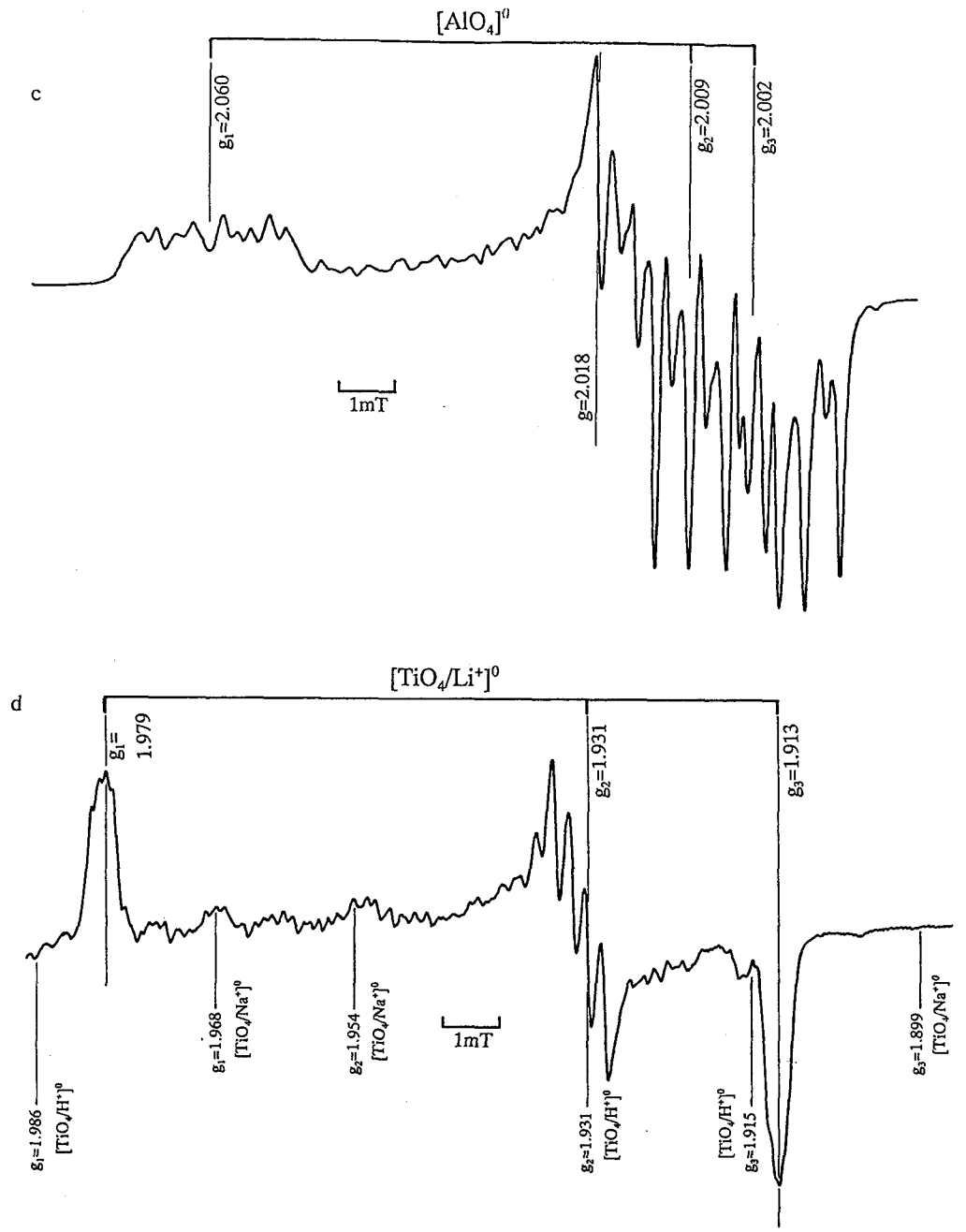

Fig.2-1 c) A powder spectrum of Al center observed at liquid nitrogen temperature with a microwave power of 5mW. d) A powder spectrum of Ti center, $[TiO_4/Li^+]^0$, observed at liquid nitrogen temperature.

(2) ESR signal assignments

Fig.2-1a shows an ESR spectrum observed at room temperature. The signals at g=2.011 and at g=2.008 were assigned to oxygen hole centers and P1 (a part of peroxy radical), respectively, by Fukuchi (1986). However, these assignments have not been established. An ESR signal at g=2.001 was assigned to be that of E' centers by Ikeya *et al.* (1982). The expanded spectrum around g=2.001 is shown in Fig.2-1b. The principal g values from this powder spectrum are consistent with those of E_1' centers obtained by Jani *et al.* (1983) (see Table 1-1).

Fig.2-1c shows a powder spectrum of Al center, $[AlO_4]^0$. The signals were the same as those observed by McMorris (1971) (see Fig.1-9). The principal g values are also shown. A powder spectrum of Ti center is shown in Fig.2-1d. The signals are also the same as those observed by McMorris (1971) (see Fig.1-9), who assigned them to $[TiO_4/M^+]$. Comparing the g values of Ti associated center in quartz (Table 1-1), the signals were assigned to those of $[TiO_4/Li^+]^0$. Observed g_3 of 1.913 is slightly different from that obtained by Okada *et al.* (1971).

(3) Results

The results of isochronal annealing experiment are shown in Fig.2-2. Spin number was calibrated by comparing the area obtained by integration of absorption line with that of DPPH where mass of DPPH was converted to spin number. The ESR intensity of Al and Ti centers began to decrease at 220°C and 170°C, and were almost completely annealed at 380°C and 260°C, respectively. The decay curve of Al centers showed a small shoulder around 260°C. The intensity of E' centers increased between 170°C and 280°C, then decreased above 300°C and was annealed out at 440°C. This behavior of E' centers is consistent with previous studies (Jani *et al.*, 1983; Miki and Ikeya, 1981). It was explained by the process that holes at Al center are released and trapped at oxygen vacancies with two electrons to form E' centers (Jani *et al.*, 1983). Correlation between increment of E' centers and decrement of Al centers was shown in their report.

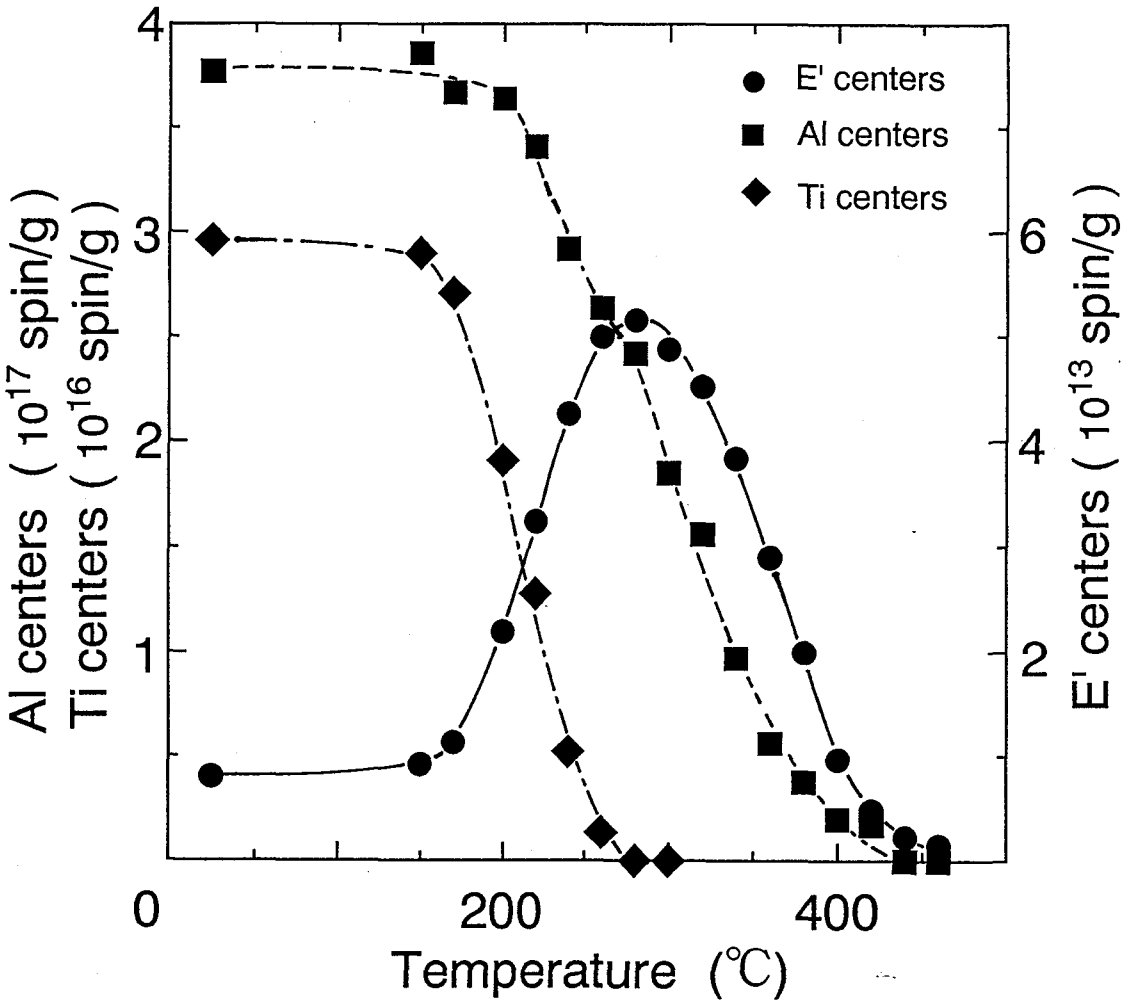

Fig.2–2 The results of an isochronal annealing experiments. The ESR intensities of Al and Ti centers decrease at 220°C and at 170°C, respectively, while that of E' centers increases between 170°C and 280°C, and then decreases above 300°C. The heating duration is 15 minutes for each temperature step.

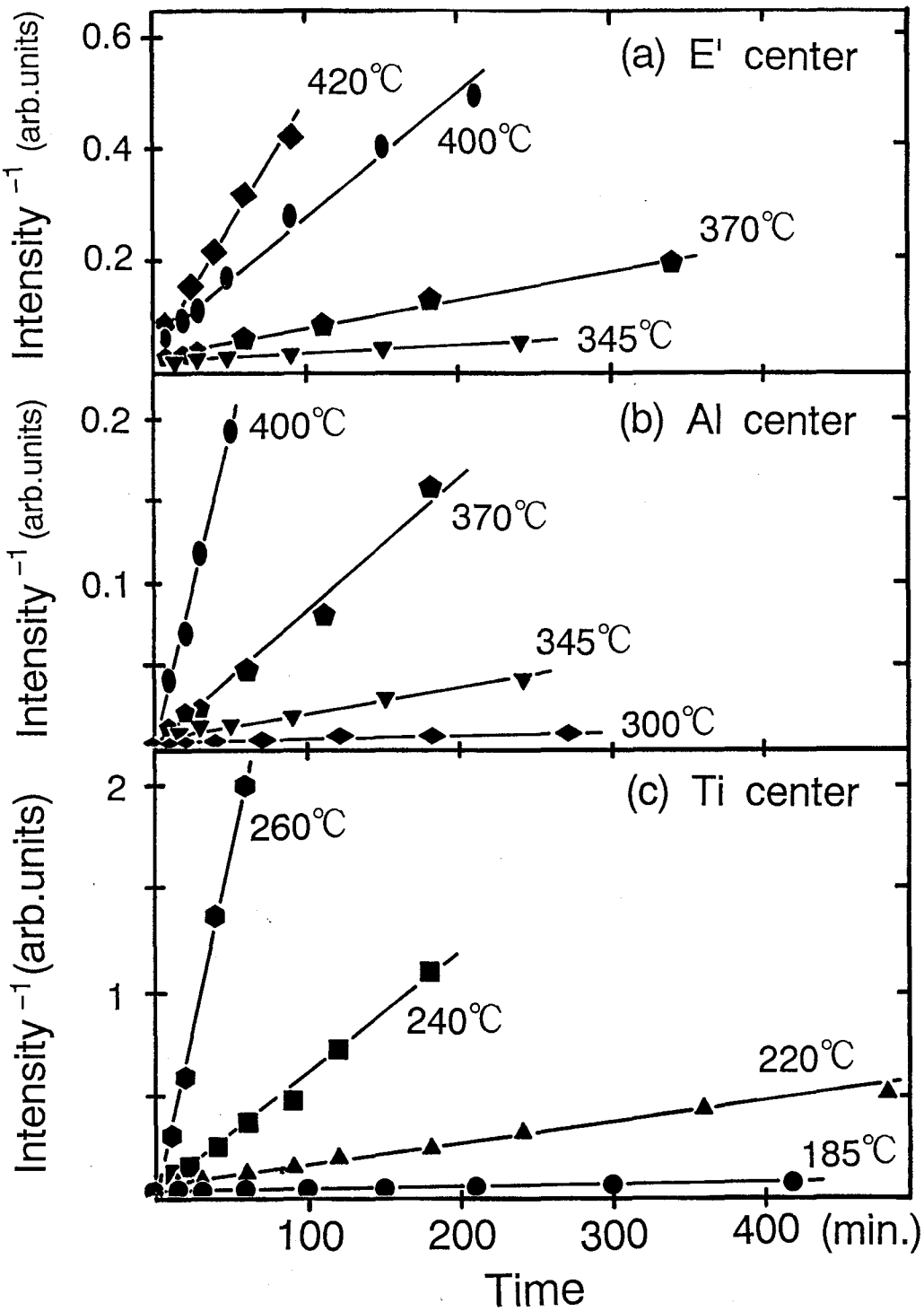

Fig.2-3 The results of isothermal annealing experiments. The reciprocals of signal intensities are plotted against time. The data points of E', Al, and Ti centers lie on a straight line indicating their second order decay kinetics.

The results of isothermal annealing experiment indicate that the intensities of E' centers do not follow an exponential decay curve on heating above 300°C, but a straight line when their reciprocals are plotted as a function of time as shown in Fig.2–3a. This behavior is explained by a second order decay as will be described in the following section. The reciprocals of intensities of Al and Ti centers also followed straight lines as shown in Fig.2–3b and 3c, respectively.

(4) Discussion

a. Decay kinetics

If a center decays with a stochastic process, the decrement of centers per unit time during heating should be proportional to the quantity of the centers, and their decreasing should follow a first order reaction, i.e.,

$$\frac{dN}{dt} = -\lambda N \qquad (2\text{–}1)$$

where N is the number of centers, t is heating time, and λ is decay constant. By integrating equation (2–1), the equation,

$$N = N_0 \exp[-\lambda t], \qquad (2\text{–}2)$$

where N_0 is the number of centers at t=0, is obtained.

If a center recombines with a complementary center, for example, an electron center for an hole center, and if its number is the same as that of the other center, the decrement of the center is proportional to the square of the number. The decay kinetics is then explained by a second order reaction with the following equation,

$$\frac{dN}{dt} = -\lambda N^2, \qquad (2\text{–}3)$$

where the notation is the same as equation (2–1). By integrating equation (3), the equation,

$$N = \frac{1}{\lambda t + \frac{1}{N_0}} \qquad (2-4)$$

is obtained. Equation (2–4) is equivalent to the following expression,

$$\frac{1}{N} = \lambda t + \frac{1}{N_0} \ . \qquad (2-5)$$

The reciprocal of the intensity should be linear against heating time in the case of second order reaction.

The reciprocals of signal intensities of E', Al, and Ti centers are on straight lines as a function of heating time as shown in Fig.2–3. Therefore, the reactions during annealing of E', Al, and Ti centers follow second order decay kinetics. The order of thermoluminescence kinetics has been discussed (e.g. Levy, 1984); the shape of some glow peaks are explained by second order reactions, but only first order decay kinetics has been considered in ESR dating (Ikeya, 1983; Shimokawa and Imai, 1987). One type of paramagnetic centers in quartz may recombine with complementary defects of about the same number. The possible recombination process is discussed in Section 2–4.

b. Arrhenius diagrams

Logarithms of decay factors of E', Al, and Ti centers are plotted as a function of reciprocal of absolute temperature of heating in Fig.2–4. Calculated activation energies are shown in Table 2–1. The points at lower temperatures for E' and for Al centers fall a little apart from the line because accurate decay factors are not obtained for the temperature where decrements of intensities are relatively small.

The obtained values of paramagnetic centers are similar to each other, and it may suggest some common process for their decay kinetics.

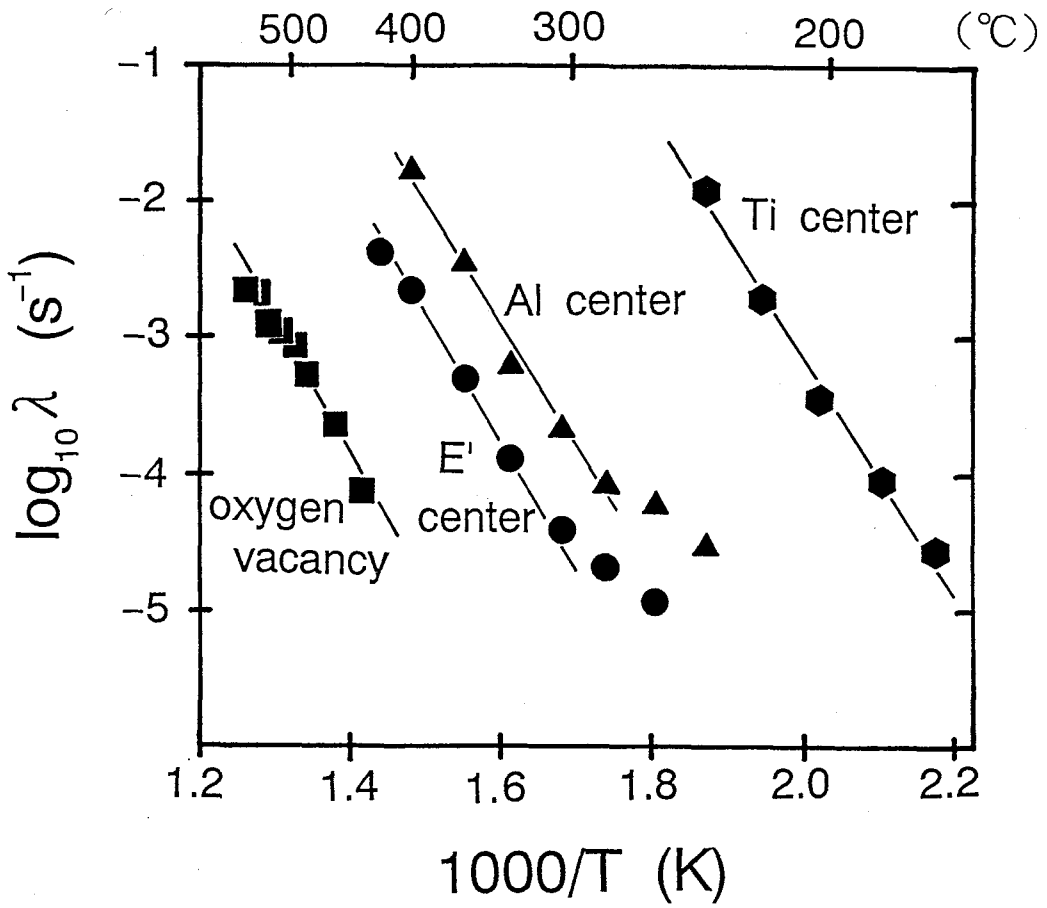

Fig.2-4 Arrhenius plots of decay factors of E', Al, and Ti centers and of oxygen vacancies. Obtained activation energies and pre-exponential factors are shown in Table 2-1.

Table 2-1 Activation energies and pre-exponential factors of decay coefficients for centers and oxygen vacancy

	Activation energy (eV)	Pre-exponential factor ($spin^{-1}$ g s^{-1})	Characteristic time** (yrs)
E'	1.8±0.1	4.7×10^{-5}	3.6×10^{11}
Al	1.7±0.2	1.2×10^{-7}	7.4×10^{9}
Ti	1.7±0.1	7.4×10^{-3}	8.0×10^{6}
Oxygen vacancy	1.9±0.1	9.6×10^{-6}	1.9×10^{15}

** defined by equation (3-3)

2-2 Measurement of oxygen vacancy amount

(1) Experiment

Nine aliquots of the second series quartz samples were heated at 430°C, and then irradiated at the dose ranged from 0 to 300 Gy. The intensities of E' centers were measured after the subsequent heating at 300°C for 15 minutes. The second ESR measurements were made after reirradiation and subsequent heating.

Another aliquot was heated at 400°C for 15 minutes to anneal Al centers out, followed by γ ray irradiation at 100 Gy. After the treatments, the sample were heated isochronally with an untreated aliquot, which was irradiated enough by natural radiation, to investigate the change in ESR intensities.

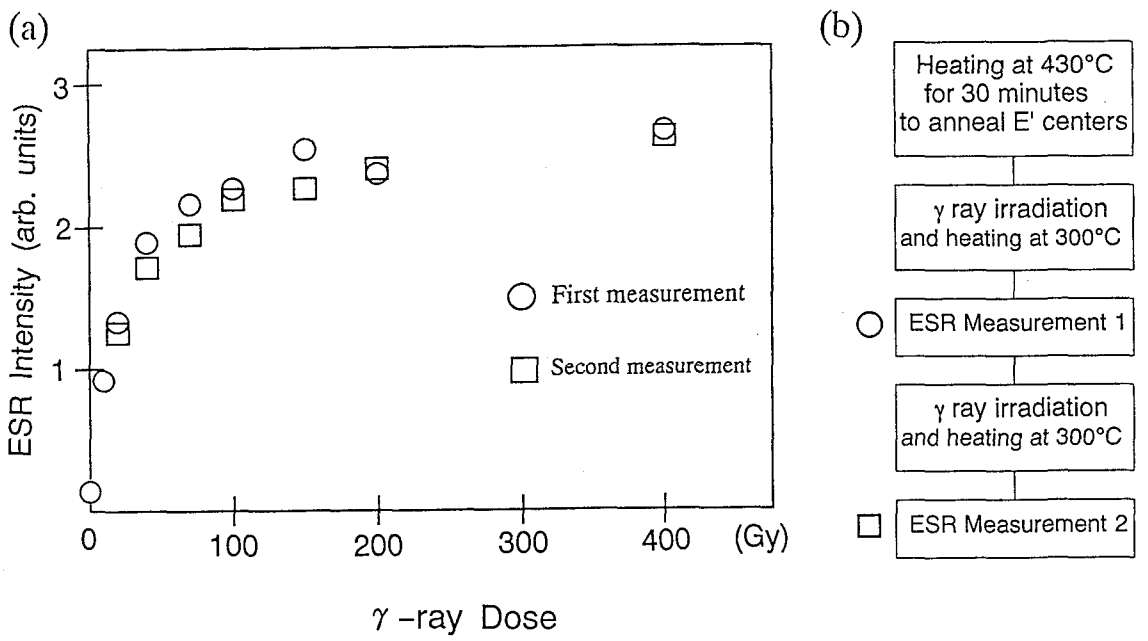

Fig.2-5 a) The intensity of E' centers increases with increasing γ ray doses where the intensity was measured after γ ray irradiation followed by heating at 300°C. After γ ray re-irradiation and heating, the intensities of E' centers, as the sum of two doses, lie on the same curve. The intensity of E' centers records γ ray dose as long as the quartz samples are not heated above 300°C. The saturation value corresponds to the amount of oxygen vacancies. b) The procedures for this experiment are summarized.

(2) Results and Discussion

E' centers were almost annealed out after heating at 430°C for 15 minutes. It appeared once again after γ ray irradiation and subsequent heating at 300°C for 15 minutes. Holes at Al centers are released on heating to be trapped at neutral oxygen vacancies with two electrons to form E' centers (Jani *et al.* 1983). The intensities of E' centers increased with increasing γ ray doses as shown in Fig.2-5. The result can be explained that the amount of holes would increase with increasing γ ray dose, hence, the intensity of E' centers may also increase after heating.

After the second γ ray irradiation and heating, the intensities of E' centers lie on the same curve as that of the first procedure, varying as a function of the sum of two doses. Accumulated dose can be measured as the intensity of E' centers as long as the heating temperature does not exceed 300°C and irradiation does not exceed 200 Gy (Fig.2-5). The E' intensity in the present sample was saturated with γ ray irradiation above 200 Gy because all oxygen vacancy sites had been changed into E' centers around this dose.

The above idea is supported by the following experimental results and discussions. Firstly, the intensity of Al centers still increases with dose range of 800 Gy to 5 kGy irradiation non-heated quartz. If the saturation behavior was due to the limitation of the amount of Al center, the intensity of Al centers would be saturated above 200 Gy. Secondly, Al centers still exist above 300°C. It indicates that Al centers remain after all neutral oxygen vacancies with two electrons are converted to E' centers.

Thirdly, if the saturation behavior is due to saturation of Al centers, E' intensity would be large relative to the first intensities in Fig.2-5 after second irradiation and heating because holes would be created by irradiation and be transferred to remaining neutral oxygen vacancies by heating.

The fourth ground for the idea is the experimental result obtained by stepwise heating experiments for the second series of samples. The changes in intensities of Al centers are shown in Fig.2-6 where Al centers decayed at a lower temperature in the aliquot irradiated at small amounts than those in untreated sample. About 50% of Al centers remained after heating at 300°C for untreated sample, while 8% of Al centers did for the sample irradiated at 100 Gy. The result is interpreted as holes in Al centers reproduced by γ ray irradiation at a light dose were all transferred to oxygen vacancies because the amount of Al centers is smaller than that of oxygen vacancies.

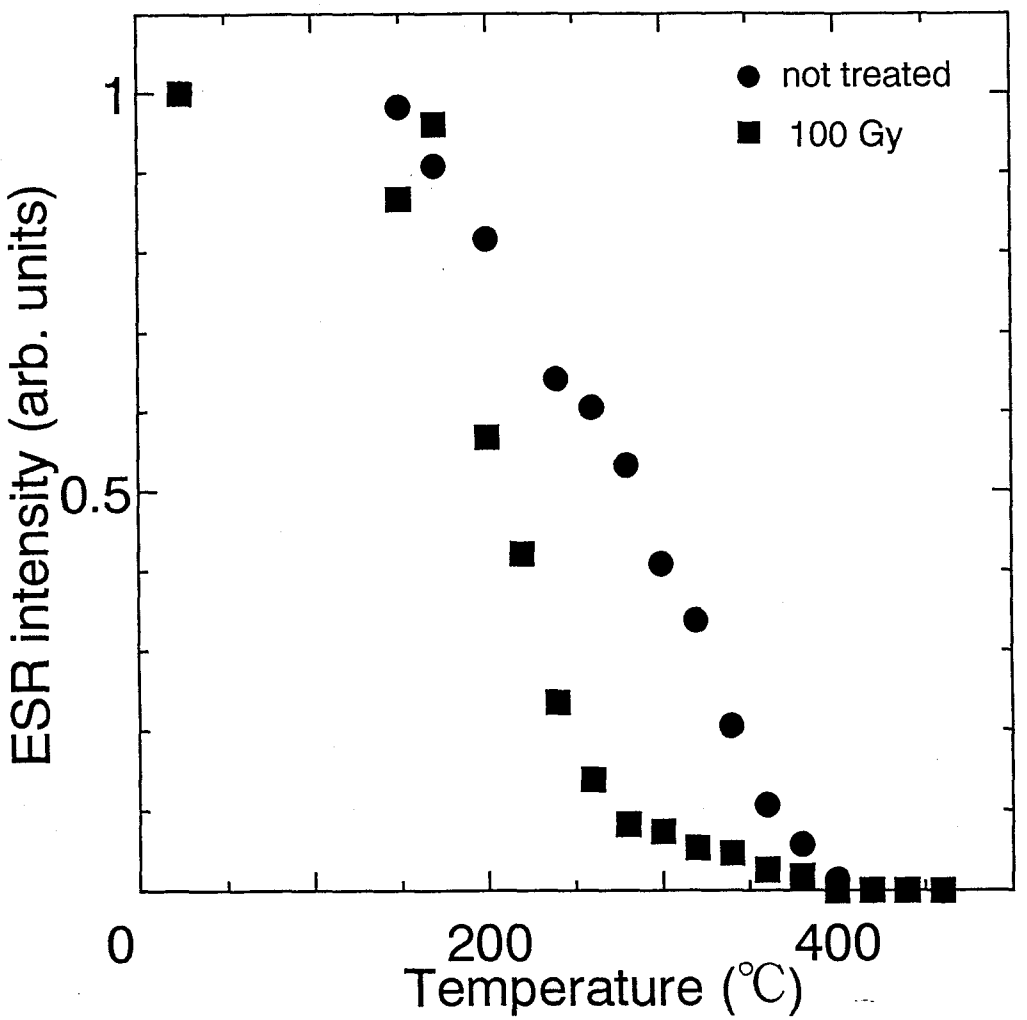

Fig.2-6 The result of an isochronal annealing experiment for the sample irradiated at 100 Gy after heating at 400°C for 15 minutes with that for untreated sample. The centers in the former sample decayed at lower temperatures than those in the latter sample did.

It can be concluded that the saturation behavior is caused by limitation of oxygen vacancy number but not by Al center number. Therefore, the number of oxygen vacancies can be measured as E' intensity after sufficient γ ray irradiation (more than 200Gy) and subsequent heating at 300°C for 15 minutes.

Recent observation on the enhancement of E' centers in quartz by heavy irradiation of 100–1000 kGy (Wieser and Regulla, 1989) is not simply taken into account as the dose of their experiments are orders of magnitude higher than the present experiment. This formation process will be investigated in Section 2-5.

2-3 Thermal stability of oxygen vacancy

(1) Experiment

Eight aliquots of quartz grains were heated at 400–500°C to investigate the thermal stability of oxygen vacancies. Another series of aliquots were heated at 450°C for 0 to 150 minutes to investigate the decay kinetics of oxygen vacancies. The samples were heated at 300°C for 15 minutes following the γ ray irradiation so that the amount of oxygen vacancies was measured as the intensity of E' centers.

(2) Results and Discussion

The amount of oxygen vacancies decreased as increasing the heating temperature as shown in Fig.2-7. The result of second experiment is shown in Fig.2-8, where reciprocal amount of oxygen vacancies are on a line as a function of heating time. The latter result indicates the second order decay kinetics also for the decay of oxygen vacancies. Therefore, the decay factors of oxygen vacancies were calculated assuming a second order reaction. Logarithms of the factors were plotted as a function of reciprocal absolute temperature in Fig.2-4. The activation energy was obtained to be 1.9 eV.

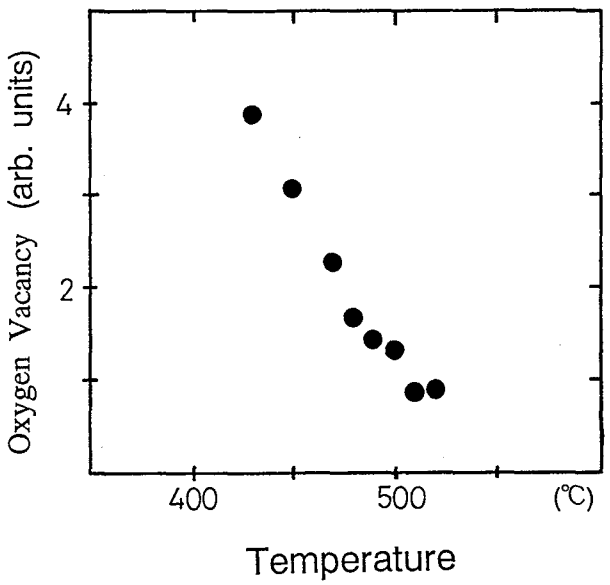

Fig.2–7 The decrease of oxygen vacancies on heating above 400°C. The heating duration is 30 minutes.

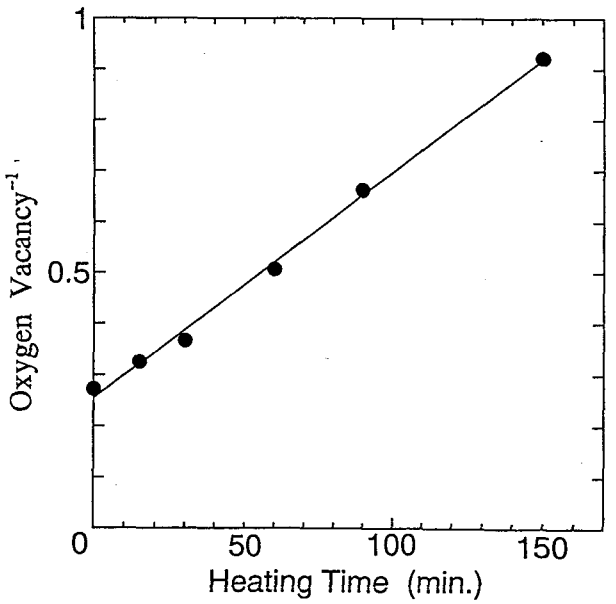

Fig.2–8 The results of the isothermal annealing experiment at 450°C for oxygen vacancies in quartz. The reciprocal intensity is on a line, indicating second order decay kinetics for oxygen vacancies.

2-4 Possible kinetics on heating for production and decay of paramagnetic defects

(1) Formation and decay kinetics below 300°C

E' intensity increased on stepwise heating below 300°C as shown in Fig.2-2 consistent with the result obtained by Jani *et al.* (1983). A neutral oxygen vacancy with two electrons traps a hole released by an aluminum hole center on heating. The correlation between increase in E' intensity and decrease in aluminum hole intensity was reported. The same correlation was also observed in the present experiment in Fig.2-2 where the intensity of aluminum hole center decreased by about 40 % with increasing E' intensity up to its maximum.

The intensity of titanium center seemed to decrease also correlating with the intensity change in Al and E' centers. It is impossible for a neutral oxygen vacancy to form an E' center by trapping an electron released by a Ti center. Therefore, decrement of Ti centers is due to recombination with holes released by Al hole centers or due to release of electrons to recombine with Al hole centers. If it is the latter case, the correlation between formation of E' centers and decay of Ti centers should be "accidental". Hence, it is probable that holes are released by Al hole centers to recombine with electrons trapped in Ti centers and to be trapped by neutral oxygen vacancies to form E' centers.

(2) Decay kinetics above 300°C

Both E' centers and remaining Al hole centers decayed above 300°C. Holes released by Al hole centers must recombine with electrons released by centers other than Ti centers in this temperature range. E' centers would decay rather due to trapping of electron than due to trapping of hole because an E' center has a positive charge. Anyway, there must be some defects that release electrons in this temperature range.

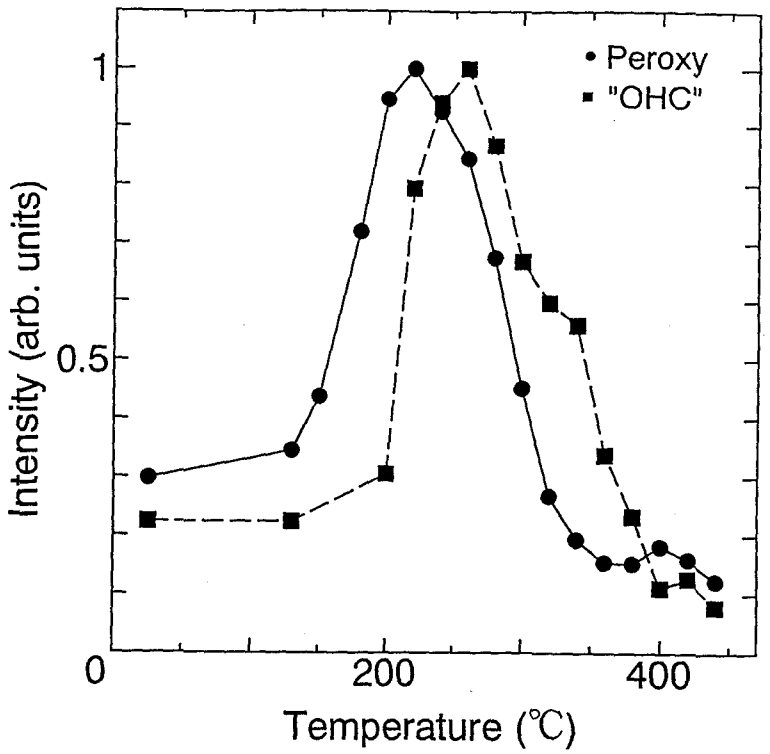

Fig.2-9 The intensity changes of peroxy and "OHC" in quartz in the isothermal experiment.

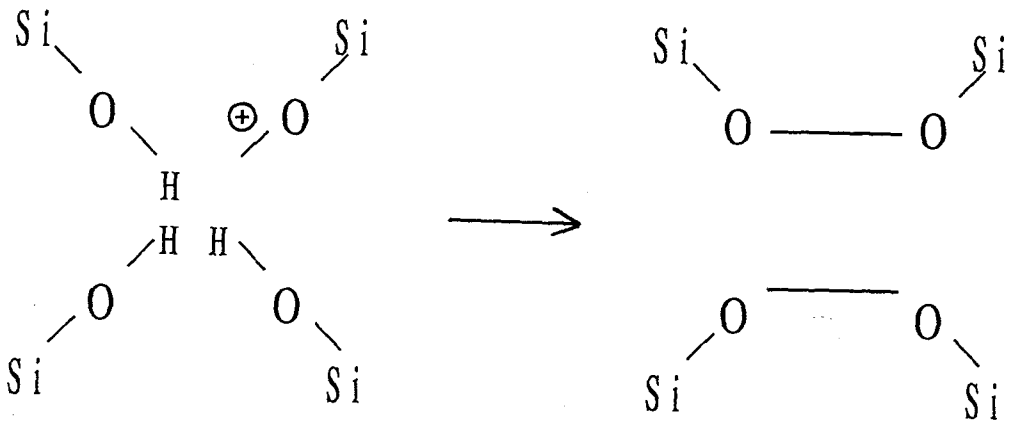

Fig.2-10 A possible process for the formation of peroxy linkages from a hydrogenic hole center $[H_3O_4]^0$ proposed by Baker and Robinson (1983).

a. Peroxy radicals as a candidate for an electron suppliers

Peroxy radical is one of candidates. It was first assigned in irradiated high purity amorphous silica by Friebele *et al.* (1979). The center is a dangling O_2^- ion whose one end is connected to a silicon ion (Stapelbroek *et al.* 1979). Garrison *et al.* (1981) assigned this radical in flints with similar g values to those of Friebele *et al.* (1979). This signal was used to date flints where the signal was enhanced by fast neutron irradiation. Garrison *et al.* (1981) did not state whether this signal was in crystalline quartz or in amorphous phase in flint but stated that the signal is similar to the one observed in crystalline quartz irradiated by fast neutrons.

Rink and Odom (1991) observed the same signal in crystalline quartz extracted from granites and denoted it as oxygen hole related center (OHRC). Therefore, if the signal observed by Garrison *et al.* (1981) were due to peroxy radicals, the signal should have been observed in crystalline quartz as was also observed in the present experiment shown in Fig.2-1. The signal height shown in Fig.2-1 was taken as its intensity following the way of Fukuchi's (1989) where he described it as "P1" center.

As a result of an isochronal heating experiment, the intensity increased below 260°C to reach its maximum and decreased above this temperature as shown in Fig.2-9. Therefore, it seems reasonable that electrons released by peroxy radicals are trapped in Al hole center and in E' center. This process explains the correlating decay of these three centers in this temperature range (260-400°C).

b. Origin of peroxy radicals

b-1. Peroxy linkages

It would be plausible that diamagnetic peroxy linkages are the origin of peroxy radicals. A peroxy linkage can be formed by trapping of interstitial oxygen between a silicon and an oxygen to be a Frenkel defect pair with an oxygen vacancy. However, if the peroxy radical is originated from this type of peroxy linkage, the number of proxy radicals would be insufficient because the number should be the same as that of oxygen vacancies. This type of peroxy radical would not have its number enough for supplying electrons to Al hole centers. Therefore, peroxy radical must be formed by other type of defects, such as silicon vacancy type, proposed by Baker and Robinson (1983) as shown in Fig.2-10.

Stapelbroek *et al.* (1971) proposed that O_2^- radical is produced by trapping a hole

at a peroxy linkage in fused silica. However, it is not the case for crystalline quartz because the peroxy radical formed in this way cannot return to peroxy linkage after releasing an electron. Therefore, a peroxy radical must be formed by trapping of an electron in a peroxy linkage. Indeed, ESR signal due to an electron trapped at peroxy linkage was observed in natural quartz at 10–30K (Baker and Robinson, 1983). It is possible that a peroxy linkage with an electron is changed into a peroxy radical on heating below 260°C. It would be impossible for peroxy linkage without an electron to trap an electron on heating below 260°C because there would be holes moving around in quartz on heating as discussed in previous section.

In summary, a peroxy radical is a candidate that serves electron to Al and E' centers on heating above 300°C. A type of peroxy radicals originated from silicon vacancy should be considered as well as those formed by trapping interstitial oxygens. However, it would be impossible for peroxy linkages to trap electrons on heating below 260°C. Therefore, we must consider a peroxy linkage with an electron (Baker and Robinson, 1983) as the candidate to be changed into peroxy radical on heating. Unfortunately, the thermal stability of the peroxy linkage with a electron has not been investigated.

b–2. Two neutral OH's

Another candidate to release electrons is two neutral OH's connected to two silicons respectively. This state might be changed into a peroxy linkage by releasing two hydrogen atoms on heating. However, it might be more probable that the state is changed into 'wet' OHC assigned in fused silica (Stapelbroek *et al.* 1979) shown in Fig.1–10.

b–3. Hydrogenic hole centers

The third candidates are a paramagnetic $[H_3O_4]^0$ and its precursor state, $[H_4O_4]^0$, which Nuttal and Weil (1980) first reported. The latter precursor is formed by trapping of four hydrogens in silicon vacancy. The authors postulated that the precursor traps a hole at irradiation and releases one proton to form the former paramagnetic center. ESR signals due to this center were observed at 25K but stable at room temperature over one year. This center may be changed into one or two peroxy radicals or into two peroxy linkages with an electron in each (Baker and Robinson, 1983). The precursor state, $[H_4O_4]^0$, may be able to release four electrons at its maximum if it is changed into two diamagnetic peroxy linkages, with releasing four hydrogen ions. It would be possible that hydrogenic hole centers and/or its precursor states trap holes to form peroxy radicals

below 260°C.

However, further studies would be needed on the process that protons are released from the precursor and/or the center because ionization potential of hydrogen atom is very high (13eV).

c. Other candidates for electron suppliers

An ESR signal at g=2.011 was observed in the present study as shown in Fig.2-1. Shimokawa and Imai (1987) and Fukuchi (1989) assigned this signal to be due to an oxygen hole center (OHC) corresponding to 'wet' OHC in fused silica (Stapelbroek *et al.*, 1979). However, Rink and Odom (1991) opposed to this assignment. One of two neutral OH's between two silicons traps a hole and releases a hydrogen ion (see Fig.1-10)to form 'wet' OHC in fused silica. If an ESR signal of OHC was observed in the present study at g=2.011, its behavior on heating shown in Fig.2-9 can be interpreted as the following. The intensity increases below 300°C because precursor state of 'OHC', which is two OH's, traps a hole released by an Al hole center. Above 300°C, it may release an electron to form a peroxy linkage.

It is possible, too, that some unknown diamagnetic electron trapping center may release electrons above 300°C. It may be related with some impurity or with some defects.

(3) Annihilation of oxygen vacancies

Oxygen vacancies trap interstitial oxygens, which may be in the form of peroxy linkages, above 400°C. Therefore, the amount of oxygen vacancies decreases with increasing temperature as shown in Fig.2-7. The activation energy of decay of oxygen vacancies was obtained to be 1.9 eV. The value is smaller than the activation energy of self diffusion coefficient of oxygen, 2.9eV (Giletti and Yund, 1984). The discrepancy would be because an oxygen atom moves substitutionally in the lattice sites for self diffusion, while an oxygen vacancy is annealed out by recombination with an interstitial oxygen ion.

(4) Moving of oxygen atoms or ions

Activation energies for decay of Ti, Al, and E' centers and of oxygen vacancies were obtained to be 1.7–1.9 eV within the error. It suggests a common process among the decays of E', Al, and Ti centers and of oxygen vacancy. The above picture in previous sections may explain that the activation energies for decays of Al and Ti centers are common because one process annihilates both centers. However, the picture must explain the common activation energy for the rest process as 'accidental' coincidence. The only candidate for this common process is the moving of oxygen atoms or ions.

It would be possible that paramagnetic centers are formed or annihilated by reacting with oxygen atoms or ions. The observation would be explained in terms of moving of oxygen atoms or ions if the reactions described in previous sections occur through the reactions with oxygen atoms or ions. Ti centers are annihilated by the reaction with oxygen atom to form oxygen ion O^-. The O^- formed by this reaction may annihilate Al hole center. An E' center can be formed by the reaction between neutral oxygen vacancy and an oxygen atom. The correlation among the above three reactions below 300°C might be because all these reactions are triggered by the activation of oxygen atoms.

It would be possible above 300°C that some electron centers are unstable, for example, hydrogenic hole centers, to supply electrons through the reaction with oxygen ions. Moving of oxygen atoms may explain the common activation energy for decay of E', Al, and Ti centers and oxygen vacancies.

2–5 Production of oxygen vacancies

(1) Fast neutron irradiation

Crystalline quartz of 99.9% purity purchased from High Purity Chemicals Co. Ltd., Japan, was heated at 600°C for 15 minutes to anneal oxygen vacancies out. Fast neutrons with their energy of 14 MeV were irradiated to quartz in the dose range of 5.2×10^{12} to 2.9×10^{14} neutron/cm^2. After subsequent γ ray irradiation and heating at 300°C for 15 minutes, E' intensity was measured by ESR to investigate the production of oxygen

vacancies by fast neutron irradiation. A small amount of E' signal was observed in a control sample. Therefore, the difference in intensity between the control and neutron irradiated samples were plotted as a function of neutron flux as shown in Fig.2-11. The production of oxygen vacancies by fast neutrons was confirmed by this experiment.

(2) γ ray irradiation

It was reported that the E' intensity measured after heating at 300°C increased with γ ray dose in the range of 0.1-100 MGy (Wieser and Regulla, 1989). This intensity should corresponds to the number of oxygen vacancies because of the similarity of their treatment with our method. Their results indicate that oxygen vacancies are created by γ ray irradiation at a high dose region.

Quartz separated from Mannari granite as previously described in Section 2-1 and 99.9 % quartz as described above were heated at 600°C for 30 minutes to anneal oxygen vacancies. Seven aliquots of samples were irradiated at the dose of 10^4 to 10^6 Gy with the dose rates of 10^3, $3x10^3$, and 10^4 Gy/h. E' intensities were measured after subsequent heating at 300°C for 15 minutes.

The amount of oxygen vacancies are plotted as a function of dose shown in Fig.2-12. The amount of oxygen vacancies was increased by γ ray irradiation, confirming the previous result (Wieser and Regulla, 1989). The intensity seem saturated in the range above $3x10^4$ Gy. Oxygen vacancies may be formed near dislocations where the vacancies are easily stabilized. The saturation behavior would be because oxygen vacancies were formed so densely.

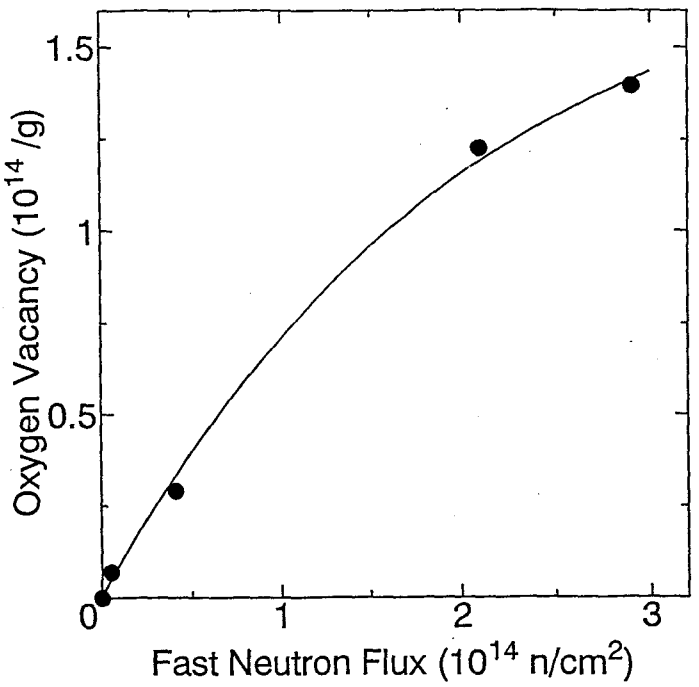

Fig.2-11 The enhancement of oxygen vacancies in quartz irradiated by fast neutron of 14 MeV.

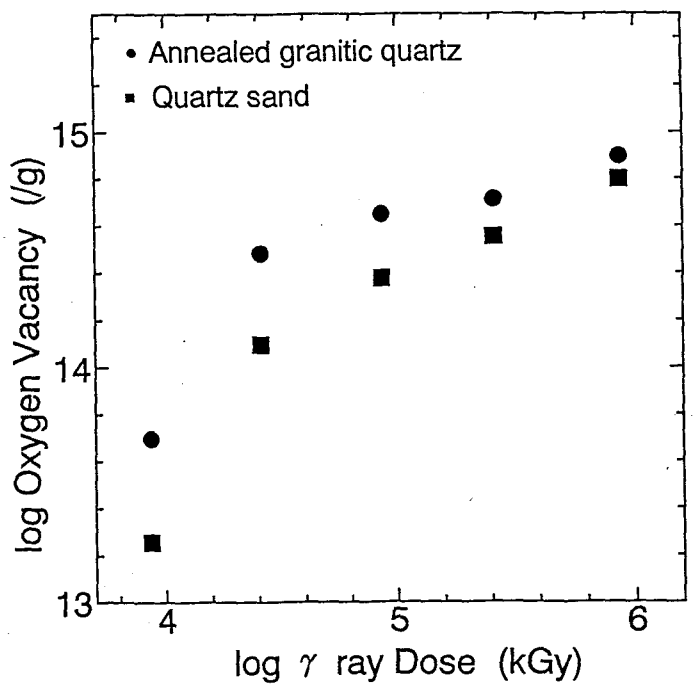

Fig.2-12 The enhancement of oxygen vacancies in quartz irradiated heavily by ^{60}Co γ rays.

2-6 Mechanical production of E' centers

(1) Experiment

About 2 g of crystalline silicon dioxide of 99.9% in purity with grain size of 1mm was heated at 600°C for 30 minutes to anneal oxygen vacancies out. The quartz grains were crushed by a pestle to powder below 75 μm in diameter. The powdered quartz was separated to 8 aliquots and irradiated by artificial γ rays with the dose ranging from 0 to 300 Gy. The signal intensity of E' centers was measured for irradiated and non-irradiated powdered samples after heating at 300°C for 15 minutes to check the thermal stability. Another series of quartz powder were prepared to investigate the E' intensity variations according to grain size. They were sieved to 7 fractions for grain diameter. ESR measurements were made for these aliquots before and after γ ray irradiation at 2 kGy.

Quartz grains extracted from Mannari granites were used for observing E'_1 centers after heating at 240°C for 3 hours to enhance the intensity. The intensity variation of E' centers was also investigated as a function of microwave power for powdered quartz and for quartz in granite.

(2) Results and Discussion

a. ESR Spectra

ESR spectra were obtained in quartz in granite and in non-irradiated and irradiated powdered quartz (<75 μm) with the microwave power of 0.01 mW as shown in Fig.2-13a-c. The signal in quartz in granite shows a typical powder spectrum with anisotropic g-factors of E_1' centers in agreement with an analysis of single crystal (Jani *et al.*, 1983). The shapes of the signals observed in powdered quartz before and after γ ray irradiation are different from this signal.

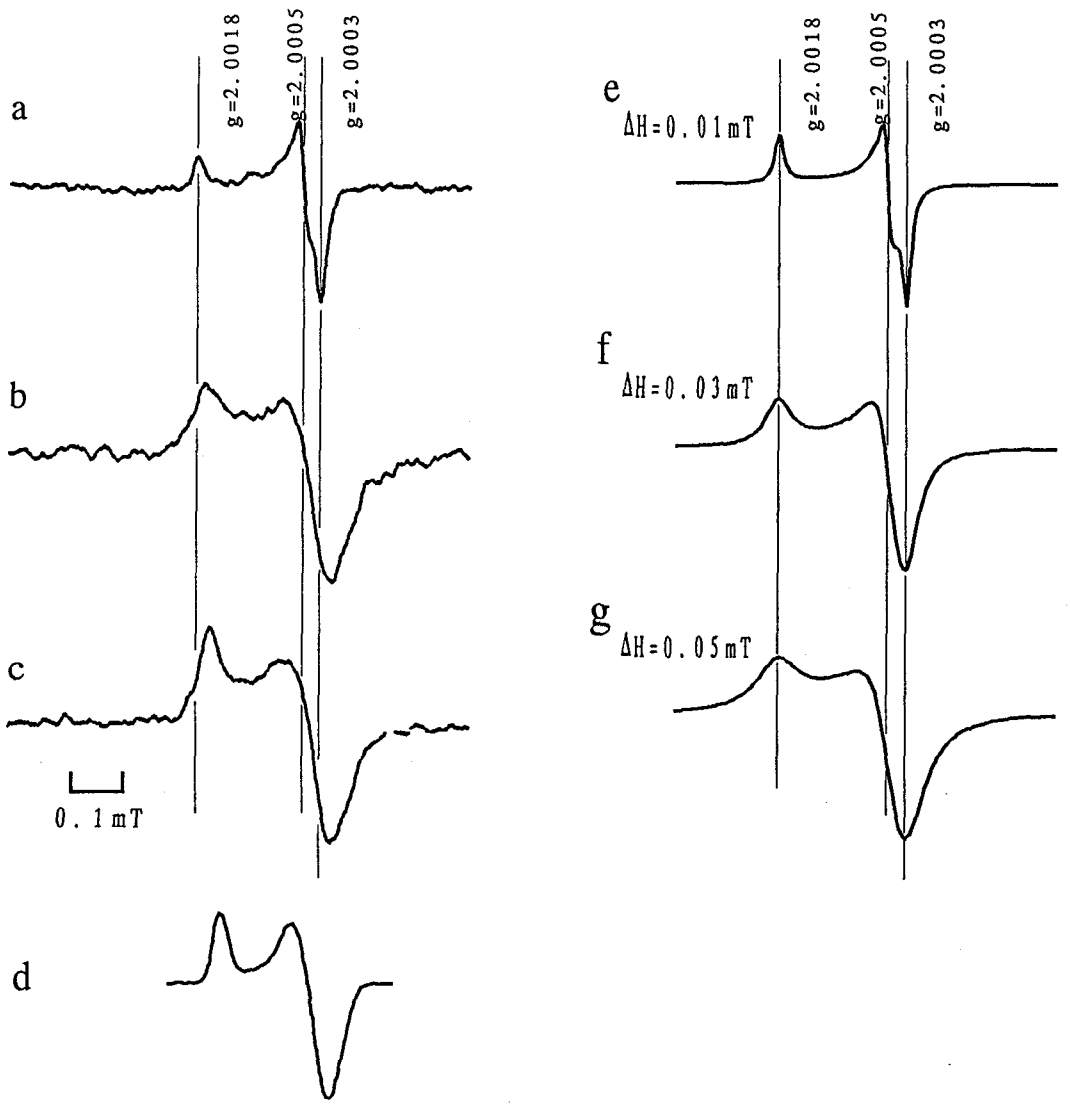

Fig.2-13 Powder ESR spectra of E' centers. a) The one observed in granitic quartz. b) The "distorted" E' signal observed in powdered quartz. c) The "distorted" one in crushed and γ rayed quartz. d) The ESR signal of E' center in quartz glass theoretically calculated by Griscom (1979). The shape is similar to c. e-g) The calculated powder ESR signals varying the linewidth assuming a Lorenzian line shape.

The line shape of the powder spectrum was numerically reconstructed by varying the linewidth of the anisotropic signals of E'_1 centers. The formula for powder spectrum of zero line width with anisotropic g-factors (Kneubühl, 1960) was given by the following expressions,

$$S(H)= \begin{cases} \frac{2}{\pi} \frac{H_1H_2H_3H^{-2}}{(H_1^2-H^2)^{\frac{1}{2}}(H_2^2-H_3^2)^{\frac{1}{2}}} K(k) & (H2 \geq H) \equiv S_1(H) \\ \frac{2}{\pi} \frac{H_1H_2H_3H^{-2}}{(H_1^2-H^2)^{\frac{1}{2}}(H_2^2-H_3^2)^{\frac{1}{2}}} K(\frac{1}{k}) & (H2 < H) \equiv S_2(H) \end{cases} \quad (1)$$

where,

$$k^2 = \frac{(H_1^2-H_2^2)(H^2-H_3^2)}{(H_1^2-H^2)(H_2^2-H_3^2)}, \qquad K(k) = \int_0^{\frac{\pi}{2}} \frac{db}{(1-k^2 \sin^2 b)^{\frac{1}{2}}}.$$

H_i is given by,

$$H_i = h\nu/g_i \qquad (i = 1,2,3),$$

where g_i were chosen from g_{xx}, g_{yy}, and g_{zz} as, $g_1 < g_2 < g_3$, and H_i denotes the resonant magnetic field, h plank's constant, and ν microwave frequency. The line shape can be constructed by integrating the line shape with one g-value, as the following expressions,

$$S_{obs}(H) = \int_{H_3}^{H_2} S_1(H')f(H-H')dH' + \int_{H_2}^{H_1} S_2(H')f(H-H')dH' \quad (2)$$

where a Lorenzian shape is assumed for the line shape, as denoted,

$$f(x) = a^2/\pi\,(a^2+x^2) \quad (3)$$

The calculated line shapes are shown in Fig.2-13e-g. The linewidth of the signal in powdered sample (Fig.2-13b) is estimated to be 0.05 mT (see Fig.2-13g), while that of E'_1 center observed in quartz in granite (Fig.2-13a) is to be 0.01 mT (see Fig.2-13e), comparing the calculated lines with those observed in samples. Apparently, the linewidth

of the signal is broadened due to lattice distortion by grinding: an X ray diffraction study confirmed the lattice distortion.

The line shape of irradiated powdered quartz is rather similar to that of E' center in quartz glass reported by Griscom (1979) as shown in Fig.2–13d. It implies that the crushing produce amorphous region in quartz and that E' centers are created in the region by γ ray irradiation.

The microwave power dependence of the signals (Fig.2–13a–c) are shown in Fig.2–14. The similar dependence of these centers indicate that the state of unpaired electron in the defect is similar to one another.

b. Enhancement in intensity by artificial γ ray irradiation

The signal intensity of powdered quartz was enhanced by γ ray irradiation as shown in Fig.2–15. Their signal intensities after heating at 300°C for 15 minutes are also plotted in the same figure. After heating, the signal intensity created by crushing became about a half as large as the one before heating. On the other hand, the decrement in intensity of the signal created by γ ray irradiation is slight relative to its intensity. This observation indicates that about a half of "distorted" E' centers formed by crushing are thermally unstable, but that those formed by γ ray irradiation is relatively stable.

c. E' intensity variation for grain diameters

The intensities of distorted E' centers are plotted as a function of grain diameters in Fig.2–16. Arends *et al.* (1963) found that the E' intensity (E_s) created by crushing, increase with decreasing the grain diameters. Our result is consistent with theirs. Similarly the intensity of distorted E' centers after γ ray irradiation increased with decreasing grain diameters as shown in the same figure. The signal intensity in crushed quartz is dominated by that from the fraction with the smallest diameter.

d. Application to ESR dating of fault movement

"Distorted E' centers" are created by artificial γ ray irradiation after crushing. A fault movement of granitic blocks crushes rocks nearby the fault plane, and grinds quartz grains into fault gouge.

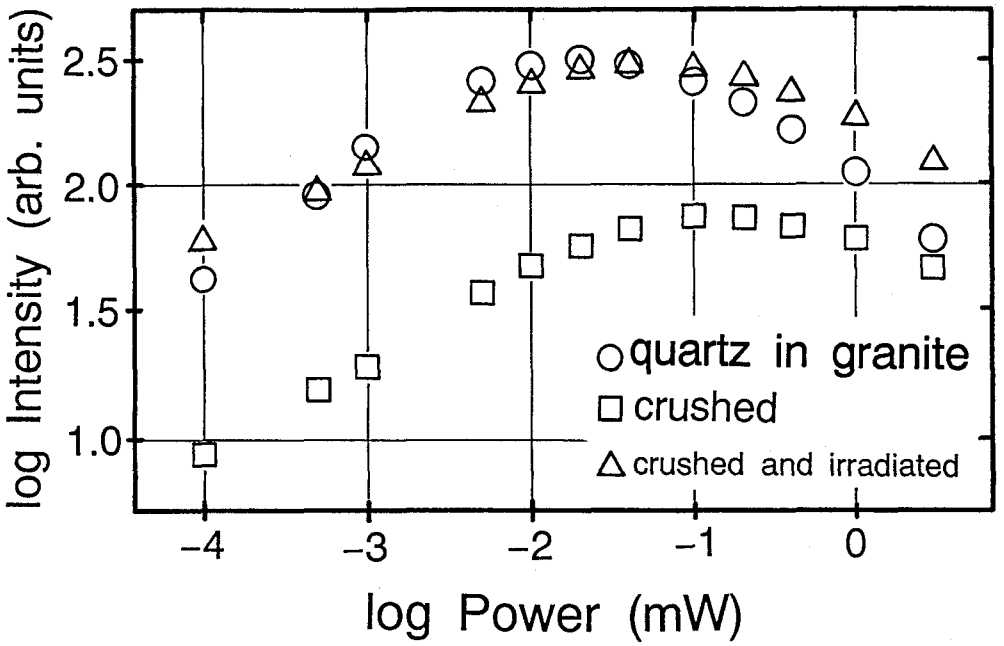

Fig.2-14 Microwave power dependence of "normal" and "distorted" E' centers were similar to one another.

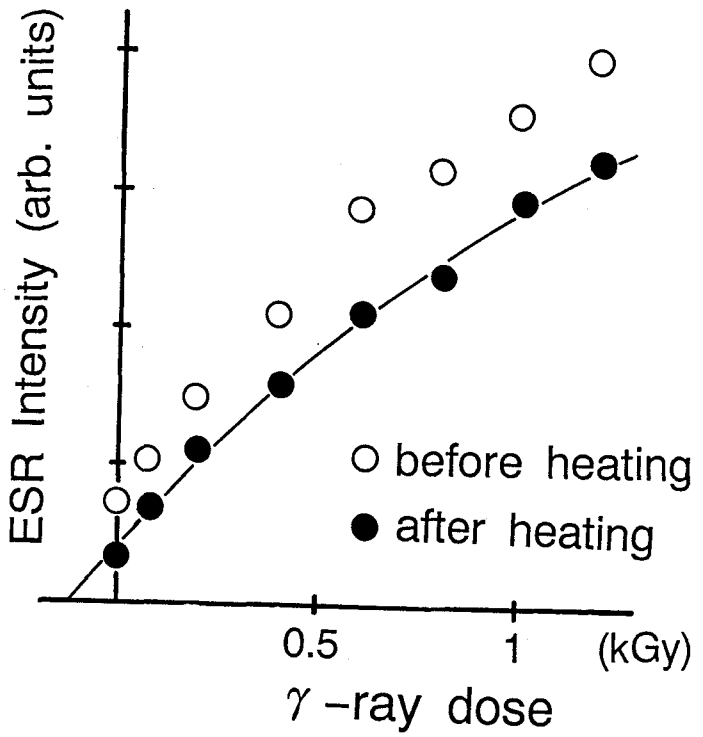

Fig.2-15 The signal intensity of distorted E' centers was enhanced by γ ray irradiation. Open and solid circles indicate the intensities before and after heating at 300°C, respectively.

Therefore, it is probable that a fault movement makes the "distorted lattice" or amorphous region in powdered quartz and that subsequent natural radiation creates "distorted E' centers".

A fault movement may also create "distorted E' centers" as indicated by the observation of the signal in non-irradiated powdered quartz, but about a half of these centers are thermally unstable. The offset of the equivalent dose of stable centers is around 100 Gy, which is obtained by extrapolating the saturation curve in Fig.2-15. The offset seems relatively large in ESR dating of fault movement of quaternary era. However, it would be reduced when a fraction less than 5 μm in diameter is used because production rate is higher in finer fraction as shown in Fig.2-16.

The ESR signal of distorted E' center has a potential applicability for dating of fault movement. The next step is to search "distorted E' centers" in natural fault gouge. It is possible that the ESR signal of "distorted" E' centers is too small to distinguish from that of "normal" E' centers. In this case, precise signal separation treatment using a computer would be necessary to extract the signal.

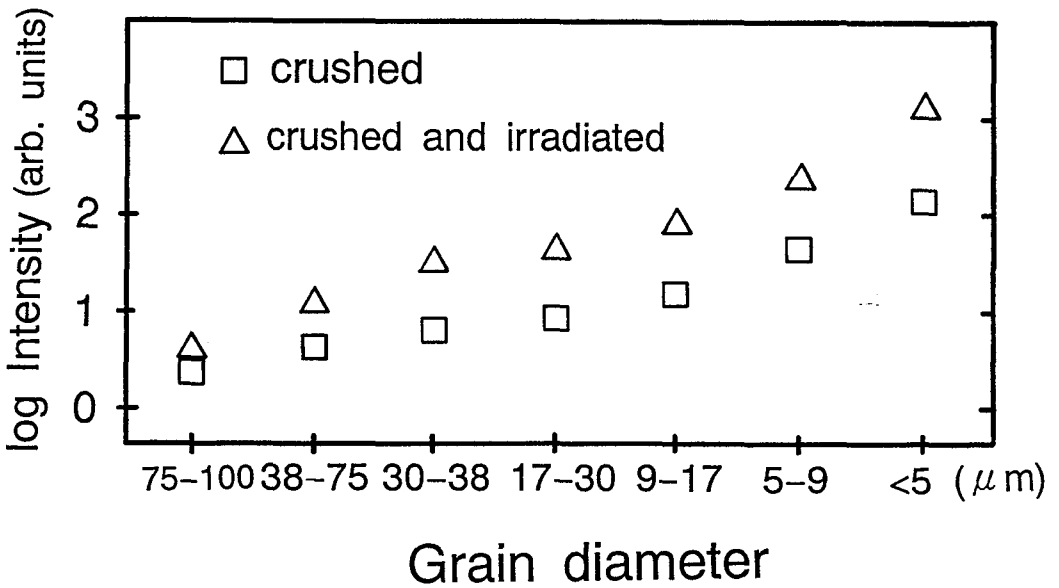

Fig.2-16 Both E' intensities before and after irradiation, and the production rate in finer fractions were larger than in coarser fractions.

3. Applications

3–1 Closure temperatures

The thermal effects of igneous intrusions on the dating of minerals have been studied by a number of workers by investigating the retentivity of radiogenic daughter elements or fission tracks in minerals. The concept of "closure temperature" was first proposed by Dodson (1973) as shown in Fig.3–1. It denotes the temperature above which radiometric age of mineral is reset due to the thermal release or homogenization of daughter elements, or due to the thermal annealing of fission tracks. Harrison *et al.* (1979) and Dodson and McClelland–Brown (1985) discussed and summarized closure temperatures for various minerals (see Table 3–1). The thermal history of rocks has been investigated by combining several minerals with ^{39}Ar–^{40}Ar and other dating methods (Harrison and McDougall, 1980; Berger and York, 1981), whereas, closure temperatures for some minerals are still in discussion (Shibata, 1991).

In electron spin resonance (ESR) dating, closure temperatures depend on their thermal stabilities. Although several workers have investigated thermal stabilities of centers, the stabilities have not well been established, especially for quartz. No papers have dealt with closure temperature in the case of ESR dating.

(1) Numerical calculation for estimation of closure temperatures

As a result of an investigation of thermal stabilities of some paramagnetic defects in quartz extracted from Mannari granite, decay of E', Al and Ti centers follow second order kinetics as described in Chapter 2. In the case of second order decay kinetics, the characteristic decay time, τ is defined by,

Table 3-1 Selected data for closure temperatures for some minerals in dating method summarized by Dodson and McClelland-Brown (1985).

Method	Mineral	Closure Temperature (°C)
K-Ar	muscovite	350±50
	biotite	300±50
	K-feldspar	150±30
	amphibole	510±25
	phlogopite	460±50
Rb-Sr	muscovite	500±50
	biotite	300±50
	K-feldspar	350±50
Fission Track	zircon	175±25
	apatite	120±20
	sphene	300±40

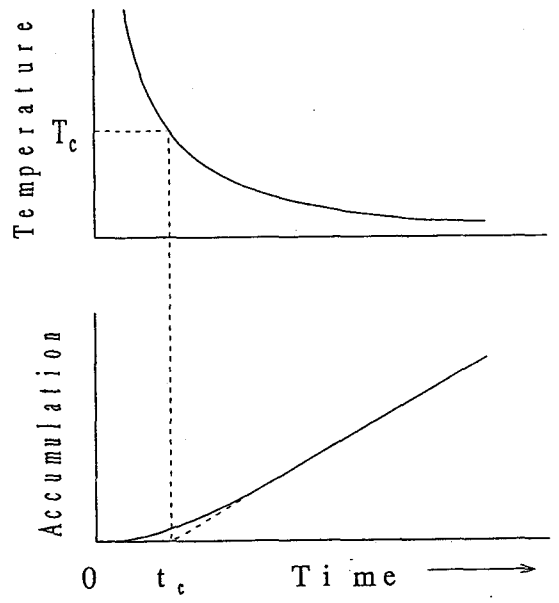

Fig.3-1 Definition of the closure temperature (T_c) proposed by Dodson (1973). The age obtained by a dating method indicates the time when the rock cooled down to T_c.

$$\tau = \frac{1}{\lambda N} , \qquad (3\text{-}1)$$

where λ is decay constant, and N is the number of centers. The obtained values at 27°C for the untreated sample are shown in Table 2-1. One can get the duration period as τ, while the concentration is reduced by half if N is taken as the concentration at present. τ depends on the present concentration as shown in the equation 3-1. A half life cannot be defined for the respective paramagnetic center. In spite of the ambiguity in the concentration of a paramagnetic species, the paramagnetic centers and oxygen vacancies are shown to be stable for more than 10^6 years if the sample is not heated.

The accumulation of centers is given by differential equations, considering that the decay reactions are second order,

$$\begin{aligned} \frac{dN}{dt} &= P - \lambda N^2 \\ \lambda &= \lambda_0 \exp\left[- \frac{E}{kT} \right] \\ T &= T(t) \end{aligned} \qquad (3\text{-}2)$$

where N is the number of centers, P is the production rate, λ is decay constant which is a function of temperature, λ_0 is a pre-exponential factor, E is activation energy, T is absolute temperature, k is Bolzmann constant, and t is time.

The accumulation of the numbers of centers in quartz was numerically calculated for two cases of temperature decrease. In one case, it was assumed that the reciprocal of the absolute temperature is linear as was in Dodson (1973), i.e.,

$$\frac{1}{T} = \frac{1}{T_0} + b\,t \qquad (3\text{-}3)$$

where t is time, T is absolute temperature at t, T_0 is initial temperature, and b is a constant. The differential equation for a first order reaction was solved and the formula concerning closure temperature was derived (Dodson, 1973). The equations (3-2) cannot be solved analytically for the second order decay kinetics. Hence, the differential equation was integrated numerically by Runge-Kutta method where production rates are the values calculated by assuming that the signal intensity increases linearly up to 100 Gy for

Al and Ti centers and up to 10^5 Gy for oxygen vacancies and that the annual dose rate is 3 mGy/y.

In the other case, a temperature decrease around dike contact was assumed, where one dimensional heat flow equation was solved numerically by assuming a heat diffusion constant to be 1.5×10^{-6} m^2/s (Calk and Naeser, 1973) and other conditions to be the same as the former case.

(2) Closure temperatures obtained for Al and Ti centers

Closure temperatures are obtained by extrapolating the linear relationship to the zero ordinate as such an example was shown in Fig.3–2 for Al centers with an intrusive dike of 500 m wide. Obtained closure temperatures are summarized in Table 3–2. When the dike intrusion is large, the signal intensity becomes saturated as the case of Ti centers shown in Fig.3–2. When the time span is large, the decay of centers cannot be neglected even at room temperature. In such a case, the closure temperature is meaningless.

Other minerals such as aragonite and calcite, which have been used for ESR dating, seldom occurs in volcanic rocks. Quartz would be the only mineral for ESR investigation of cooling history of rock bodies and of dike contacts. The closure temperatures for Al and Ti centers are lower than that for fission track dating of apatite having the lowest closure temperature, 120°C (Dodson and McClelland–Brown, 1985). Thus, the ESR method using Al and Ti centers can solve the thermal history at temperatures lower than that other dating methods can deal with.

(3) Closure temperature obtained for oxygen vacancy

Oxygen vacancies in quartz are much more stable than Al and Ti centers as discussed in Chapter 2. Oxygen vacancies have not been used in ESR dating. Recently, Odom and Rink (1989) reported that the intensities of E' centers are correlated with ages in the range between 0.1 and 1400 Ma. However, the formation mechanism of oxygen vacancies in natural quartz has not been established as will be discussed in Section 3–5.

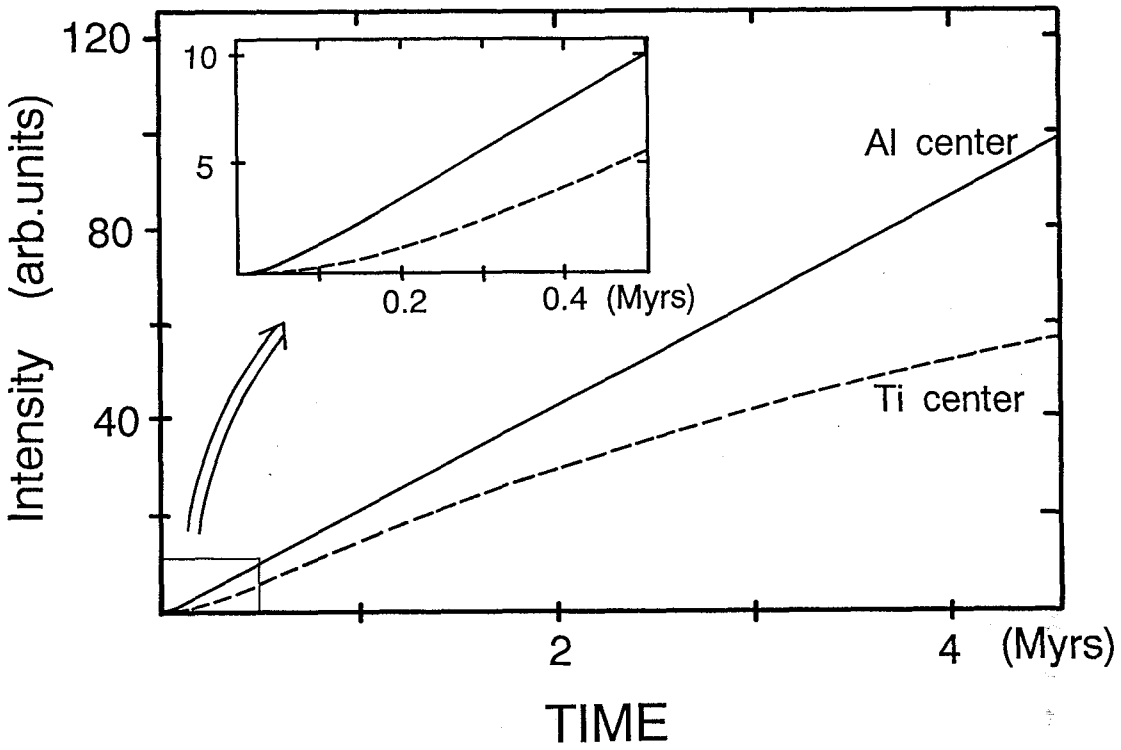

Fig.3-2 Calculated intensity of Al (solid line) and Ti (broken line) centers in quartz after intrusion of a dike 500 m wide. The differential equation (3-2) was integrated numerically by Runge-Kutta method assuming the annual dose rate of 3 mGy/y. The temperature decrease was calculated assuming one-dimensional heat flow. The closure temperature is obtained by extrapolating the linear increase of the defect concentration to the zero ordinate. The signal intensity of Al centers increases linearly, while that of Ti centers shows a saturation in this condition of cooling.

Table 3–2 Closure temperatures calculated by equation (3–2) for two cases of cooling.

CASE 1: The reciprocal of absolute temperature is linear as indicated by Dodson (1973).

b* (/deg Myr)	Cooling Rate (deg/Myr)	Closure temperature (°C) Oxygen vacancy	Al centers	Ti centers
10^{-4}	~ 10	190	78	31
3.3×10^{-4}	~ 30	210	96	45
10^{-3}	~ 100	240	110	55
10^{-2}	~ 1000	290	150	82

* This parameter is given in the equation (3–3).

CASE 2: A dike intrusion. It is assumed that ESR dating procedure is made at the time when the rock cools down to 27°C.

Width of dike (m)	Closure temperature (°C) Oxygen vacancy	Al center	Ti center
30	430	350	160
100	410	240	48*
300	390	140	28*
700	320	58*	27*

* The accumulation of centers in quartz shows saturation like the accumulation of Ti centers in Fig.3–2.

Oxygen vacancies were formed by heavy γ ray irradiation shown in Section 2-5. If it is assumed that natural β and γ rays create oxygen vacancies in quartz, the closure temperature can be defined for oxygen vacancies. On the assumption, accumulation of oxygen vacancies were calculated using the equations (3-2) for two cases of cooling as in the cases for Al and Ti centers. The production rate was calculated assuming that the signal intensity increases linearly up to 10^5 Gy in Fig.2-12, and that the annual dose rate is 3 mGy/y.

The results of calculation are shown in Table 3-2. If ESR dating method using oxygen vacancies is established, as will discussed in Section 3-5, the method will define the age at about the same temperature as fission track dating method using zircon does.

(4) Summary

The different ages when the rock reached respective closure temperatures may be obtained for different centers and for oxygen vacancy. Cooling histories can be solved more precisely by combining conventional dating method with various minerals with the ESR method with several centers and vacancies in quartz.

Discussion in Chapter 2 showed that the thermal stabilities might depend on the element and its concentration of the impurity, thus, that the closure temperatures defined for respective centers might do, too. Closure temperatures might have to be defined for individual sample in that case.

3-2 Thermal effect in metamorphic rock around an intrusion zone

Mineralogical structures in metamorphic rocks were changed by heat, pressure or permeation of other substances. Hornfels are clays or shales metamorphosed through the action of heat from nearby igneous rocks. Heat releases electrons trapped by impurities and defects. The clock time based on the accumulated amount of trapped electrons is set to zero as is made in thermoluminescence (TL) dating of fired clays or pottery (Aitken 1986, McKeever 1978). Some lattice defects would have been annealed out by the tem-

perature rise at the time of intrusion. Hence, metamorphic rocks are objects of ESR dating or of geological heat assessment by ESR. The ESR age of volcanic eruption was investigated using quartz in sediment baked by lava flow (e.g. Yokoyama *et al.*, 1985). However, no systematic work on metamorphic rocks using ESR has been reported so far, although thermal effect of intrusion was assessed by fission track method (e.g. Calk and Naeser 1973).

Present work in this section describes ESR studies of igneous intrusion rocks and of the hornfels formation as well as of mudstones as a function of the distance from the site of intrusion. It is suggested that ESR assessment of geological heat as well as the age can be made by spatially sampling altered rocks around the intrusion.

(1) Experimentals

Intrusion rhyolite, hornfels, and mudstone along the valley of Mino National Park, Osaka, are collected along a river as shown in Fig.3–3. The width of the intrusion was 17 m. Mineralogical identifications of the samples were made using a polarization microscope.

Quartz grains were extracted from hornfels and mudstone samples with the procedure described in Chapter 2. Oxygen vacancy concentrations in the samples were obtained with the treatment and with the condition of ESR measurement as described in Chapter 2.

(2) Experimental Results and Discussion

The size of quartz grains is larger in metamorphosed rocks than in mudstone confirmed by polarized microscope observation indicating the growth of quartz grains by heat under pressure owing to the intrusion. Metamorphism was identified mineralogically in samples within about 80 m from the intrusion.

Fig.3–4 shows an ESR spectra of hornfels (60 m apart from the intrusion) at room temperature. A signal associated with E' centers at g = 2.001 was observed.

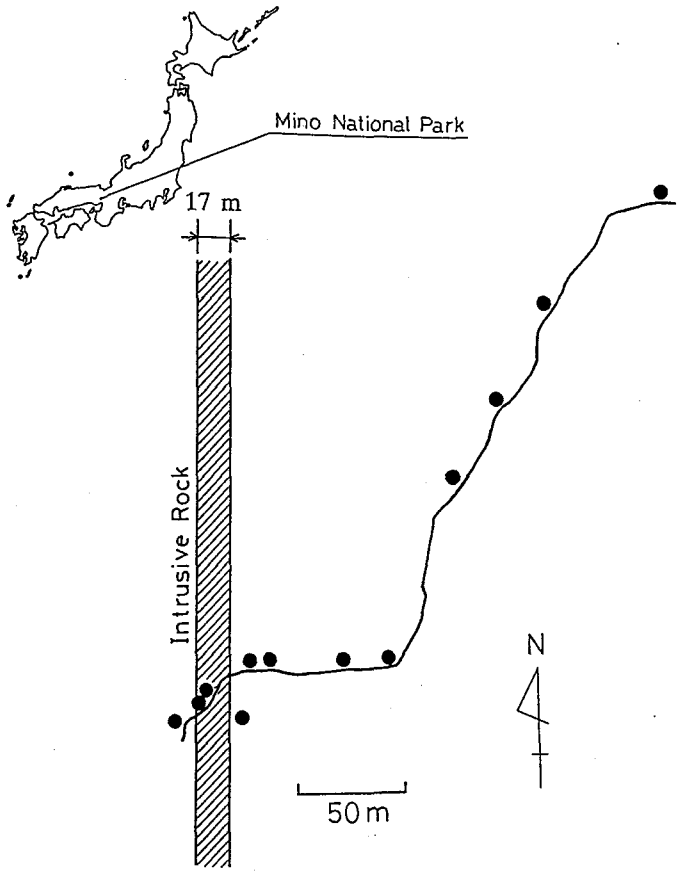

Fig.3-3 The sampling locations at Mino National Park along the Mino river in the vicinity of an igneous intrusive rock.

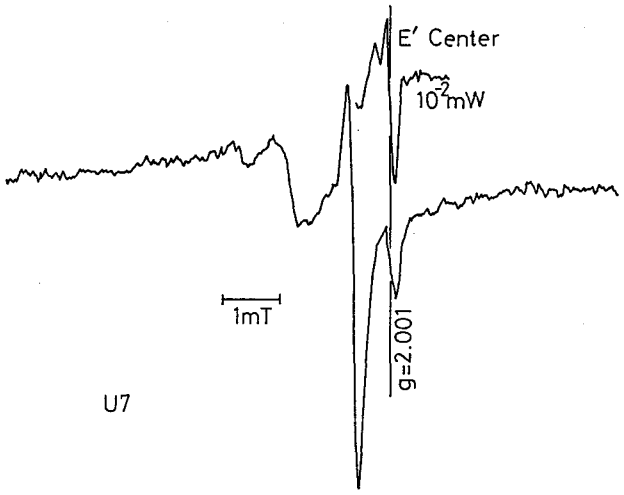

Fig.3-4 A room temperature ESR spectrum obtained for a piece of hornfels near the intrusive rock.

Fig.3–5 shows the concentration of oxygen vacancies in quartz as a function of distance from the site of the intrusion rock. The concentration is low near the intrusion relative to that far from the intrusion except two points at about 120 and 160 m. The following thermal history may explain the tendency of Fig.3–5 assuming that oxygen vacancies in quartz are created by natural radiation. When the intrusion of rhyolite took place, the defects (oxygen vacancy) in quartz grains in mudstone near the intrusion were completely annealed out, while those in grains of further samples might have been only partly annealed out. Quartz grains in mudstone adjacent to the intrusion may have been recrystallized to anneal oxygen vacancies out. After the intrusion, defects were created by natural radiation again. Therefore, the concentration in the sample near the intrusion are small while quartz grains in samples further from the intrusion show large signal intensities of oxygen vacancies.

(3) Calculation of Heat Flow around Intrusion and of its effect on oxygen vacancies

A calculation of heat flow was made to estimate the rough temperature rise around the rhyolite intrusion and mudstones based on a simplified model of one–dimensional heat flow. The intrusion with the thickness of 17 m at the temperature of 1200°C was assumed to be a heat source. The heat diffusion constant was assumed to be 1.5×10^{-6} (m^2/s) (Calk and Naeser, 1973). The temperature distributions are shown in Fig.3–6 as a function of the distance at several times after the intrusion.

The change of concentration of defects was calculated by the equations (3–2), where T(t) was obtained by heat flow equation for several points with the following assumptions: 1) Oxygen vacancies are created by external β and γ rays. 2) The production rate is the same as the one in section 3–1. 3) The annual dose rate is 5 mGy/y. 4) The initial concentration of oxygen vacancies was 3.2×10^{15} /g. 5) The rhyolite dike intruded in the mudstone 1×10^7 years ago. The calculated distribution of oxygen vacancies is shown also in Fig.3–5 by a solid line.

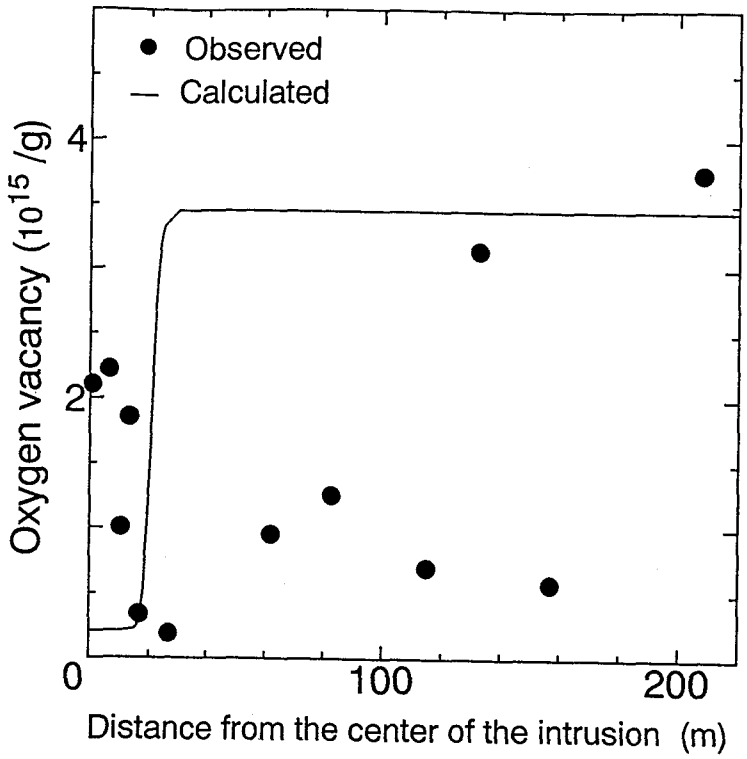

Fig.3-5 The distribution of concentrations of oxygen vacancies in quartz extracted from hornfels and mudstone. The solid line indicates the predicted distribution of oxygen vacancies.

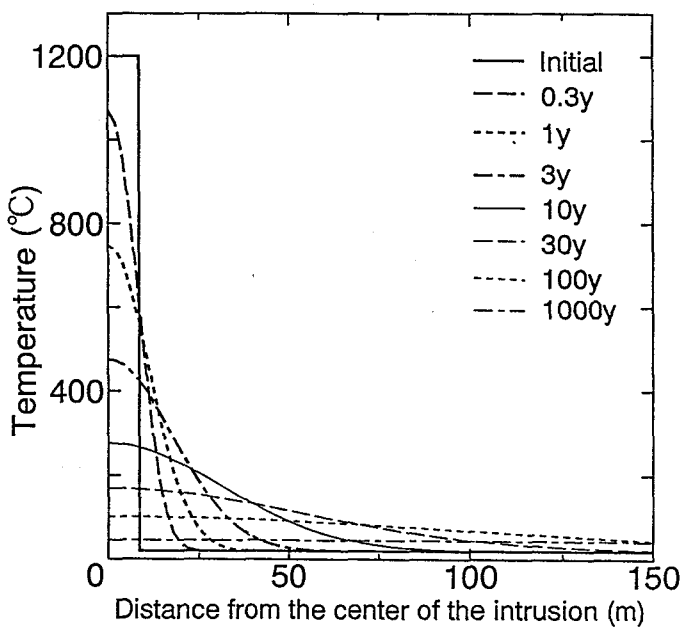

Fig.3-6 Theoretical calculation of the temperature distributions after intrusion of rhyolite magma of 1200°C with a thickness of 17 m for one-dimensional thermal conduction of mudstone.

The result of calculation is not consistent with the observed distribution. The result of the calculation indicates that the heat of the intrusion gives no effect on oxygen vacancies in samples further than 30 m from the intrusion. The model does not explain the observation that the concentrations of oxygen vacancies in the rhyolite intrusion are larger than those of hornfels adjacent to the intrusion.

Geothermal fluid may have been supplied continuously to the intrusion for some duration to anneal the oxygen vacancies around 60–80 m apart from the intrusion. Some other geothermal events might happen around 60–80 m as is indicated by the observation that the concentrations are low at the points, 120 m and 160 m. Higher annual dose rate or higher production rate of oxygen vacancies in the rhyolite than in hornfels may have caused higher concentration.

Although the present calculation is too simplified to predict the metamorphism and thermal annealing of lattice defects quantitatively, the numerical simulation clearly predict that metamorphism in the vicinities had certainly caused the temperature rise differently at several sites and that several lattice defects would have been annealed out.

3–3 Assessment of prehistoric heat treatment of stone implements

The lithic tool fragments made of heated chert have been used to investigate the firing technology for studying the history of ancient human beings. Although heat treatment as a frequent component in lithic technology has been well established for two decades, there are major problems in the identification of heat treatment in archaeological assemblages using macroscopic attributes such as color and luster (e.g., Purdy and Brooks 1971). Even when raw material from the geologic source is available for comparison, the range of these attributes may overlap between heated and unheated materials.

Thermoluminescence analysis is an established method for the secure identification of heat treatment (Aitken 1986, Melcher and Zimmerman 1977). Because one is simply contrasting the relatively modern thermoluminescence of artificial heating with the ancient luminescence centers induced by radiation in the chert, such assessments are not nearly as demanding in terms of samples or as time consuming in analysis as is the relatively expensive TL dating process.

Electron spin resonance (ESR) offers an equally secure method of identifying heat treatment without many of the liabilities of TL analysis. For example, repeated measure–

ments are possible in contrast to TL in which heating destroys trapped electron or hole centers. Trapped electrons (holes) created by natural radiation during a geological time can be measured with ESR: heating releases these from traps to recombine. The oxidation state of paramagnetic impurities such as Fe^{3+} can be also monitored with ESR. Ancient technology of pottery was assessed from the change in ESR spectra (Warashina *et al.*, 1981). ESR is inherently less sensitive in its measurement than TL; however, while it may impact dating applications to geological materials other than dating archaeological ones, the difference in precision is of no importance in the detection of heat treatment for archaeological lithics.

A new method to assess the ancient heat treatment of cherts using E' centers, an unpaired electron at an oxygen vacancy site, is proposed in this section. It is based on the thermal property of E' centers in quartz contained in chert. This method is checked by a control experiment and is applied to lithic tool fragments made of cherts.

The intensity of E' centers increases when the sample is heated below 300°C, while it decreases when it is heated above 300°C as shown in an experiment in Chapter 2. This behavior of E' centers is specific in contrast to impurity centers in quartz, whose intensities only decrease on heating and do not increase.

An oxygen vacancy, which traps electron and becomes E' center, was shown to be thermally more stable than E' centers. They decrease in number when the sample is heated above 400°C. A method to obtain the number of oxygen vacancies as the intensity of E' center has been proposed in Chapter 2. The procedure used is the irradiation of the quartz sample by γ rays at a dose above 200 Gy followed by heating at 300°C for 15 minutes to convert oxygen vacancies with two electron into E' centers.

(1) The Method to Estimate the Heating Temperature

a. Experimental Basis

E' centers and oxygen vacancies have respective thermal stabilities. The method is based on that the ratio of E' centers to oxygen vacancies and the heating temperature show one to one correspondence in a temperature range.

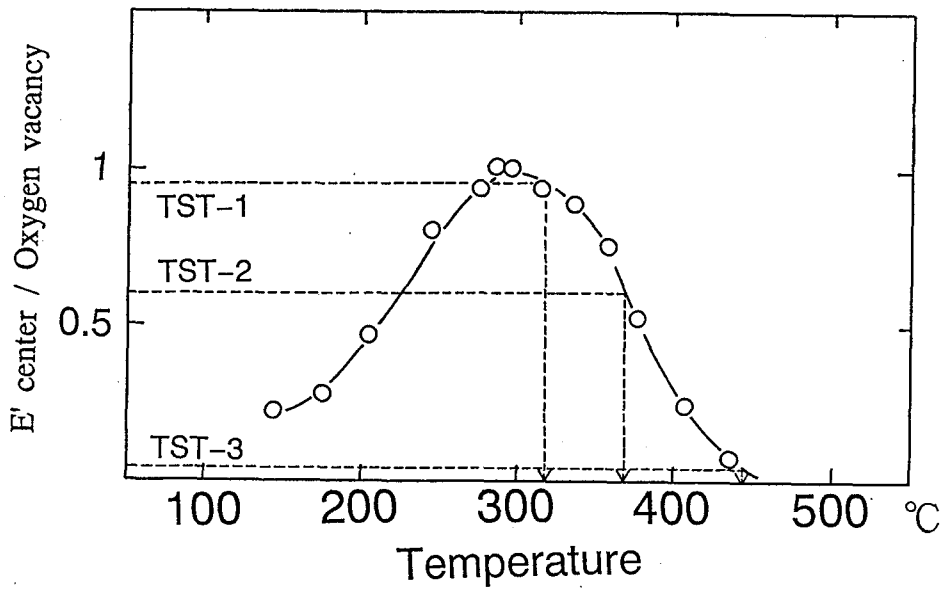

Fig.3-7 E' to oxygen vacancy ratio plotted as a function of heating temperature for quartz in granite. The value and the temperature show one to one correspondence in each range below and above 300°C. The heating temperature can be estimated from E' center to oxygen vacancy ratio if one knows the temperature range. The results of a control experiment (TST-1, 2, 3) show that the estimated temperatures agree with the actual ones (see Table 3-3 for summary).

Quartz grains were separated for an experiment to confirm the basis from Take-fushi granite at Okazaki city, Aichi prefecture, Japan. ESR measurements were made for the extracted quartz grains. Their conditions of sample preparation and of ESR measurements are the same as described in Chapter 2.

The E' intensity of quartz in granite increased after heating below 300°C and decreased above 300°C as was the same for Mannari granite (Fig. 2-2). The change in intensity by heating an aliquot with stepwise temperature elevation is almost the same as that by heating several aliquots at respective several temperatures.

The latter aliquots were irradiated at 3 kGy and annealed at 300°C for 15 minutes. The value obtained by dividing the E' intensity after the first heating by the one after irradiation and annealing is the ratio between E' centers and oxygen vacancies after the first heating because the amount of oxygen vacancies is obtained as E' intensity after the treatment. The ratios are plotted as a function of the temperature of first heating as shown in Fig.3-7.

The ratio and the temperature of first heating show one to one correspondences below 300°C and above 300°C respectively. Therefore, the temperature at which a sample had been heated can be obtained using the curve shown in Fig.3-7 if one knows the E' intensity to oxygen vacancy ratio and the temperature range. The range, above or below 300°C, can be determined by comparing the E' intensities before and after annealing at 300°C. If the sample had been heated below 300°C, the E' intensity would increase by annealing because remaining holes would be transferred to oxygen vacancies and would form E' centers. If the sample had been heated above 300°C, the E' intensity would be the same or become slightly less because there are no remaining holes to be transferred.

The temperature range in which the sample had been heated can be determined by the comparison between the E' intensities measured before (no treatment) and after heating at 300°C without a reference sample because the qualitative characteristics of E' centers would be common for all quartz.

On the other hand, reliable result would be obtained by using a non-heated reference sample to determine temperature. The decay of E' intensity follow second order kinetics as described in Chapter 2. Therefore, it depends on its concentration. It is necessary to determine oxygen vacancy concentration in quartz (not average concentration for bulk). In the case of lithic tool fragments, especially in the case of chert, it is almost impossible to separate quartz phase from the sample. However, if we use a reference sample, bulk measurement without quartz separation is enough for the estimation of heat treatment temperature by comparing the decay curve.

The reduction of E' intensity by γ ray irradiation for heated quartz was reported by Sato et. al. (1985). Considering their result, the temperature estimated for the sample had been irradiated above 100 Gy after heating would not be correct because the E' intensity would have been affected by irradiation. The procedures are summarized as below to estimate the temperature at which a sample had been heated in the past.

b. Semi-quantitative temperature assessment

The procedure is the one described in the previous section to determine the temperature range. It is summarized as the following. If the E' intensity increase after heating at 300°C for 15 minutes, it is estimated that the sample had been heated below 300°C or never been heated. This heating degree is named "0". If the E' intensity is the same or slightly less after heating at 300°C, the sample is estimated to have been heated above 300°C. This degree is "1".

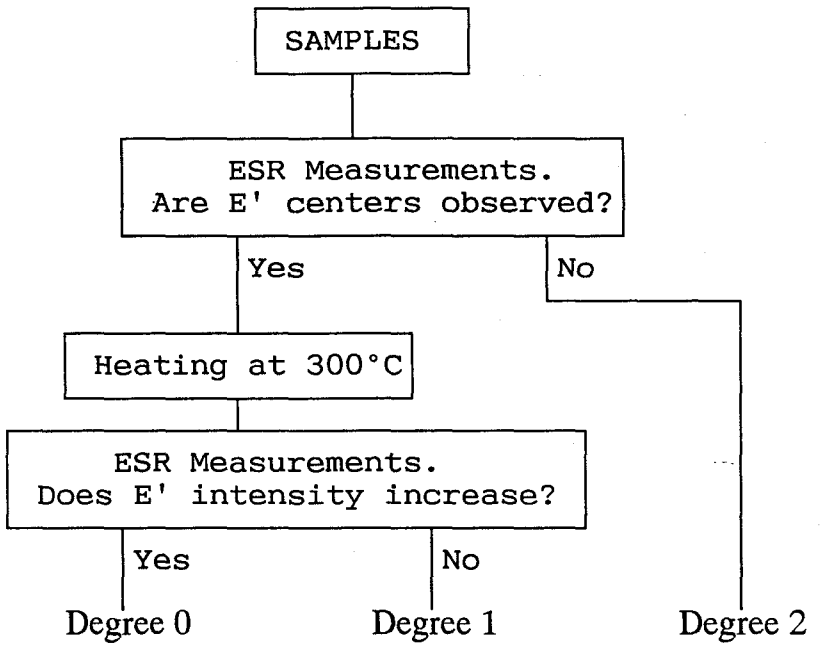

Degree 0 : unheated or heated below 300°C if it has been heated
Degree 1 : heated between 300°C and 450°C
Degree 2 : heated above 450°C

Fig.3-8 The algorithm proposed for semi-quantitative estimation of the temperature of ancient heat treatment.

In the case that the sample had been heated above 450°C, E' centers would not be observed: this degree is "2". When the signal of E' centers is observed after heating at 300°C following γ ray irradiation, it indicates that oxygen vacancies had not been annealed by heating. Oxygen vacancies can be annealed out above 600°C as shown in Chapter 2, therefore, in this case, the heating temperature is estimated between 450°C and 600°C (degree "2-1"). If no E' signal is obtained after the treatment, it would be estimated that it had been heated above 600°C (degree "2-2"). The procedure to judge the degree of heat treatment is summarized to an algorithm shown in Fig.3-8.

c. Determination of heating temperature

The temperature of heat treatment is obtained as the following in the case of heating degree "0" and "1". After the heating degree is obtained by the procedure shown in the previous section, E' to oxygen vacancy ratio is obtained by dividing E' intensity observed in the original sample by the one after γ ray irradiation and heating. E' center to oxygen vacancy ratio and the heating temperature show one-to-one correspondence in each region of "degree 0" and in "degree 1" as in Fig.3-7. Therefore, the heating temperature is obtained from the E' to oxygen vacancy ratio by using the curve as the procedure shown in Fig.3-7. The algorithm to estimate the heating temperature is summarized in Fig.3-9. If the degree is "2", the temperature cannot be determined.

d. A control experiment

Several aliquots of quartz grains from a granite were heated at temperatures shown in Table 3-3 for 30 minutes. The heating and irradiation procedures were followed the algorithm shown in Fig.3-9. The E' to oxygen vacancy ratios obtained and the temperatures estimated are summarized in Table 3-2. The procedure is also shown in Fig.3-7. Actual heating temperature and those estimated by the procedure agree completely.

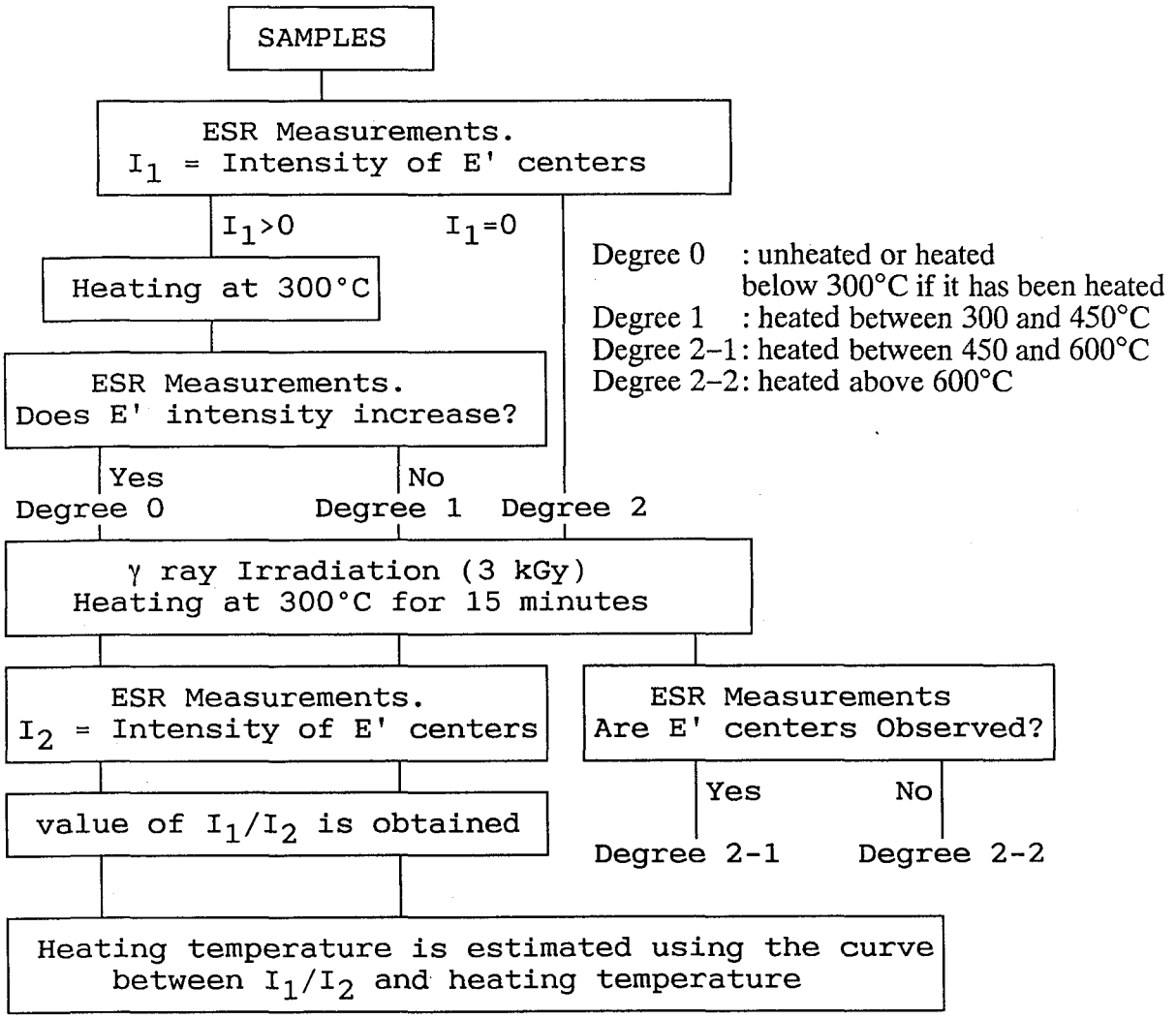

Fig. 3-9The algorithm proposed to estimate the temperature of ancient heat treatment.

Table 3-3 The results of a control experiment. Estimated temperatures agreed with heating temperatures.

Sample	I_1/I_2	Heating Temperature (°C)	Estimated Temperature (°C)
TST-1	0.95	315	310
TST-2	0.60	373	370
TST-3	0.04	445	440

(2) Application to lithic tool fragments

a. Sample description

Our initial application involved the examination of ten specimens from the central Mississippi valley representing two distinctive and well known cherts, the Mill Creek chert from southern Illinois and the Dover chert from western Tennessee. Both cherts are tough materials and were widely traded in the form of hoes in the Late Prehistoric period (e.g., Winters 1981). Two samples represent the raw materials collected at quarry sites were served as referents for the unheated material characteristics. These materials present two common situations with respect to heat treatment.

The Mill Creek chert, typically a light gray (10YR7/1), does change color quite markedly upon heating to a light red (7.5YR6/6) (Dunnell *et al.*, submitted). A minor color variant in the natural material is also light red, presumably from oxidation of iron at ambient temperatures. The Dover chert, on the other hand, is a chert that changes little upon heat treatment, either in color or luster (Dunnell *et al.*, submitted).

The remaining eight specimens are archaeological and originate from two late Mississippian sites, County Line and Langdon, on the Malden Plain in the Eastern Lowlands in the Mississippi valley of Southeast Missouri (see Fig.3-10). The specimens represent various stages in destruction and recycling of hoes. While heat treatment is inimical to the hoe function, recycling for other uses changes the selective conditions. Refashioning into smaller tools may have required it if the material was to be used at all. Hence ascertaining the presence of heat treatment is of particular interest in understanding the consumer reuse of traded lithic material.

b. Results and Discussion

ESR signals observed in some stone implements and a chert are shown in Fig.3-11. The signal of E' centers was observed in the chert of control samples and in LAN279, but not in LAN1035-1.

About 200 mg of raw cherts were heated with a stepwise temperature elevation. The E' intensities expressing the amount of oxygen vacancies were the same as the peak values in stepwise heating for the cherts. This fact indicates that the natural radiation had created sufficient amount of holes which, when the sample is annealed, are transferred to oxygen vacancies and form E' centers.

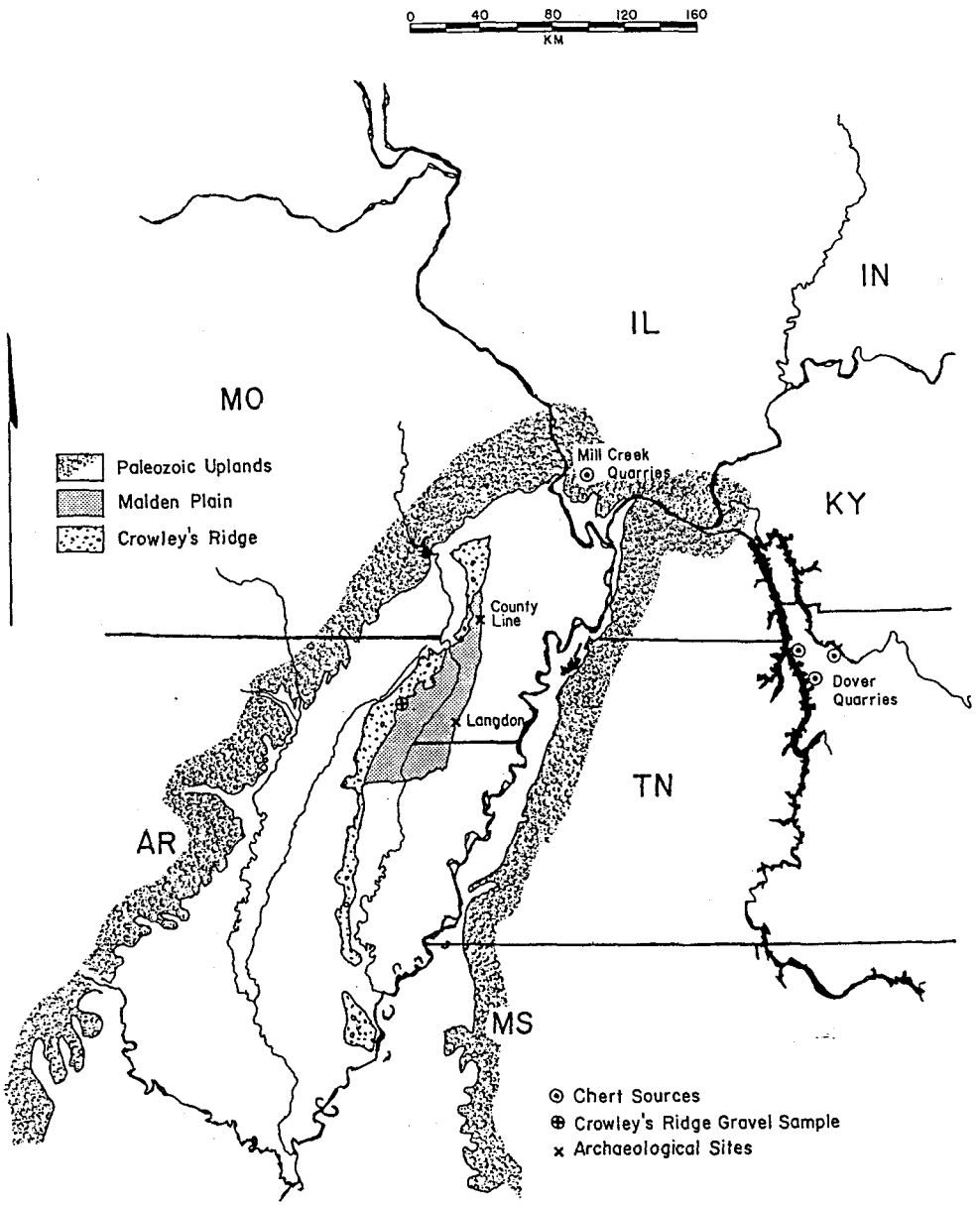

Fig.3-10 A map showing the sample localities of stone implements and of cherts for control experiments.

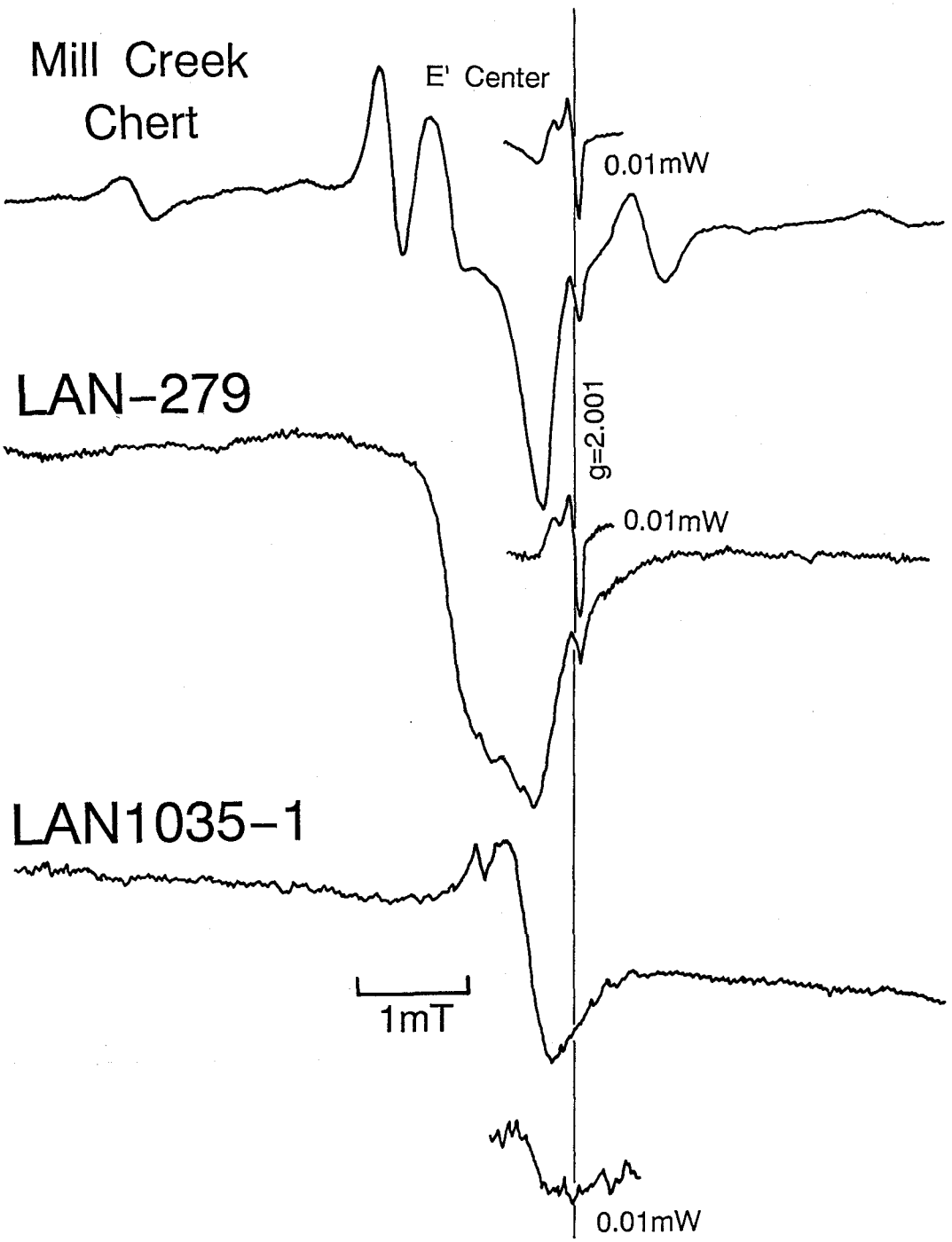

Fig.3-11 ESR spectra obtained at room temperature for stone implements and for a source chert.

The curves between heated temperature and E' to oxygen vacancy ratio were obtained as shown in Fig. 3-12a and 3-12b. The heating temperatures were estimated for lithic tool fragments using these curves and the algorithm shown in Fig. 3-9.

The heating degrees of CL253 and LAN 279 were judged to be "1" because their E' intensities decreased or did not change by heating at 300°C. The temperatures were estimated as shown in Fig.3-12a. E' centers were not observed in LAN1035-1 and in LAN88, but observed after γ ray irradiation and annealing. Therefore, their heating degree was judged to be "2". The increments of E' intensities by heating up to 300°C were rather small for Dover chert. Therefore, the heating temperature for the sample, LAN-1052 the range of which were in "0", could not be determined precisely.

Al centers in these samples gave a complementary information for temperature estimations of these samples. Al centers were observed in LAN946, CL176, and LAN1038, and in both cherts, but not in LAN1052. After γ ray irradiation, they were observed in all samples, and annealed out after subsequent heating at 300°C. These observations imply that Al centers were observed in former samples because of no heat treatment and that they were not in the latter one because of moderate heating. The results are summarized in Table 3-4 and consistent with the method using color of the material.

It is clear from the results of this study that whether or not heat treatment was employed in the manufacture of hoes from either the Mill Creek or Dover cherts (Cobb 1988). Down-the-line consumers, at least in rock poor areas like the Malden Plain did make use of heat treatment when recycling exhausted hoes and hoe resharpening flakes. The size of our sample is too small to identify exactly at what stage in the recycling process heat treatment was introduced or the degree to which this point might have varied to accommodate specific materials or the intended end product. Nonetheless, the suggestion is that heat treatment was not used for large pieces but applied in the final stages of manufacture of small items such as points.

(3) Some problems involved in the method

The change in intensity of E' centers by natural radiation after heating can be neglected because the natural radiation dose would be within 5 Gy for the annual dose rate of 5 mGy/y since the hoe fragments were made in 10th century. This method is applicable only to the materials whose accumulated doses given by natural radiation after heating are within 100 Gy, where the reduction of E' intensity can be neglected.

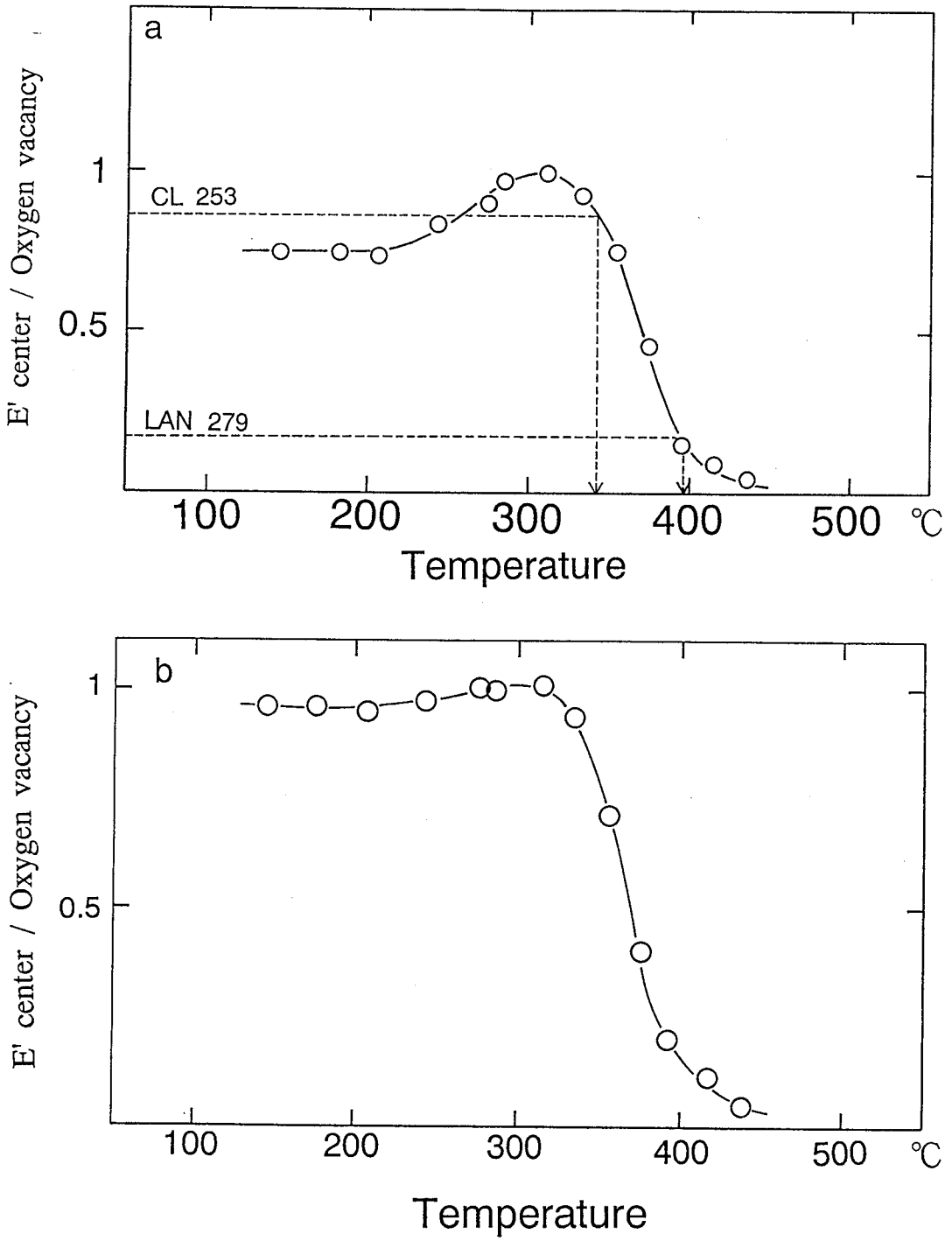

Fig.3-12 a) E' to oxygen vacancy ratio plotted as a function of heating temperature for Mill creek chert. The heating temperatures were estimated for CL253 and LAN279. b) E' to oxygen vacancy ratio plotted as a function of heating temperature for Dover chert.

The duration of prehistoric heat treatment is assumed to be 30 minutes. A simple calculation indicate that temperature is more effective than time. The obtained temperature ranges from 380°C to 355°C when the duration ranges from 20 to 60 minutes, where E' to oxygen vacancy ratio is 0.5, using the parameters obtained for E' centers in Mannari granite as described in Chapter 2.

Table 3–4. The results of an application to lithic tool fragments. The observation of E' centers at each step of the procedures, that of Al centers, and the estimated temperatures are shown.

Sample	Source Chert	Change after heating	I_1/I_2	Al center	Estimated Temperature (°C)
LAN946	M	i	0.71	+	not heated
CL176	M	i	0.78	+	not heated
LAN1035–1	M		0	–	450–600
CL253	M	d	0.85	–	340
LAN279	M	d	0.17	–	400
LAN1038	D	i	0.86	+	not heated
LAN88	D		0	–	450–600
LAN1052	D	i	0.97	–	<300

D: Dover Chert
M: Mill Creek Chert
i: The E' intensity increased by heating at 300°C.
d: The E' intensity slightly decreased or did not change by heating at 300°C.
+ : observed
– : not observed
I_1/I_2: E' to oxygen vacancy ratio

3–4 ESR dating of Ma–Ga range

The ESR signal to noise ratio sets the limitation of about several thousand years to the youngest age of this method (Ikeya, 1988), while thermal stability of the signal impose the oldest limitation of about 2 Ma (e.g. Shimokawa and Imai, 1987). Recently,

Odom and Rink (1989) reported that the intensity of E' centers and of peroxy centers in quartz in granite are correlated with the age in the time range of 0.1 to 1400 Ma. They suggested that these centers in quartz may be used as geochronometer of the above age range, far beyond the limitation so far considered. Recoiled nuclides by α decays were proposed to be the possible cause of defect formation. Their subsequent paper (Rink and Odom, 1991) investigated the α emitters in quartz and tried to evaluate the α-recoil effect.

It has been thought that E' centers are not formed by γ ray irradiation (e.g. Garrison *et al.*, 1981) except for quartz grains at geological faults (e.g. Ikeya *et al.*, 1982). However, Wieser and Regulla (1989) used signal intensity of E' centers in quartz for ESR dosimetry of high dose range (0.1-100 MGy) where E' centers are produced by γ ray irradiation.

The experimental results described in Chapter 2 indicate that two processes are necessary to form E' centers, i.e., formation of oxygen vacancies and transfer of holes to oxygen vacancies with tow electrons. Two interpretations are possible to explain the correlation between age and E' intensities observed by Odom and Rink (1989). One is that oxygen vacancies are created by some pocess in geologic time scale, therfore, the amount of their paramagnetic states, E' centers, also increased with ages. The other is that the amount of oxygen vacancies is constant, but the fraction of paramagnetic states increased with age. E' intensity was observed to increase on heating around 200°C. It would be possible that E' intensity increases with aging at a lower temperature.

(1) Experimental

Quartz grains extracted from granites and from tuffs shown in Table 3-5 were offered for ESR measurement. The procedures for sample preparation and ESR measurement are the same as described in Chapter 2.

The number of oxygen vacancies were measured as E' intensity after ^{60}Co γ ray irradiation at the dose of 3kGy was made prior to heating at 300°C to attain E' intensity to its maximum.

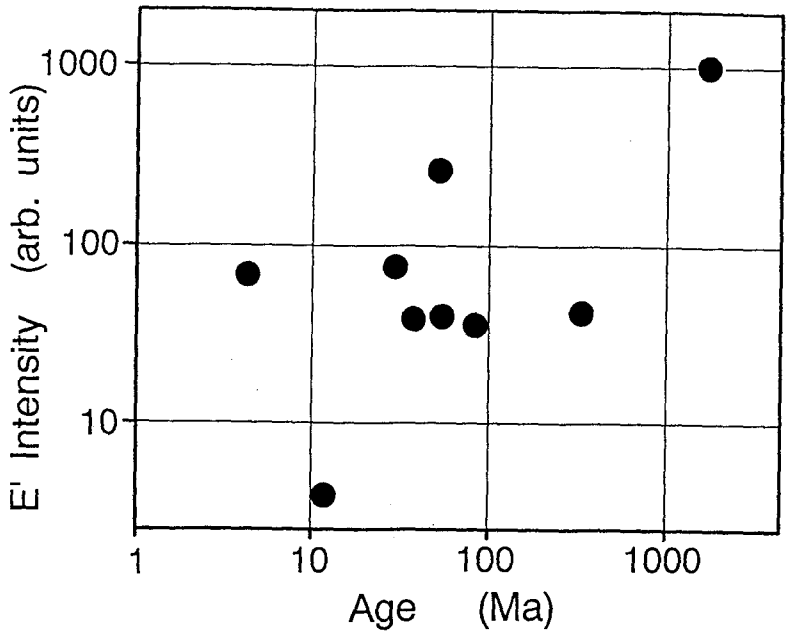

Fig.3-13 ESR intensities of E' centers are plotted as a function of geologic ages in a logarithmic scale. There seems a rough correlation between them.

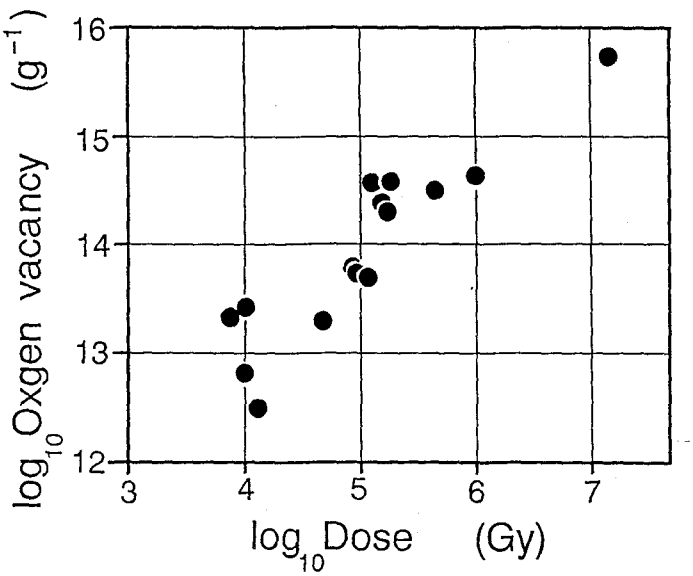

Fig.3-14 The oxygen vacancy concentrations are plotted as a function of absorbed dose calculated from the concentrations of radioactive elements and geologic age (see Table 3-5). The correlation is better than Fig.3-13. The correlation in this figure would suggest the formation of oxygen vacancies in quartz by external β and γ ray radiation.

Table 3–5 Sample description, radiometric age references, and experimental results. Total accumulated doses were calculated from the content of U, Th, and K obtained by γ ray spectroscopy and radiometric ages considering the decays of the elements.

Sample	Age (Ma)	Method	K_2O (%)	U (ppm)	Th (ppm)	Calculated Total Accumulated Dose (Gy)	E' intensity (arb. units)	Amount of Oxygen Vacancy (g^{-1})	Age Reference
Minamihirasawa[1]	3.7–5.1	fossil	2.0	2.4	3.0	8.6×10^{3}	68	2.6×10^{13}	Ohmura *et al.* (1990)
Tentokuji[1]	4.8	F.T.	2.6	1.3	3.2	1.2×10^{4}	n.d.	6.5×10^{12}	Ohmura *et al.* (1990)
Mizuguchi[2]	6.0	F.T.	2.7	1.5	2.8	1.0×10^{4}	n.d.	3.1×10^{12}	Ohmura *et al.* (1990)
Baba[1]	12	^{40}Ar–^{39}Ar	0.36	n.d.	4.2	7.4×10^{3}	3.9	2.2×10^{13}	Takahashi *et al.* (submitted)
Tsukushimori[2]	15	K–Ar	3.6	2.2	5.5	1.3×10^{4}	n.d.	1.9×10^{13}	Ohmura *et al.* (1990)
Masayama[2]	24	F.T.	4.6	3.6	5.0	4.6×10^{4}	n.d.	4.9×10^{13}	Ohmura *et al.* (1990)
Iwamisugisawagawa[2]	24	F.T.	5.4	3.0	2.9	1.1×10^{5}	n.d.	5.3×10^{13}	Ohmura *et al.* (1990)
Oga–1[3]	30	F.T.	3.5	1.2	4.7	9.0×10^{4}	77	6.2×10^{13}	Ohmura *et al.* (1990)
Shimofuruya[4]	38	K–Ar	2.5	1.8	10	1.3×10^{5}	38	4.0×10^{14}	Kawano and Ueda (1966)
Nyudozaki[5]	53	F.T.	2.8	5.2	5.4	8.4×10^{4}	280	2.4×10^{14}	Ohmura *et al.* (1990)
JG–3[4*]	55	K–Ar	2.6	2	8	1.8×10^{5}	39	4.0×10^{14}	Uchiumi *et al.* (1989)
Oga–2[4]	61	F.T.	3.5	2.9	6.8	1.5×10^{5}	n.m.	1.9×10^{14}	Ohmura *et al.* (1990)
JG–1[4*]	85	K–Ar	4.0	3.3	14	4.5×10^{5}	36	3.3×10^{14}	Shibata (1968)
Hikami[4]	339	Rb–Sr	2.5	n.d.	7.3	9.9×10^{5}	42	4.8×10^{14}	Shibata (1974)
Rapakivi[4]	1750	Rb–Sr	4.3	3.1	11	1.4×10^{7}	970	5.8×10^{15}	Piper (1980)

* U, Th, and K concentrations were obtained by Ando *et al.* (1989).

U, Th, and K concentrations of the samples, the ages of which are referred in Ohmura *et al.* were obtained by the authors.

The numbers in the superscription denotes tuff[1], rhyolite[2], quartz porphyry[3], granite[4], and dacite[5].

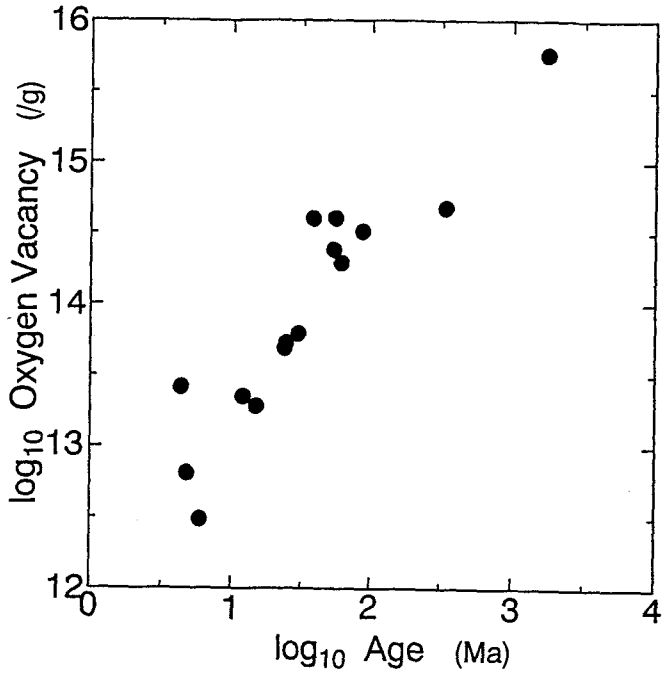

Fig.3-15 The amount of oxygen vacancies are plotted as a function of geologic ages in a logarithmic scale. It suggests that some process creates oxygen vacancies in quartz in geologic time scale.

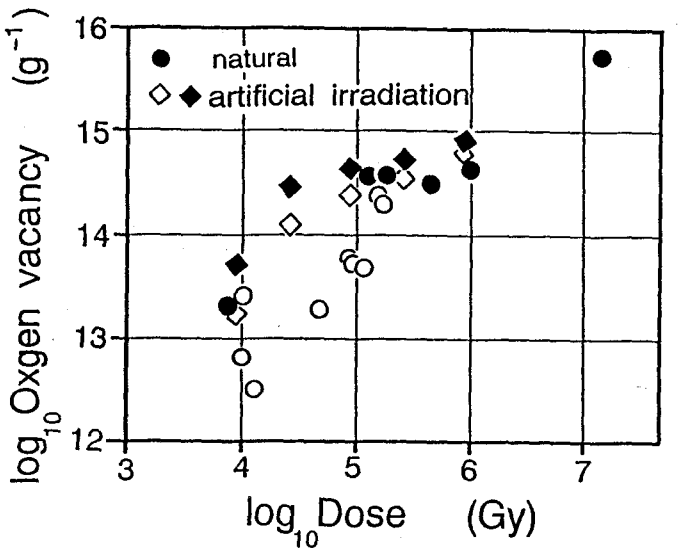

Fig.3-14 The oxygen vacancy concentrations are plotted as a function of absorbed dose with the results of artificial γ irradiation (Fig. 2-12). This figure indicates that external β and γ ray can create the amount of oxygen vacancies observed in quartz in granite.

Average U, Th and K concentration in each granite were measured with γ ray spectroscopy. Annual dose rate was calculated using the table obtained by Nambi and Aitken (1986).

(2) Results and Discussion

The annual dose rate for each sample calculated from U, Th, and K concentrations is listed in Table 3-5. The E' intensities (no treatment) are plotted as a function of age in Fig.3-13. The amount of oxygen vacancies measured as E' intensities are plotted as a function of age (Fig. 3-15) and of total absorbed dose (Fig. 3-14) which are calculated from the annual dose rate and the radiometric age. The correlation factor was remarkably improved in both cases. Fig. 3-15 shows that the amount of oxygen vacancies increases with radiometric ages. It suggestes that oxygen vacancies were accumulated in geologic time but not that the fraction of paramagnetic states increased.

Another problem is what process creates oxygen vacancies in quartz in beologic tiem. Odom and Rink (1989) postulated that α recoil nuclides produce E' centers as well as oxygen vacancies. However, it was reported that the E' intensity measured after heating at 300°C increased with γ ray dose in the range of 0.1-100 MGy (Wieser and Regulla, 1989). This intensity should corresponds to the number of oxygen vacancies because of the similarity of their treatment with our method. Their results indicate that oxygen vacancies are created by γ ray irradiation at a high dose region.

Total accumulated dose for these granite samples are calculated to be $8x10^3$ to $1x10^7$ Gy from the external annual dose rate and the age. It is no wonder that oxygen vacancies are created in this dose range, considering the result of Wieser and Regulla (1989). Indeed, an experiment in Section 2-5 confirmed their result as shown in Fig.2-12. Comparing Fig.2-12 with Fig.3-14, the amounts of oxygen vacancies in natural quartz are consistent with those created by artificial γ ray irradiation.

The ESR signal intensity of E' centers increases on heating below 300°C (e.g. Jani *et al.*, 1983) but decreases by subsequent γ ray irradiation with the dose of around 1 kGy (Sato *et al.*, 1985). Therefore, E' intensity might be affected by some shallow heating event or by natural dose rate as well as by the number of oxygen vacancies. The number of oxygen vacancies would be a better value because it is not affected on heating below 400°C as shown in Chapter 2. In fact, the correlation factor was improved for plotting of the number of oxygen vacancy.

Some variation in the number of oxygen vacancies (Fig.3–14) may be caused by the cooling rate of granite. Oxygen vacancies would be accumulated when the temperature decreased around 200°C, as discussed in Section 3–1. Wieser and Regulla (1989) pointed out that production rate increases with temperature, and that the rate at 150–200°C is about twice as much as the one at room temperature. It implies that oxygen vacancy would be created more in the case of slow cooling than in the case of rapid one.

In conclusion, it is probable that the β and γ ray create oxygen vacancies in quartz in granite. The possibility of creation by α recoil nuclides included in quartz grains cannot be excluded, but at least the amount created by β and γ ray cannot be neglected. Further studies would be needed to evaluate both efficiencies and to investigate creation of peroxy centers by γ ray irradiation, which has been discussed in terms of α recoil effect (Rink and Odom, 1991).

Summary

Formation and decay kinetics of E', Al, and Ti centers and of oxygen vacancies were investigated. An experimental procedure to estimate the number of oxygen vacancies was proposed. The results of isochronal and isothermal heating experiments indicate that all these centers decay following the second order decay kinetics implying that the centers decay by recombining with another center whose numbers are about the same. Oxygen vacancies decay following second order decay kinetics, too. It was confirmed that oxygen vacancies are created not only by fast neutron irradiation, but also by γ ray irradiation at a heavy dose more than 1000 Gy. Using the results obtained above, the following problems on ESR dating were discussed.

1. Closure temperatures for ESR dating using E', Al, and Ti centers were estimated to be 91°C, 78°C, and 31°C, respectively, with a cooling rate of about 10°C/Ma by numerical calculation with considering accumulation and decay following second order kinetics.

2. A thermal history around an intrusive rock was investigated using oxygen vacancies in quartz extracted from metamorphic rocks. The distribution of the concentrations of oxygen vacancies was not consistent with the one predicted by numerical simulation. However, the simulation clearly show that the temperature rise caused by a dike intrusion would anneal several lattice defects near the intrusion.

3. As an Archaeological application, a new technique was proposed to estimate heat treatment for ancient stone implements. A control experiment gave successful results. The method was first practically applied to implements of American Indians' about 10th century.

4. Concentration of oxygen vacancies in quartz from volcanic rocks was found to be correlated with total accumulated dose calculated by using the radiometric ages and external β and γ ray dose rates ranging from 10 to 1400 Ma. The possibility of formation of oxygen vacancies by β and γ rays was tested and discussed.

These findings and new approaches will hopefully contribute for ESR dating method to expand its field of applications.

Acknowledgements

I wish express my sincere gratitude to my promoter, Professor Motoji Ikeya for introducing me to this field of research and for many invaluable suggestions for the studies. I also express my gratitude to Dr. T. Miki (Yamaguchi University) for giving me a useful suggestions on formation kinetics on E'_1 center in quartz. I would like to appreciate Dr. T. Nagatomo's (Nara University of Education) invaluable discussions on ESR dating and his kindness in γ ray spectroscopy.

I am indebted to Prof. R.C. Dunnell, Dr. K. Saito, Dr. F. Goff, Dr. Y. Tsuji, and Dr. S. Ito for sample provisions. I also thank Dr. T. Tanaka for age references. I express my appreciation to Dr. J. Rink for encouraging discussion.

I acknowledge Dr. I. Katakuse, Dr. C. Yamanaka, Dr. S. Ikeda, Dr. M. Furusawa, Mr. T. Ichihara, and Dr. M. Kasuya for useful discussions and experimental cooperation. I also express my thank to Mr. H. Kohno, Mr. K. Ogoh, Mr. K. Meguro, Ms. J. Morikawa, Mr. H. Minamibayashi, and Mr. K. Yamamoto for their helpful cooperation.

The γ ray irradiation was made at the Industry of Scientific and Industrial Research Osaka University. This work is partially supported by Grant-in-Aid for Encouragement of Young Scientists (No. 04854028, 03854034, 02854035) provided by the Ministry of Education, Science and Culture, by Itoh Science Foundation and by Inoue Science Foundation.

References

Aitken, M.J. (1985) Thermoluminescence Dating: Academic Press, London.

Anderson, J.H. and Weil, J.A. (1959) Paramagnetic resonance absorption of color centers in germanium-doped quartz, *J. Chem. Phys.*, 31, 427-434.

Anderson, J.H., Feigl, F.J., and Schlesinger, M. (1974) The effects of heating on color centers in germanium-doped quartz, *J. Phys. Chem. Solids*, 35, 1425-1428.

Ando, A., Kamioka, H., Terashima, S., and Ito, S. (1989) 1988 values for GSJ rock reference samples, "Igneous rock series", *Geochem. J.*, 23, 143-148.

Arends, J., Dekker, A. J. and Perdok, W. G. (1963) Color centers in quartz produced by crushing, *Phys. Status Solidi*, 3, 2275-2279.

Ariyama, T. (1985) Conditions of resetting the ESR clock during faulting, *ESR Dating and Dosimetry*, 251-258.

Baker, J.M. and Robinson, P.T. (1983) EPR of a new defect in natural quartz: possibly O_2^-, *Solid State Commun.*, 48, 551-554.

Barker, P.R. (1975) Hyperfine parameters of the Al centre in smoky quartz, *J. Phys. C: Soid State Phys.*, 8, L412-414.

Becker, W. and Lehmann, G. (1980) Anomolous hyperfine splitting of ^{57}Fe in alpha-quartz, *Solid State Commun.*, 35, 367-369.

Berger, G.W. and York, D. (1981) Geothermometry from $^{40}Ar/^{39}Ar$ dating experiments, *Geochim. Cosmochim. Acta*, 45, 795-811.

Bossoli, R.B., Jani, M.G., and Halliburton, L.E. (1982) Radiation-induced E" centers in crystalline SiO_2, *Solid State Commun.*, 44, 213-217.

Bossoli, R.B. and Halliburton, L.E. (1983) ^{27}Al hyperfine and quadrupole interactions for the $[AlO_4]^0$ center in quartz, *Phys. Status Solidi B*, 136, 709-714.

Buhay, W. M., H. P. Schwarcz and R. Grun (1988) ESR dating of fault gouge: the effect of grain size, *Quat. Sci. Rev.*, 7, 515-522.

Calk, L.C. and Naeser, C.W. (1973) The thermal effect of a basalt intrusion of fission tracks in quartz monzonite, *Journal of Geology*, 81, 189-198.

Chandra, H., Symons, M.C.R., and Griffith, D.R. (1988) Stable perinaphthenyl radicals in flints, *Nature*, 332, 526-527.

Cobb, C.R. (1988) Mill Creek chert biface production: Mississippian Political Economy in Illinois., *Ph. D. Dissertation, Department of Anthropology, Southern Illinois University, Carbondale. University Microfilms, Ann Arbor.* .

Cox, R.T. (1976) ESR of an S=2 center in amethyst quartz and its possible identification as the d^4 ion Fe^{4+}, *J. Phys C: Solid State Phys.*, 10, 3355-3361.

Davis, P.H. and Weil, J.A. (1978) Silver atom center in alpha-quartz, *J. Phys. Chem. Solids*, 39, 775-780.

Dodson, M.H. (1973) Closure temperature in cooling geochronological and petrological systems, *Contr. Mineral. and Petrol.*, 40, 259-274.

Dodson, M.H. and McClelland-Brown, E. (1985) Isotopic and paleomagnetic evidence for rates of cooling, uprift and erosion, *Geol. Soc. Mem.*, no.10, 315-325.

Duchesne, J., Depireux, J., and van der Kaa, J.M. (1961) Origin of free radicals in carbonaceous rocks, *Geochim. Cosmochim. Acta*, 23, 209–218.

Dunnell, R.C., Ikeya, M., McCutcheon, P.T., and Toyoda, S. (submitted) Heat treatment of Mill creek and Dover cherts on the Malden Plain, Southeast Missouri, *J. Archaeol. Sci.*

Feigl, F.J., Fowler, W.B., and Yip, K.L. (1974) Oxygen vacancy model for the E_1' center in SiO_2, *Solid State Commun.*, 14, 225–229.

Friebele, E.J., Griscom, D.L., and Stapelbroek, M. (1979) Fundamental defect centers in glass: The peroxy radical in irradiated high–purity, fused silica, *Physical Rev. Lett.*, 42, 1346–1349.

Fukuchi, T. (1986) ESR dating of fault movement using various defect centers in quartz; the case in the western south Fossa Magna, Japan, *Earth Planet. Sci. Lett.*, 78, 121–128.

Fukuchi, T. (1988) Applicability of ESR dating using multiple centres to fault movement — the case of the Itoigawa Shizuoka Tectonic line, a major fault in Japan, *Quat. Sci. Rev.*, 7, 509–514.

Fukuchi, T. (1989) ESR dating of fault movement and frictional heating by faulting, *Ph. D. Thesis, University of Tsukuba, Japan* .

Garrison, E.G., Rowlett, R.M., Cowan, D.L., and Holroyd, L.V. (1981) ESR dating of ancient flints, *Nature*, 290, 44–45.

Garrison, E.G. (1989) Characterization of an ESR Geochronological dating center in flints, *Phys. Chem. Minerals*, 16, 767–773.

Giletti, B.J. and Yund, R.A. (1984) Oxygen diffusion in quartz, *J. Geophys. Res.*, 89, 4039–4046.

Griffith, D.R., Seeley, N.J., Chandra, H., and Symons, M.C.R. (1983) ESR dating of heated chert, *PACT J.*, 9, 399–409.

Griffith, D.R., Robins, G.V., Seeley, N.J., Chandra, H., McNeil, D.A.C., and Symons, M.C.R. (1982) Trapped methyl radicals in chert, *Nature.*, 300, 435–436.

Griffith, J.H.E., Owen, J., and Ward, I.M. (1954) Paramagnetic resonance in neutron–irradiated diamond and smoky quartz, *Nature*, 173, 439–442.

Griscom, D.L. (1979) E' center in glassy SiO_2: Microwave saturation properties and confirmation of the primary 29Si hyperfine structure, *Phys. Rev. B*, 20, 1823–1834.

Griscom, D.L. (1980) E' center in glassy SiO_2: ^{17}O, ^{1}H, and "very weak" ^{29}Si superhyperfine structure, *Phys. Rev.*, 22, 4192–4202.

Grün, R. and Invernati, C. (1985) Uranium accumulation in teeth and its effect on ESR dating — A detailed study of a mammoth tooth, *Nucl. Tracks*, 10, 869–878.

Halliburton, L.E., Perlson, B.D., Weeks, R.A., Weil, J.A., and Wintersgill, M.C. (1979) EPR study of the E_4' center in alpha–quartz, *Solid State Commun.*, 30, 575–579.

Harrison, T.M., Armstrong, R.L., Naeser, C.W., and Harakal, J.E. (1979) Geochronology and thermal history of the Coast Plutonic Complex, near Prince Rupert, British Columbia, *Can. J. Earth Sci.*, 16, 400–410.

Harrison, T.M. and McDougall, I. (1980) Investigations of an intrusive contact, northwest Nelson, New Zealand I. Thermal, chronological and isotopic constraints, *Geochim. Cosmochim. Acta*, 44, 1985–2003.

Hitt, K.B. and Martin, J.J. (1983) Radiation–induced mobility of lithium and sodium in alpha–quartz, *J. Appl. Phys.*, 54, 5030–5031.

Ikeda, S., Kasuya, M., and Ikeya, M. (1991) ESR Ages of Middle Pleistocene Corals from the Ryukyu Islands, *Quatern. Res.*, 36, 61–71.

Ikeya, M. (1975) Dating of a stalactite by electron paramagnetic resonance, *Nature*, 255, 48–50.

Ikeya, M. and Miki, T. (1980) Electron spin resonance dating of animal and human bones, *Science*, 207, 977–979.

Ikeya, M. and Ohmura, K. (1981) Dating of fossil shells with electron spin resonance, *J. Geol.*, 89, 247–251.

Ikeya, M., Miki, T., and Tanaka, K. (1982) Dating of a Fault by Electron Spin Resonance on Intrafault Materials, *Science*, 215, 1392–1393.

Ikeya, M., Miki, T., Tanaka, K., Ohmura, K., and Sakuramoto, Y. (1983) ESR dating of faults at Rokko and Atotsugawa, *PACT J.*, 9, 411–419.

Ikeya, M. and Ohmura, K. (1983) Comparison of ESR ages of corals from marine terraces with ^{14}C and $^{230}Th/^{234}U$ ages, *Earth Planet. Sci. Lett.*, 65, 34–38.

Ikeya, M. (1983) ESR studies of geothemal boring cores at Hachobara power station, *Jpn. J. Appl. Phys.*, 22, 763–769.

Ikeya, M. (1985) Electron spin resonance, *In Dating method of Pleistocene deposits and their problems. Rutter, N.W. ed. Geological Society of Canada Publications, Tronto.*, 73–87.

Ikeya, M. and Miki, T. ed. (1985) ESR DATING AND DOSIMETRY, IONICS, Tokyo.

Ikeya, M. (1988) Dating and Radiation Dosimetry with Electron Spin resonance, *Magn. Reson. Rev.*, 13, 91–134.

Ikeya, M., Toyoda, S. and Minamibayashi, H. (1990) ESR studies of thermal effect in metamorphic rock around an intrusion zone, *J. ESR Appl. Metrol.*, 6, 2–10.

Imai, N. Shimokawa, K., and Hirota, M. (1985) ESR dating of volcanic ash, *Nature*, 314, 81–83.

Imai, N. and Shimokawa, K. (1988) ESR dating of quaternary tephra from Mt. Osore–zan using Al and Ti centers in quartz, *Quart. Sci. Rev.*, 7, 523–527.

Ishii, H., Ikeya, M., and Meguro, K. (submitted) Dosimetry of tooth enamels and defects in synthetic apatite, *Appl. Radiat. Isot.* .

Isoya, J. and Weil, J.A. (1979) Uncompensated titanium(3+) center in alpha–quartz, *Phys. Status Solidi A*, 52, K193.

Isoya, J., Bowman, M.K., Norris, J.R., and Weil, J.A. (1983a) An electron spin echo envelope modulation study of lithium nuclear hyperfine and quadrupole coupling in the A(Ti–Li) center of a–quartz, *J. Chem. Phys.*, 15, 1735–1746.

Isoya, J., Weil, J.A., and Davis, P.H. (1983b) EPR of atomic hydrogen 1H and 2H in alpha–quartz, *J. Phys. Chem. Solids*, 44, 335–343.

Jani, M.G., Bossoli, R.B., and Halliburton L.E. (1983) Further characterization of the E'1 center in crystalline SiO2, *Phys. Rev. B.*, 27, 2285–2293.

Kawano, Y. and Ueda, Y. (1966) K–A dating on the igneous rocks in Japan (V) —Granitic rocks in southwestern Japan —, *The Journal of Japanese association of mineralogists, petrologists, and economic geologists*, 56, 191–211.

Kneubühl, F.K. (1960) Line shapes of electron paramagnetic resonance signals produced by powders, glasses, and viscous liquids, *J. Chem. Phys.*, 33, 1074–1078.

LePage, Y.L. and Donnay, G. (1976) Refinement of the crystal structure of low–quartz, *Acta Cryst.*, B32, 2456–2459.

Levy, P.W. (1984) Thermoluminescence systems with two or more glow peaks described by anomalous kinetic parameters, *Nucl. Inst. Method Phys. Res.*, B1, 436–444.

Mackey, J.H. Jr. (1963) EPR study of impurity-related color centers in germanium-doped quartz, *J. Chem. Phys.*, 39, 74–83.

Maschmeyer, D. and Lehmann, G. (1982) An Al O– P radiation defect in rose-colored quartz, *Solid State Chem. Proc. Second European Conf., Veldhoven, Holland. in Studies in Inorganic Chemistry, ed. by Metsclaar, R., Heijligers, H.J.M., Schoonman, J. Elsevier, Amsterdam*, 315–318.

McKeever, S.W.S. (1978) Thermoluminescence of solids, Cambridge University Press.

McMorris, D.W. (1971) Impurity color centers in quartz and trapped electron dating: electon spin resonance, thermoluminescence studies, *J. Geophys. Res.*, 76, 7875–7887.

Melcher, C.L. and Zimmerman. D.W. (1977) Thermoluminescence Determination of prehistoric heat treatment chert artifacts, *Science*, 197, 1359–1362.

Miki, T. and Ikeya, M. (1981) The physical basis of ESR dating of fault movements (Japanese title translated), *The Earth Monthly*, 3, 500–504.

Miki, T. and M. Ikeya (1982) Physical basis of a fault dating with ESR, *Naturwissenschaften*, 69, 390–391.

Mombourquette, M.J., Tennant, W.C., and Weil, J.A. (1984) EPR study of Fe3+ in alpha-quartz: a re-examination of the so-called I-center.

Nambi, K.S.V. and Aitken, M.J. (1986) Annual dose conversion factors for TL and ESR dating, *Archaeometry*, 28, 202–205.

Nuttal, R.H.D. and Weil, J.A. (1980) Two hydrogenic trapped-hole species in alpha-quartz, *Solid State Commun.*, 33, 99–102.

Nuttal, R.H.D. and Weil, J.A. (1981a) The magnetic properties of the oxygen-hole aluminum centers in crystalline SiO2. I. $[AlO_4]^0$, *Can. J. Phys.*, 59, 1696–1708.

Nuttal R.H.D. and Weil, J.A. (1981b) The magnetic properties of the oxygen-hole aluminum centers in crystalline SiO_2 II $[AlO_4/H^+]^+$ and $[AlO_4/Li^+]^+$, *Can. J. Phys.*, 59, 1709–1718.

Nuttal R.H.D. and Weil, J.A. (1981c) The magnetic properties of the oxygen-hole aluminum centers in crystalline SiO2 III $[AlO_4]^+$, *Can. J. Phys.*, 59, 1886–1892.

O'Brien, M.C.M. (1955) The structure of the colour centers in smoky quartz, *Proc. Roy. Soc. A*, 231, 404–414.

Odom, A.L. and Rink, W.J. (1989) Natural accumulation of Shottky-Frenkel defects: Implications for a quartz geochronometer, *Geology*, 17, 55–58.

Ohmura, K., Okazaki, K., Ishiguchi, M., and Sakuramoto, Y. (1989) A report on ESR dating of Tertiary volcanic rocks, *Ed. Japan National Oil Corp., Studies on genesis and development of sedimentary basin* .

Okada, M., Rinneberg, H., Weil, J.A., and Wright, P.M. (1971) EPR of Ti^{3+} centers in a-quartz, *Chem. Phys. Letters*, 11, 275–276.

Piper, J.D.A. (1980) Paleomagnetic study of the Swedish Rapakivi Suite: Proterozoic tectonics of the Baltic shield, *Earth Planet. Sci. Lett.*, 46, 443–461.

Porat, N. and Schwarcz, H.P. (1991) Use of signal subtraction methods in ESR dating of burned flint, *Nucl. Track Radiat. Meas.*, 18, 203–212.

Purdy, B.A. and Brooks, H.K. (1971) Thermal alteration of silica materials: An archaeological approach, *Science*, 173, 322–325.

Rink, W.J. and Odom, A.L. (1991) Natural alpha recoil particle radiation and ionizing radiation sensitivities in quartz detected with EPR: implications for geochronometry, *Nucl. Tracks Radiat. Meas.*, 18, 163–173.

Rinneberg, H. and Weil, J.A. (1972) EPR studies of Ti^{3+}–H^{+} centers in x–irradiated alpha–quartz, *J. Chem. Phys.*, 56, 2019–2028.

Robins, G.V., Seeley, N.J., McNeil, D.A.C., and Symons, M.C.R. (1978) Identification of ancient heat treatment in flint aftefacts by ESR spectroscopy, *Nature.*, 276, 703–704.

Rudra, J.K., Fowler, W.B., and Feigl, F.J. (1985) Model for the E_2' center in alpha quartz, *Phys. Rev. Lett.*, 55, 2614–2617.

Rudra, J.K. and Fowler, W.B. (1987) Oxygen vacancy and the E'_1 center in crystalline SiO_2, *Phys. Rev. B*, 35, 8223–8230.

Sato, T., Suito, K., and Ichikawa, Y. (1985) Characteristics of ESR and TL signals on quartz from fault regions, *ESR Dating and Dosimetry*, 267–273.

Schinadt, R. and Schneider, J. (1970) The electronic structure of the trapped–hole center in smorky quartz, *Phys. Kondens. Materie*, 11, 19–42.

Schnadt, R. and Räuber, A. (1971) Motional effects in the trapped–hole center in smorky quartz, *Solid State Commun.*, 9, 159–161.

Shibata, K. (1968) K–Ar age determinations on granitic and metamorphic rocks in Japan, *Chishitsu Chosasho Hokoku*, No.227, 71.

Shibata, K. (1974) Rb–Sr geochronology of the Hikami granite, Kitakami mountains, Japan, *Geochem. J.*, 8, 193–207.

Shibata, K. (1991) K–Ar ages of potassium feldspar and its closure temperature (Japanese title translated), *Chishitsu News*, no.437, 7–14.

Shimokawa, K., Imai, N., and Hirota, M. (1984) Dating of a volcanic rock by electron spin resonance, *Isotope Geoscience*, 2, 365–373.

Shimokawa, K. and Imai, N. (1985) ESR dating of quartz in tuff and tephra, *ESR Dating and Dosimetry, IONICS, Tokyo*, 181–185.

Shimokawa, K. and Imai, N. (1987) Simultaneous determination of alteration and eruption ages of volcanic rocks by electron spin resonance, *Geochimica et Cosmochimica Acta*, 51, 115–119.

Shimokawa, K., Imai,N., and Moriyama, A. (1988) ESR dating of volcanic and baked rocks, *Quaternary Sci. Rev.*, 7, 529–532.

Silsbee, R.H. (1961) Electron spin resonance in neutron–irradiated quartz, *J. Appl. Phys.*, 32, 1459–1462.

Stapelbroek, M., Griscom, D.L., Friebele, E.J., and Sigel, G.H., Jr. (1979) Pxygen–associated trapped–hole centers in high–purity fused silicas, *J. Non–crystal. Solids*, 32, 313–326.

Taguchi, S., Harayama, M., and Hayashi, M. (1985) ESR signal of zircon and geologic age, *ESR Dating and Dosimetry*, 191–196.

Takahashi, M. and Saito, K. (1992) K–Ar and ^{39}Ar–^{40}Ar ages of miocine Kitamura and Baba tuffs, Gunma prefecture — with special reference to the N.13–N.14 boundary of planktonic forminiferal zones —, *Jour. Geol. Soc. Japan*, 98, 323–335.

Tanaka, T., Sawada, S., and Ito, T. (1985) ESR dating of late Pleistocene nearshore and terrace sands, in southern Kanto, Japan, *ESR Dating and Dosimetry, IONICS, Tokyo*, 219–228.

Tanaka, K. (1989) Dating of fault movement by ESR method — basis and application, *Ph. D. Thesis, University of Kyushu, Japan* .

Taylor, A.L. and Farnell, G.W. (1964) Spin-lattice interaction experiments on colour centers in quartz, *Can. J. Phys.*, 42, 595-607.

Tsukamoto, Y., Yamanaka, C., and Ikeya, M. (in press) Fundamental study on ESR dating of outer planets and the satellites, *Appl. Radiat. Isot.* .

Uchida, Y., Isoya, J., and Weil, J.A. (1979) Dynamic interchange among three states of phosphorus(4+) in alpha-quartz. I, *J. Phys. Chem.*, 83, 3462-3467.

Uchiumi, S., Uto, K., and Shibata, K. (1989) K-Ar ages of rock reference materials, *Mass Spectrometry*, 37, 375-381.

Weeks, R.A. (1956) Paramagnetic resonance of lattice defects in irradiated quartz, *J. Appl. Phys.*, 27, 1376-1381.

Weeks, R.A. and Nelson, C.M. (1960) Trapped electrons in irradiated quartz and silica: II. Electron spin resonance, *J. Am. Ceram. Soc.*, 43, 399-404.

Weil, J.A. and Anderson, J.H. (1961) Direct field effects in electron paramagnetic resonance hyperfine spectra, *J. Chem. Phys.*, 35, 1410-1417.

Weil, J.A. (1971a) The analysis of large hyperfine splitting in paramagnetic resonance spectroscopy, *J. Mag. Reson.*, 4, 394-399.

Weil, J.A. (1971b) Germanium-hydrogen-lithium center in a-quartz, *The Journal of Chem. Phys.*, 55, 4685-4698.

Weil, J.A. (1984) A Review of Electron Spin Spectroscopy and Its Applications to the Study of Paramagnetic Defects in Crys-talline Quartz, *Phys. Chem. Minerals*, 10, 149-165.

Warashina, T., Higashimura, T., and Nakao, Y. (1981) Determination of firing temperatures of ancient pottery by means of ESR spectroscopy, *British Museum Occasional Papers*, 19, 117-128.

Wieser, A. and Regulla, D.F. (1989) ESR dosimetry in the "Giga-rad" range, *Appl. Radiat. Isot.*, 40, 911-913.

Wieser, A., Göksu, Y., and Regulla, D.F. (1986) The ESR spectrum as an indicator of the archaeological heating temperature of flints, *Proceedings of the 1st International Conference on Prehistoric Flint Mining and Lithic Raw Material Identification in the Carpathian Basin, Budapest-Sumeg*, 175-182.

Winters, H.D. (1981) Excavating in Museums: Notes on Mississippian hoes and Middle Woodland copper Gouges and cherts, *In, Research Potential of Anthropological Museum Collections, edited by A.E. Cantwell, J,B. Griffin, and N.A. Rothschild, Annals of the New York Academy of Science, No.376. New York.*, 17-34.

Wright, P.M., Weil, J.A., Buch, T., and Anderson, J.H. (1963) Titanium color centers in rose quartz, *Nature*, 197, 246-248.

Yokoyama, Y., Quaegebeur, J.P., Bibron, R., Leger, C., Nbuyen, H., and Poupeau, G. (1982) Datation du site de l'Homme de Tautavel par la resonance de spin electronique (ESR), *Comptes Rendus des Searces de l'academie des Sciences, paris Series II*, 294, 759-764.

Yokoyama, Y., Falgueres, C., and Quaegebeur, J.P. (1985) ESR dating of sediment baked by lava flows: Comparison of paleo-doses for Al and Ti centers, *ESR Dating and Dosimetry, Ikeya, M. and Miki, T., Eds. (IONICS, Tokyo)*, 197-204.

Zeller, E.J. (1968) Use of electron spin resonance for measurement of natural radiation damage, *in Thermoluminescence of Geological Materials. ed. McDougall, D.J., Academic Press, London*, 271–279.

APPENDIX

Annual Dose Rate from Atmospheric Radon Activities

Abstract

The effect of atmospheric radon activities on the annual dose rate of natural radiation is calculated so that the electron spin resonance (ESR) and thermoluminescence (TL) ages of limestone cave deposits are refined. When the surface of a cave is dry, both the dose rate from α rays and that from β rays were calculated to be comparable to that from β rays assuming 1 working level (1WL = 3700 Bq/m^3) of ^{222}Rn activity. Although the surface is wet, 0.2 mGy/y of β rays from daughter elements would be given, taking shielding and wash-out effect of water into account. The effect is evaluated for ESR dating of Petralona cave deposits in Mausoleum.

1. Introduction

Extremely high radon activity especially in summer in a cave was discovered during 1976 investigation of Akiyoshi cave for clarifying radiation environment to refine ESR dating method. The preliminary result was reported in Anthropos (Ikeya, 1977). Detailed analysis of radon emanation for a cave was published using a model of cylinder (Miki and Ikeya, 1980). The effect of the atmospheric radioactivity was simply neglected in the ESR dating of carbonate deposits because the effect seemed negligibly small at Akiyoshi cave (Ikeya, 1977). The high total dose of natural radiation (TD) of some cave travertine at the surface was detected with ESR both at Akiyoshi and at Petralona. The

possibility was cited that the effect may be due to atmospheric radon activities but again neglected considering the dose rate estimated to be low and a continuous growth of the travertine (Ikeya, 1980).

Petralona cave dating controversy again raised this question as the external dose rate to the cranium encrust was extraordinary high as 1.90 mGy/y observed by Hennig *et al.* (1981;1982) in contrast to other results (Ikeya, 1978, Liritzis and Poulianos, 1980). Recent remeasurement by Greek nuclear physicists at the site of cranium gave the external γ ray dose rate of 0.35 mGy/y (Papastefanou et al. 1986) roughly in agreement with our earlier result of 0.50 mGy/y (Ikeya, 1977) and with that of 0.80 mGy/y (Ikeya, 1978). However, Greek physicists did not revise the age of Petralona carbonate and cranium with the new dose rate presumably due to the high activity of atmospheric radon, 1.28×10^4 and 1.72×10^4 Bq/m^3 (Papastefanou *et al.*, 1986). Although it is not clear whether the effect of the daughters is excluded in their α ray track detection, the result might give the high annual dose rate from atmospheric radon.

In this paper, we estimate the annual dose rate to the surface of the material from the activity of ^{222}Rn and its daughter nuclides in air and on the surface of the material.

Table A–1 Half lives, Decay Constants, and Energies of α and β decays of Radioactive nuclides after ^{222}Rn in ^{238}U–series disintegration.

i	Nuclides	Half Life	Decay Constant (y^{-1})	Energy of α Decay(MeV)	Energy of β Decay(MeV)
1	^{222}Rn	3.82 day	66.6	5.49	
2	^{218}Po	3.05 min.	1.18×10^5	6.00	
3	^{214}Pb	26.8 min.	1.35×10^4		1.03(6%),0.67(94%)
4	^{214}Bi	19.7 min.	1.82×10^4		3.26(19%),1.88(9%),1.51(40%) 1.0(23%),0.4(9%)
5	^{214}Po	0.164 msec.	1.29×10^{11}	7.69	
6	^{210}Pb	22.3 year	3.15×10^{-2}		0.061(19%),0.015(81%)
7	^{210}Bi	5.01 day	50.6		1.160(99+%)
8	^{210}Po	139 day	1.81	5.31	

2. The Energy Given by α particles

α particles are produced in the decays of ^{222}Rn and its daughters, ^{218}Po, ^{214}Po, and ^{210}Po (see Table A–1). The relation between the energy and the range of an α particle is obtained by integrating the stopping power for energy as follows,

$$R = 3.18 \times 10^{-3} E^{3/2} \qquad (1)$$

E (MeV): Energy of α particle

R (m): Range of α particle with energy E in air

In the case that an α particle produced at x m from a plane of the surface enters into the carbonate from a perpendicular direction to its plane, the relation between the residual range, R–x, and the energy, $E_\alpha(x)$, given to the surface is,

$$R - x = 3.18 \times 10^{-3} E_\alpha(x)^{3/2} \qquad (2)$$

where R is given by equation (1). From equation (2), we get

$$E_\alpha(x) = 46.2\,(R-x)^{2/3} \qquad (\text{MeV}) \qquad (3)$$

The energy of α particles given to a very small region, $dS(m^2)$, from radioactive elements in air is obtained by integrating the contribution from a very small volume in air from which α particles can reach the considered surface. The very small volume in air is given by the following expression (see Fig.A–1).

$$dV = x^2 \sin\theta \, dx \, d\theta \, d\psi \qquad (4)$$

The ratio of the α particles which reach dS to total α particles from dV, i.e., the ratio of the solid angle of dS to the total solid angle, is

$$\frac{dS \cos\theta}{4 \pi x^2} \qquad (5)$$

Then, the energy of α particles given to dS is given by (3), (4) and (5)

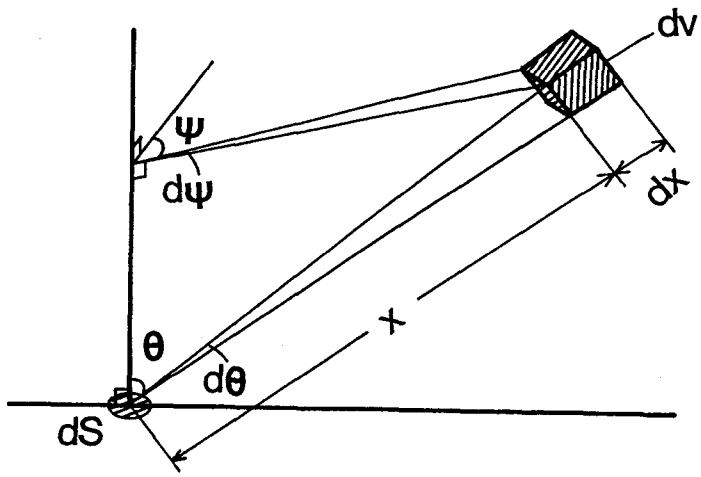

Fig.A–1 The energy given to dS by α and β rays are obtained by integrating the energy from the radioactive elements in a very small volume, dV, in air of a cylindrical cave.

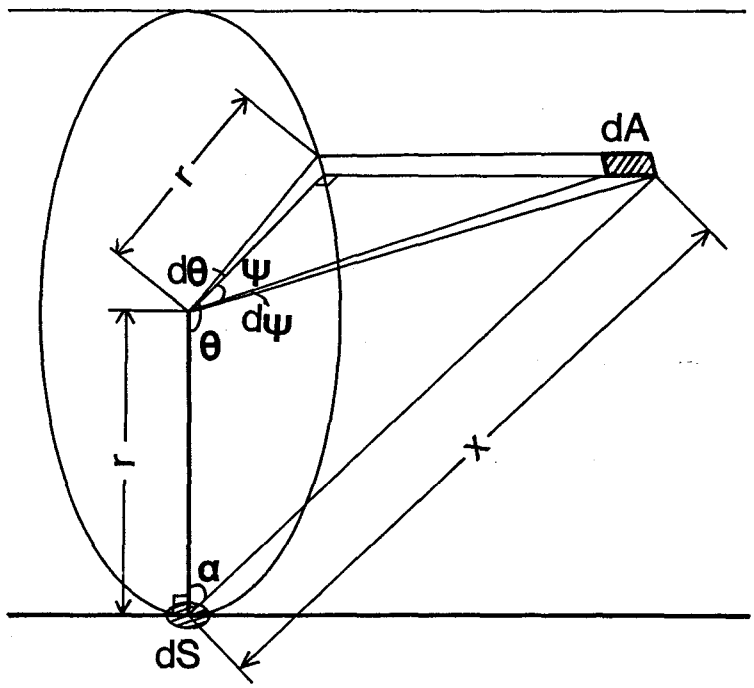

Fig.A–2 The energy given to dS by β rays are obtained by integrating the energy from the radioactive elements adsorbed on a very small area, dA, in the surface of a cylindrical cave.

$$E^{\alpha}_{A,i}\, dS = C_i \int_0^{\pi/2} d\theta \int_0^{2\pi} d\psi \int_0^{Ri} dx\, 46.2\,(R_i - x)^{2/3} \frac{dS\cos\theta}{4\pi x^2} x^2 \sin\theta$$

$$= 6.94\, C_i R_i^{5/3}\, dS$$

$$= 4.77\times10^{-4}\, C_i E_i^{5/2}\, dS$$

where C_i is the radioactivity of an element i in Bq/m^3, and E_i and R_i are the energy and the range respectively of α particle from a decay of an element i. The relation between E_i and R_i is given by equation (1). Therefore, the energy per unit surface given by α particles produced in air is,

$$E^{\alpha}_{A,i} = 4.77\times10^{-4}\, C_i\, E_i^{5/2} \quad (Mev / m^2\, s) \qquad (6)$$

The energy given by α particles from the elements adsorbed on the surface is,

$$E^{\alpha}_{S,i} = \frac{S_i E_i}{2} \quad (Mev / m^2 s) \qquad (7)$$

where S_i is the radioactivity of an element i on the surface in Bq/m^2 and E_i is the energy of α particle from a decay of an element i. Considering the solid angle, the half of the energy is taken.

From equations (6) and (7), the annual dose rate from an element i can be calculated for two models. One is that the carbonate grew with a constant speed v (cm/y). In this case the total dose by α particles from an element i in air ($TD^{\alpha}_{A,i}$) and the total dose from the one adsorbed on the surface ($TD^{\alpha}_{S,i}$) are calculated to be,

$$TD^{\alpha}_{A,i} = 3.31\times10^{-6} \left(\frac{1}{v}\right)\left(\frac{2.7\times10^3}{\rho}\right)\left(\frac{C_i}{37}\right) E^{5/2} \quad (mGy) \qquad (6)\text{-}1$$

$$TD^{\alpha}_{S,i} = 3.46\text{x}10^{-5}\left(\frac{1}{v}\right)\left(\frac{2.7\text{x}10^{3}}{\rho}\right)\left(\frac{S_i}{0.37}\right)E \qquad (\text{mGy}) \qquad (7)\text{-}1$$

v (cm/y) : a speed of growth
ρ (kg/m^3) : the density of the carbonate
E_i (Mev) : energy of α decay of an element i
C_i (Bq/m^3) : the radioactivity of an element i in air
S_i (Bq/m^2) : the radioactivity of an element i absorbed on the surface

The other model is that a carbonate had grown in a very short duration period and α particle effect is limited at the very surface (within the range of about 10 μm). However, we usually take the sample with a thickness of d mm. The "effective" annual dose rates given by radioactive elements in air and on the surface depend on the thickness of the sample and are given by,

$$YD^{\alpha}_{A,i} = 3.31\text{x}10^{-5}\left(\frac{1}{v}\right)\left(\frac{2.7\text{x}10^{3}}{\rho}\right)\left(\frac{C_i}{37}\right)E^{5/2} \qquad (\text{mGy/y}) \qquad (6)\text{-}2$$

$$YD^{\alpha}_{S,i} = 3.46\text{x}10^{-4}\left(\frac{1}{v}\right)\left(\frac{2.7\text{x}10^{3}}{\rho}\right)\left(\frac{S_i}{0.37}\right)E \qquad (\text{mGy/y}) \qquad (7)\text{-}2$$

d (mm) : thickness of the sample

3. The Energy Given by β Rays

We also calculated the energy given by β rays sticked to the wall from radioactive elements (^{214}Pb, ^{214}Bi, ^{210}Pb, and ^{210}Bi, see Table A–1) in a cave. The energy from the elements in air is also different from the energy from the one on the surface.

The relation between the energy and the range of a β ray is given by,

$$R = \begin{cases} 4.19\,E - 103 & (0.8 < E) \\ 3.15\,E^{1.38} & (E < 0.8) \end{cases} \qquad (8)$$

E (MeV) : the energy of β decay

R (m) : the maximum range of β ray with energy E in air

In the case that a β ray produced at x m from a plane of the a carbonate enters into the carbonate from a perpendicular direction to its plane, the relation between the residual range, R−x, and the energy, E', is,

$$R - x = \begin{cases} 4.19\,E_\beta - 103 & (0.8 < E_\beta) \\ 3.15\,E_\beta^{1.38} & (E_\beta < 0.8) \end{cases} \qquad (9)$$

where R is given by equation (8). From equation (9) and considering that the average energy depends on the shape of the energy spectrum and that it is approximately one third of the maximum energy, i.e. the energy of β decay, we obtain,

$$E_\beta(x) = \begin{cases} 7.96\times10^{-2}\,(R - x) + 0.0819 \text{ (Mev)} & (2.32 < R - x) \\ 0.145\,(R - x)^{0.725} \text{ (Mev)} & (R - x < 2.32) \end{cases} \qquad (10)$$

The intensity of β rays decreases with distance as the following expression.

$$I = I_0 \exp(-\mu\rho x) \qquad (11)$$

where μ is an absorption factor given by,

$$\mu = 1.7\,E^{-1.43} \quad (m^2/kg) \qquad (12)$$

ρ is the density of air, which is 1.29 kg/m^3, and x is a distance in m from the position where β ray is produced.

The energy of β ray from radioactive elements in air is calculated by the same way as that of α particle using a model of a cylindrical cave (see Fig.A–2). The region of integration is different from the one in the case of α particle because the range of β ray is much longer than that of α particle. The energy of β ray given to a unit surface is ob–

tained from (4), (5), (10), and (11),

$$E^{\beta}_{A,i} = C_i \int_0^{R_i} dx \int_0^{\pi/2} d\theta\, 4 \int_0^{\psi_0} d\psi\, x2 \sin\theta \frac{\cos\theta}{4\pi x^2} \exp(-\mu\rho x)\, E_{\beta}(x)$$

where x, θ, and ψ are restricted by the shape of the cave, that is a column in our model. In the case that the range is smaller than the diameter (R < 2r), after integration for ψ, we obtained,

$$E^{b}_{A,i} = Ci \int_0^{R_i} dx \left(\frac{1}{4} - \frac{1}{2\pi} \int_{\theta_0}^{\pi/2} \psi_o \sin 2\theta\, d\theta \right) \exp(-\mu\rho x)\, E_{\beta}(x) \quad (13)\text{–a}$$

where,

$$\theta_0 = \cos^{-1} \frac{x}{2r} \quad (14)$$

and,

$$\psi_0 = \cos^{-1} \frac{\{(2r\cos\theta)/x - \cos_2\theta\}^{1/2}}{\sin\theta} \quad (15)$$

In the other case that the range is larger than the diameter (R > 2r), after integration for ψ, we obtained,

$$E^{\alpha}_{A,i} = C_i \left[\int_0^{2r} dx \left(\frac{1}{4} - \frac{1}{2\pi} \int_{\theta 0}^{\pi/2} \psi_0 \sin 2\theta\, d\theta \right) \exp(-\mu\rho x)\, E_{\beta}(x) \right. \quad (13)\text{–b}$$

$$\left. + \int_{2r}^{R} dx \left(\frac{r^2}{x^2} - \frac{1}{2\pi} \int_{\theta 1}^{\pi/2} \psi_0 \sin 2\theta\, d\theta \right) \exp(-\mu\rho x)\, E_{\beta}(x) \right]$$

where θ_0 and ψ_0 are given by (14) and (15) respectively and θ_1 is given by,

$$\theta_1 = \cos^{-1}\frac{2r}{x}$$

$E^{\beta}_{A,i}$ is calculated from the given value of E (the energy of a β decay) and r (the radius of a cave) by numerical integration of (13)–a or (13)–b.

There are two kind of β rays from radioactive elements adsorbed on the surface, which give the surface their energy. One is the β ray produced by the elements adsorbed on the same region of the surface. The energy is given as the same in the case of α particle by,

$$E^{\beta}_{S,i,1} = \frac{S_i E_i}{6} \qquad (MeV / m^2 s) \qquad (16)$$

where S_i is a radioactivity of the element i per unit area in Bq/m^2, E_i is the energy of β decay in MeV. It is considered that the average energy of β rays is one third of the energy of β decay. The other kind of β rays that produced by the elements adsorbed on other region pass through the air and give the considered region their energy. The energy of β ray from a very small region, dA, to the considered small region, dS, is calculated (see Fig.A–2). The area of the very small region is given by,

$$dA = \frac{r^2}{\cos^2\psi} d\theta\, d\psi \qquad (17)$$

The ratio of the solid angle of dS to the total solid angle is,

$$\frac{dS \cos\alpha}{4\pi x^2} \qquad (18)$$

where cosα is represented by,

$$\cos\alpha = \frac{(x^2+ r^2)\cos^2\psi - r^2}{2\,r\,x\cos^2\psi} \tag{19}$$

Then, the energy given to a unit area is obtained by (10), (11), (17), (18), and (19),

$$E^{\beta}_{S,i,2} = S_i \int_0^{\theta 2} d\theta\, 4 \int_0^{\psi 2} d\psi \frac{r^2}{\cos^2\psi} \frac{\cos\alpha}{4\pi x^2} \exp(-\mu\rho x)\, E_{\beta}(x)$$

where,

$$\theta_2 = \begin{cases} \pi & (R > 2r) \\ 2\sin^{-1}(R/2r) & (R < 2r) \end{cases}$$

and,

$$\psi_2 = \tan^{-1}\left(\frac{R^2}{r^2} - 4\sin^2\frac{\theta}{2}\right)^{1/2}$$

Using the relation among x, θ, and ψ;

$$x = r\left(4\sin^2\frac{\theta}{2} + \tan^2\psi\right)^{1/2} \tag{20}$$

we obtained,

$$E^{\beta}_{S,i,2} = S_i \int_0^{\theta 2} d\theta\, 4 \int_0^{\psi 2} d\psi \frac{(1-\cos\theta)\, r^3}{\pi x^3 \cos^2\psi} \exp(-\mu\rho x)\, E_{\beta}(x) \tag{21}$$

where x is given by (20). This integration is also calculated numerically. The total energy of β ray from a radioactive element on the surface is summation of (16) and (21);

$$E^{\beta}_{S,i} = E^{\beta}_{S,i,1} + E^{\beta}_{S,i,2} \qquad (22)$$

In the case that stalactite grew with a constant speed v (cm/y), total doses from radio-activity in air and from that on the surface are given by,

$$TD^{\beta}_{A,i} = 1.87 \left(\frac{1}{v}\right)\left(\frac{2.7\text{x}10^{3}}{\rho}\right) E^{\beta}_{A,i} \quad \text{(mGy)} \qquad (23)\text{-}1$$

$$TD^{\beta}_{S,i} = 1.87 \left(\frac{1}{v}\right)\left(\frac{2.7\text{x}10^{3}}{\rho}\right) E^{\beta}_{S,i} \quad \text{(mGy)} \qquad (24)\text{-}1$$

In the case that stalactite had grown rapidly in a short time and exposed to β ray after the termination of the growth, the annual dose rate is given by,

$$YD^{\beta}_{A,i} = 3.74 \left(\frac{2.7\text{x}10^{3}}{r}\right) E^{\beta}_{A,i} \quad \text{(mGy/y)} \qquad (23)\text{-}2$$

$$YD^{\beta}_{S,i} = 3.74 \left(\frac{2.7\text{x}10^{3}}{r}\right) E^{\beta}_{S,i} \quad \text{(mGy/y)} \qquad (24)\text{-}2$$

where we assume that β ray penetrate to the stalactite to the depth of 5 mm. When the sample is thicker than 5 mm, annual dose should be multiplied by (5/d), where d is the thickness of the sample in mm.

4. An Adsorption model

The energy given to a stalactite depends on whether the elements are in air or adsorbed on the surface (see equation (6) and (7), and (23) and (24)). Half lives of ^{218}Po, ^{214}Pb, ^{214}Bi, and ^{214}Po are very short and the one of ^{210}Pb is relatively long. It is probable

that, in a cave, the elements before ^{210}Pb (i=1,2,...5 in Table A–1) decay in air and ^{210}Pb and the elements after it (i=6,7,8) decay after adsorption onto the surface. According to this model, total dose (the case that stalactite grew with a speed v) and annual dose (the case that stalactite had grown rapidly and the effect of α particle and β ray is limited near the surface) are calculated assuming radioactive equilibrium after ^{222}Rn in ^{238}U–series disintegration. When a radioactive equilibrium is attained, the radioactivity of each element is the same, i.e.

$$\lambda_1 N_1 = \lambda_2 N_2 = \lambda_i N_i = \text{const.} \qquad (i=3,4,....8) \qquad (25)$$

where $\lambda_i N_i$ is a radioactivity of an element i. Then, the relation between the radioactivity of a element i per unit volume in air, C_i, and the one of an element j per unit area adsorbed on the surface, S_j, is the following;

$$S_j = \frac{r}{2} C_i \qquad (i=1,2,...5,\ j=6,7,8) \qquad (26)$$

where the shape of the cave is assumed to be a column. After summing (6), (7) for i considering the relation of (25), (26) and the energies of α decay (Table A–1), we obtain,

$$TD^{\alpha} = (1.07\text{x}10^{-3} + 9.19\text{x}10^{-3}\ r)\left(\frac{1}{v}\right)\left(\frac{2.7\text{x}10^{3}}{\rho}\right)\left(\frac{C_1}{37}\right) \quad (\text{mGy}) \qquad (27)\text{–}1$$

$$YD^{\alpha} = (1.07\text{x}10^{-2} + 9.19\text{x}10^{-4}\ r)\left(\frac{1}{d}\right)\left(\frac{2.7\text{x}10^{3}}{\rho}\right)\left(\frac{C_1}{37}\right) \quad (\text{mGy/y}) \qquad (27)\text{–}2$$

v (cm/y) : growing speed of stalactite
d (mm) : thickness of a sample
ρ (kg/m^3) : density of stalactite
r (m) : radius of a cave
C_1 (Bq/m^3) : radioactivity of ^{222}Rn in air

The effect of β ray cannot be described for any radius and any radioactivity as (27)

because $E_{A,i}^{\beta}$ and $E_{S,i}^{\beta}$ depends on the radius of the cave and the energy of the β decay. When the radius is 1 m and 2 m, the total dose and the annual dose from β rays are given by the following expressions;

$$TD^{\beta} = G_{TD}(r)\left(\frac{1}{v}\right)\left(\frac{2.7\times10^{3}}{\rho}\right)\left(\frac{C_1}{37}\right) \quad \text{(mGy)} \qquad (28)\text{–}1$$

$$YD^{\beta} = G_{YD}(r)\left(\frac{2.7\times10^{3}}{\rho}\right)\left(\frac{C_1}{37}\right) \quad \text{(mGy)} \qquad (28)\text{–}2$$

where, $G_{TD}(1) = 1.75\times10^{-3}$ $G_{YD}(1) = 3.45\times10^{-3}$
$G_{TD}(2) = 2.57\times10^{-3}$ $G_{YD}(2) = 5.14\times10^{-3}$

Table A–2 Annual Dose rates from α and β rays assuming that the radioactivity of ^{222}Rn is 1 WL, that the radius of a cave is 1 m, that the thickness of a sample is 5 mm and that the carbonate had grown rapidly and exposed to α and β ray after the termination of the growth.

	α (mGy/y)	β (mGy/y)
Air	0.214	0.196
(^{222}Rn)	(0.0467)	
Surface	1.84	0.154
Total	2.05	0.350

The annual dose rate and the contribution of radioactive elements in air and on the surface are listed in Table A-2 in the case that the radioactivity of ^{222}Rn in the cave is 3700 Bq/m^3 (= 1WL), the density of stalactite is 2.7×10^3 kg/m^3 and the thickness of the sample of stalactite is 5 mm.

More precise estimation of ^{222}Rn effect can be obtained by considering adsorption process of daughter elements. The differential equations of these processes are below:

$$\frac{dN_i}{dt} = \lambda_{i-1} N_{i-1} - \lambda_i N_i - A_d N_i \qquad (i = 2,3.....8)$$

$$\frac{dQ_i}{dt} = \lambda_{i-1} Q_{i-1} - \lambda_i Q_i + A_d N_i \qquad (i = 2,3.....8) \qquad (29)$$

N_i : The abundance of an element i in the air of the cave
Q_i : The abundance of an element i adsorbed on the surface of the cave
λ_i : Decay constant of an element i
A_d : Adsorption factor

where we assumed that, A_d, an adsorption factor which is the ratio of the abundance of an element absorbing onto the surface to the abundance in air in a unit duration period is the same for all elements.

We have already obtained a preliminary result that the effect of α particles is controlled strongly by A_d value, which can be determined by observing the deposition velocity of radon daughters. The relation between adsorption factor, A_d (y^{-1}) and deposition velocity v_d (cm/y) is the following;

$$A_d = \frac{2 v_d}{r} \qquad (30)$$

where we assume a cylindrical shape of a cave with a radius of r.

5. Shielding and Washing out Effect

The a rays produce defects densely along the track leading to the high recombination rate. The α ray efficiency, k–value ranging from 0.1 to 0.3 (Yokoyama et al. 1982) must be multiplied to the α ray dose rate for evaluating the effective dose rate. The energy from α particles (Table A–2) is decreased and seems comparable to the annual dose rate of γ ray (see section 1) after multiplied by k–value. The energy from β ray seems also comparable to that of γ ray (Table A–2). However, we should consider some factors that decrease the dose rates from α particles and β ray.

In the case that stalactites or carbonate deposits are dry, the effect of α particles and β rays from ^{222}Rn and its daughters on annual dose rate is probably large. Indeed, a high total dose at the surface of cave deposits has been already observed (Ikeya, 1980). However, in most cases where the carbonate deposits are growing, the whole energy of α particle and a part of the energy of β ray from elements in air would be shielded by the surface water, the thickness of which is estimated to be more than 100 μm by the result of fluid dynamics. The water would also wash out the deposited radioactive nuclides. Hence, the effect of ^{222}Rn activity would be only the energy of β ray produced by daughter elements in air. This dose rate is estimated to be 0.2 mGy/y for 1 working level (see Table A–2). For more precise estimation, we should consider the contribution from ^{222}Rn and its daughters solved in the cave water in this case.

We have neglected the radon effect taking the summer activity of 111 Bq/m^3 in Akiyoshi cave into account (Miki and Ikeya, 1980) and we have shown in this paper that this assumption was appropriate. But the result of a measurement of radon activity of about 4 WL with a solid state detector at Petralona is extraordinary large (Papastefanou et al. 1986), where the precise experimental procedures were not described. If they have measured α particles from not only ^{222}Rn but also from its daughters, the radioactivity only from ^{222}Rn would be one third of the measured activity, and if they have also measured the α tracks due to daughter elements adsorbed on the surface and regarded that the number of tracks solely as due to ^{222}Rn α rays, the radioactivity only from ^{222}Rn would be one tenth (see Table A–2). Hence, we refrain from calculating the accurate dose rate at the moment. It is clear that the external dose rate of 1.90 mGy/y by Hennig et al. was incorrect leading to the underestimated age of 200 ky. The present atmospheric ^{222}Rn activity should be reinvestigated with α track and preferably with other methods.

6. Conclusion

We have calculated the dose rate of α and β rays produced by ^{222}Rn and its daughters in air and on the surface of the cave, which cannot be measured by a commercial TL dosimeter in a glass capsule. The results of calculation using a model of a cylindrical cave suggest that, if the surface is dry, the effect of α particles and β rays are comparable to that of γ ray when radioactivity of ^{222}Rn is 1 WL. In this case, it should be noted that the k-value becomes extremely small down to 0.05 (Koba et al. 1986) for heavily damaged surface. Thus, further investigation is necessary to clarify the dose dependence of the k-value. However, if there are the shielding and washing out effect by water, the effect would be limited to that of β ray from air, which is about 0.2 mGy/y at radioactivity of ^{222}Rn of 1WL.

It is most important that the activity only from ^{222}Rn in air should be measured for more precise estimation of effect from ^{222}Rn. A deposition velocity of daughter elements and concentrations of radioactive elements in cave water should be measured, too. The age of the Petralona cranium encrust should be left to further investigation.

References

Hennig, G. J., Herr, W., Weber, E., and Xirotiris, N.I. (1981) ESR-dating of the fossil hominid cranium from Petralona Cave, Greece. *Nature*, 292, 533-536.

Hennig,G.J., W.Herr, E.Weber, and N.I.Xirotiris. (1982) Petralona Cave dating controversy. *Nature*, 299, 280-282.

Ikeya, M. (1977) Electron spin resonance dating and fission track detection of Petralona stalagmite. *Anthropos*, 4, 152-168.

Ikeya, M. (1978) Natural Radiation at Petralona Cave. *Anthropos*, 5, 54-59.

Ikeya, M. (1980) ESR dating of carbonates at Petralona Cave. *Anthropos*, 7, 143-151.

Koba, M., Tamura, M., Ikeya, M., and Kaigara, T. (1986) Quartenary shorelines and crustal movements on Minamidaitoh-Jima, Northwest Pacific. in, ed. Yushan and Songling, Z., *Late Quartenary Sea Level Changes*.

Liritzis and Poulianos (1980) A radiation survey of Petralona Cave. *Anthropos*, 7, 252-259.

Miki, T. and Ikeya, M. (1980) Accumulation of atmospheric radon in calcite caves. *Health Physics*, 39, 351-354.

Papastefanou, C., Manolopoulou, M., Savvides, E., and Charalambous, Stef. (1986) Dose rate measurements in Petralona Cave for Archanthropus. *Anthropos*, 11, 41-48.

Yokoyama, Y., Nguyen, H. V., Quaegebeur, J. P., and Poupeau, G. (1982) Some problems encountered in the estimation of annual dose-rate in the electron spin resonance dating of fossil bones. *Pact. J.*, 6, 103-115.